

การแยกอิแนนทิโอเมอร์ของแอลกอฮอล์ด้วยแก๊สโครมาโทกราฟี  
ที่ใช้อนุพันธ์ของแอลฟาไซโคลเดกซ์ทรินเป็นเฟสคงที่

นาย ทศพล โปธิสมุทโรยธิน

วิทยานิพนธ์นี้เป็นส่วนหนึ่งของการศึกษาตามหลักสูตรปริญญาวิทยาศาสตรมหาบัณฑิต

สาขาวิชาเคมี ภาควิชาเคมี

คณะวิทยาศาสตร์ จุฬาลงกรณ์มหาวิทยาลัย

ปีการศึกษา 2549

ลิขสิทธิ์ของจุฬาลงกรณ์มหาวิทยาลัย

GAS CHROMATOGRAPHIC ENANTIOMERIC SEPARATION  
OF ALCOHOLS USING DERIVATIZED  $\alpha$ -CYCLODEXTRIN  
STATIONARY PHASE



Mr. Todsapon Pothisamutyothin

A Thesis Submitted in Partial Fulfillment of the Requirements  
for the Degree of Master of Science Program in Chemistry

Department of Chemistry

Faculty of Science

Chulalongkorn University

Academic Year 2006

Copyright of Chulalongkorn University

Thesis Title                    GAS CHROMATOGRAPHIC ENANTIOMERIC  
SEPARATION OF ALCOHOLS USING DERIVATIZED  
 $\alpha$ -CYCLODEXTRIN STATIONARY PHASE

By                                    Mr. Todsapon Pothisamutyothin

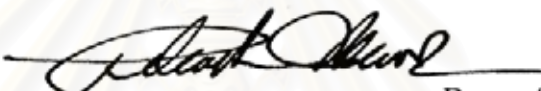
Field of Study                    Chemistry

Thesis Advisor                 Assistant Professor Aroonsiri Shitangkoon, Ph.D.

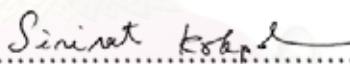
Thesis Co-advisor             Associate Professor Vudhichai Parasuk, Ph.D.


---

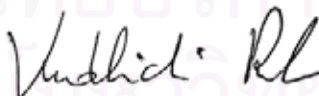
Accepted by the Faculty of Science, Chulalongkorn University in  
Partial Fulfillment of the Requirements for the Master's Degree

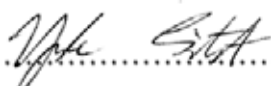
  
..... Dean of the Faculty of Science  
(Professor Piamsak Menasveta, Ph.D.)

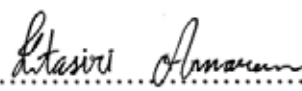
THESIS COMMITTEE

  
..... Chairman  
(Associate Professor Sirirat Kokpol, Ph.D.)

  
..... Thesis Advisor  
(Assistant Professor Aroonsiri Shitangkoon, Ph.D.)

  
..... Thesis Co-advisor  
(Associate Professor Vudhichai Parasuk, Ph.D.)

  
..... Member  
(Assistant Professor Yongsak Sritana-anant, Ph.D.)

  
..... Member  
(Amarawan Intasiri, Ph.D.)

ทศพล โพธิสมุทโรยชิน : การแยกอิแนนทิโอเมอร์ของแอลกอฮอล์ด้วยแก๊สโครมาโทกราฟี  
ที่ใช้อนุพันธ์ของแอลฟาไซโคลเดกซ์ทรินเป็นเฟสคงที่. (GAS CHROMATOGRAPHIC  
ENANTIOMERIC SEPARATION OF ALCOHOLS USING DERIVATIZED  $\alpha$ -  
CYCLODEXTRIN STATIONARY PHASE) อ.ที่ปรึกษา: ผศ. ดร. อรุณศิริ ชิตางกูร,  
อ.ที่ปรึกษาร่วม: รศ. ดร. วุฒิชัย พาราสุข, 126 หน้า.

ได้แยกคู่อิแนนทิโอเมอร์ของแอลกอฮอล์ 90 ชนิด ด้วยอะพิลลารีแก๊สโครมาโทกราฟีที่มี  
เฮกซะคิส(2,3-ได-โอ-เมทิล-6-โอ-เทอร์ท-บิวทิล ไดเมทิลไซลิล)ไซโคลมอลโตเฮกซะไอส (หรือ  
ASiMe) เป็นเฟสคงที่ชนิดโครัล โดยได้ทำการศึกษาค่าผลของชนิด ตำแหน่งและจำนวนของหมู่  
แทนที่ ตำแหน่งโครัล และ โครงสร้างหลักที่แตกต่างกัน ที่มีผลต่อค่ารีเทนชันและค่าการเลือก  
จำเพาะของอิแนนทิโอเมอร์ นอกจากนี้ ยังได้คำนวณค่าทางเทอร์โมไดนามิกส์ และสร้าง  
แบบจำลองโมเลกุลด้วยวิธีค็อกกิง เพื่ออธิบายถึงแรงกระทำระหว่างอิแนนทิโอเมอร์กับเฟสคงที่  
และกลไกการแยกคู่อิแนนทิโอเมอร์ของแอลกอฮอล์ที่นำมาศึกษา จากการทดลองพบว่าอิแนนทิโอ  
เมอร์ของแอลกอฮอล์ที่นำมาศึกษาทุกตัว สามารถแยกได้ด้วยเฟสคงที่ ASiMe ยกเว้น 12, 15, 17,  
4OMe, 4OMeBen และ 2but โดย 1-(2,5-ไดฟลูออโรฟีนิล)เอทานอล ให้ค่าการแยกของคู่อิแนนทิ  
โอเมอร์ดีที่สุดจากแอลกอฮอล์ 90 ชนิดที่นำมาศึกษา ผลของตำแหน่งของหมู่แทนที่ต่อการแยกของ  
คู่อิแนนทิโอเมอร์เห็นได้ชัดจาก 1-ฟีนิลเอทานอลที่มีหมู่แทนที่ 1 หมู่ โดยการแยกของคู่อิแนนทิโอ  
เมอร์จะเพิ่มขึ้นเมื่อตำแหน่งของหมู่แทนที่เป็น พารา- < เมตา- << ออร์โท- แต่ไดฟีนิลเอทานอลที่มี  
หมู่แทนที่ที่ตำแหน่งออร์โท จะมีค่าการแยกของคู่อิแนนทิโอเมอร์ต่ำกว่า 1-ฟีนิลเอทานอลที่มีหมู่  
แทนที่เหมือนกัน ซึ่งแสดงถึงผลของโครงสร้างหลัก การแยกของคู่อิแนนทิโอเมอร์ของแอลกอฮอล์  
กลุ่มอื่น ๆ ไม่เห็นแนวโน้มที่ชัดเจน ผลการคำนวณทางทฤษฎียังแสดงให้เห็นว่า รูปร่างของการเกิด  
สารประกอบเชิงซ้อนระหว่างแอลกอฮอล์กับ ASiMe จะขึ้นอยู่กับชนิด ตำแหน่ง และรูปร่างของหมู่  
แทนที่เช่นกัน

ภาควิชา .....เคมี.....      ลายมือชื่อนิสิต ..... ทศพล โพธิสมุทโรยชิน .....

สาขาวิชา .....เคมี.....      ลายมือชื่ออาจารย์ที่ปรึกษา ..... อรุณศิริ ชิตางกูร .....

ปีการศึกษา ..... 2549.....      ลายมือชื่ออาจารย์ที่ปรึกษาร่วม ..... วุฒิชัย พาราสุข .....

## 477 23096 23 : MAJOR CHEMISTRY

KEYWORD: CAPILLARY GAS CHROMATOGRAPHY / DERIVATIZED  
CYCLODEXTRIN / CHIRAL SEPARATION / ALCOHOLS

TODSAPON POTHISAMUTYOTHIN: GAS CHROMATOGRAPHIC  
ENANTIOMERIC SEPARATION OF ALCOHOLS USING DERIVATIZED  
 $\alpha$ -CYCLODEXTRIN STATIONARY PHASE.

THESIS ADVISOR: ASSIST. PROF. AROONSIRI SHITANGKON, Ph.D.,  
THESIS CO-ADVISOR: ASSOC. PROF. VUDHICHAJ PARASUK, Ph.D.,  
126 pp.

Enantiomeric separations of 90 alcohols were studied by means of capillary gas chromatography using hexakis(2,3-di-*O*-methyl-6-*O*-*tert*-butyldimethylsilyl)cyclo-maltohexaose (or ASiMe) as chiral stationary phase. The influence of type, position and number of substituent, position of chiral center, and main-structure of alcohols, on retention and enantioselectivity was systematically investigated. Thermodynamic data and molecular docking calculation were also acquired to clarify the strength of analyte-stationary phase interaction and the mechanism of chiral recognition towards the selected groups of alcohols. The gas chromatographic results indicated that all tested analytes, except for **12**, **15**, **17**, **4OMe**, **4OMeBen** and **2but**, could be successfully enantioseparated with ASiMe. Among 90 alcohols studied, the best enantioseparation was observed on 1-(2,5-difluorophenyl)ethanol. The effect of position of substituent towards enantioseparation was clearly seen from mono-substituted 1-phenylethanol. The enantioseparation increased as the position of substituent was in the order of *para*- < *meta*- << *ortho*-. Nevertheless, *ortho*-substituted diphenylmethanols displayed low enantioseparation compared to 1-phenylethanol with similar substitution, demonstrating the effect of main-structure. The enantioseparation of other series of alcohols did not show a distinct trend. Results from molecular docking suggested that the orientation of complexes between alcohol and ASiMe were dependable on the type, position and structure of substituent.

Department .....Chemistry.....

Field of study .....Chemistry.....

Academic year..... 2006.....

Student's signature .....

Advisor's signature .....

Co-advisor's signature .....

*Todsapon Pothisamutyothin*  
*A. Shitangkoon*  
*Vudhichai Parasuk*

## ACKNOWLEDGEMENTS

First of all, I would like to express my deep thankfulness to my advisor, Assistant Professor Dr. Aroonsiri Shitangkoon, and my co-advisor, Associate Professor Vudhichai Parasuk, for their precious suggestion, encouragement, together with careful and critical reading. I would like to thank Associate Professor Dr. Sirirat Kokpol, Assistant Professor Dr. Yongsak Sritana-anant and Dr. Amarawan Intasiri for their valuable comments, suggestions and reading. Also, I am greatly thankful to Assistant Professor Dr. Somsak Pianwanit for his advice on docking calculation problems.

Appreciation is also expressed to the Department of Chemistry, Chulalongkorn University for the financial support as a part of this research work. I thank all the staffs in the Department of Chemistry for the continuous support throughout my study.

My special thank go to Professor Gyula Vigh for his kind provision of cyclodextrin derivative used in this research.

Warm thanks also extend to many best friends for their encouragement, kind assistance and social support; particularly, I am thankful to everybody in my research group, giving me enjoyable time during the years.

Finally, my warmest thanks go to my beloved parents and my lovely family for their care, understanding, encouragement and unlimited support throughout my entire education. Without them, I would have never been able to achieve this goal.

# CONTENTS

	<b>PAGE</b>
ABSTRACT (IN THAI) .....	iv
ABSTRACT (IN ENGLISH) .....	v
ACKNOWLEDGEMENTS .....	vi
CONTENTS .....	vii
LIST OF TABLES .....	ix
LIST OF FIGURES .....	x
LIST OF ABBREVIATIONS AND SIGNS .....	xiii
CHAPTER I INTRODUCTION .....	1
CHAPTER II THEORY .....	4
2.1 Gas chromatographic separation of enantiomers .....	4
2.2 Cyclodextrins and their derivatives .....	5
2.3 Parameters affecting enantioseparation .....	6
2.4 Molecular modeling studies for enantioseparation .....	9
2.5 Thermodynamic investigation of enantiomeric separation by gas chromatography .....	11
2.6 Study interaction between CD and alcohol derivatives by molecular modeling .....	14
CHAPTER III EXPERIMENTAL .....	24
3.1 Preparation of alcohol derivatives .....	24
3.2 Gas chromatographic analyses .....	34
3.3 Methods of molecular modeling calculations .....	35
CHAPTER IV RESULTS AND DISCUSSION .....	38
4.1 Synthesis of alcohol derivatives .....	38
4.2 Gas chromatographic separation of alcohol derivatives .....	38
4.3 Thermodynamic investigation by van't Hoff approach .....	42
4.4 Molecular modeling of the interaction between chiral solute and selector .....	76
CHAPTER V CONCLUSION .....	83

	viii
	<b>PAGE</b>
REFERENCES .....	85
APPENDICES .....	91
Appendix A      Glossary .....	92
Appendix B      NMR Spectra .....	94
Appendix C      Thermodynamic studies .....	100
Appendix D      Docking configuration .....	110
VITA .....	112



สถาบันวิทยบริการ  
จุฬาลงกรณ์มหาวิทยาลัย



**LIST OF TABLES**

<b>TABLE</b>		<b>PAGE</b>
2.1	Some physical properties of native $\alpha$ -, $\beta$ - and $\gamma$ -CDs .....	5
3.1	Structure and abbreviation of all alcohol derivatives used in this study .....	26
4.1	The docking results of selected analytes and ASiMe .....	77
4.2	Comparison of the binding energy difference obtained for the analyte and ASiMe complex .....	82



สถาบันวิทยบริการ  
จุฬาลงกรณ์มหาวิทยาลัย

## LIST OF FIGURES

FIGURE		PAGE
1.1	Structures of propranolol, thalidomide and lavandulol .....	1
2.1	(a) A structure of cyclodextrin molecule with n glucose units (b) The side view of cyclodextrin showing primary hydroxyls on a narrow rim and secondary hydroxyls on a larger rim of a ring .....	6
2.2	Structure of praziquantel .....	11
3.1	Grid base energy evaluation .....	36
4.1	Retention factors ( $k'$ ) of selected alcohols on OV-1701 column at 160 °C .....	39
4.2	Retention factors ( $k'_2$ ) of the more retained enantiomers of selected alcohols on ASiMe column at 160 °C .....	40
4.3	Separation factors ( $\alpha$ ) of the enantiomeric pairs of selected alcohols on ASiMe column at 160 °C .....	41
4.4	Enthalpy change ( $-\Delta H$ , kcal/mol) of alcohol analytes on OV-1701 column obtained from van't Hoff approach ( $\bar{x} = 12.75$ ; SD = 2.73) .....	45
4.5	Entropy change ( $-\Delta S$ , cal/mol·K) of alcohol analytes on OV-1701 column obtained from van't Hoff approach ( $\bar{x} = 17.15$ ; SD = 1.56) .....	46
4.6	Enthalpy change ( $-\Delta H_2$ , kcal/mol) of the more retained enantiomers of alcohol analytes on ASiMe column obtained from van't Hoff approach ( $\bar{x} = 14.42$ ; SD = 1.78) .....	47
4.7	Entropy change ( $-\Delta S_2$ , cal/mol·K) of the more retained enantiomers of alcohol analytes on ASiMe column obtained from van't Hoff approach ( $\bar{x} = 21.02$ ; SD = 1.92) .....	48
4.8	Difference in enthalpy values ( $-\Delta(\Delta H)$ , kcal/mol) of the enantiomers of alcohol analytes on ASiMe column .....	50

## FIGURE

4.9	Difference in entropy values ( $-\Delta(\Delta S)$ , cal/mol·K) of the enantiomers of alcohol analytes on ASiMe column .....	51
4.10	Difference in enthalpy values ( $-\Delta(\Delta H)$ , kcal/mol) of the enantiomers of mono-substituted 1-phenylethanol derivatives on ASiMe column .....	53
4.11	Plots of $\ln \alpha$ versus $1/T$ of <b>2Cl</b> , <b>3Cl</b> and <b>4Cl</b> on ASiMe column .....	54
4.12	Chromatograms of (a) <b>2Cl</b> , (b) <b>3Cl</b> , (c) <b>4Cl</b> on ASiMe column at (left) 150 °C and (right) 140 °C .....	54
4.13	Chromatograms of (a) <b>4OCF<sub>3</sub></b> and (b) <b>4OMe</b> on ASiMe column at 120 °C .....	56
4.14	Chromatograms of (a) <b>4Me</b> (b) <b>4Et</b> , (c) <b>4Bu</b> and (d) <b>4tBu</b> on ASiMe column at 140 °C .....	56
4.15	Difference in enthalpy values ( $-\Delta(\Delta H)$ , kcal/mol) of the enantiomers of di-substituted 1-phenylethanol derivatives on ASiMe column .....	58
4.16	Chromatograms of (a) <b>25F</b> , (b) <b>34F</b> , (c) <b>25Me</b> and (d) <b>34Me</b> on ASiMe column at 150 °C .....	59
4.17	Difference in enthalpy values ( $-\Delta(\Delta H)$ , kcal/mol) of the enantiomers of alcohols in series 3 on ASiMe column .....	61
4.18	Difference in enthalpy values ( $-\Delta(\Delta H)$ , kcal/mol) of the enantiomers of alcohols in series 3.1 on ASiMe column .....	62
4.19	Chromatograms of (a) <b>triF</b> , (b) <b>tetraF</b> and (c) <b>pentaF</b> on ASiMe column at 110 °C .....	63
4.20	Difference in enthalpy values ( $-\Delta(\Delta H)$ , kcal/mol) of the enantiomers of alcohols in series 3.2 on ASiMe column .....	64
4.21	Chromatograms of (a) <b>4</b> and (b) <b>5</b> on ASiMe column at 130 °C .....	66
4.22	Chromatograms of (a) <b>2</b> and (b) <b>3</b> on ASiMe column at 150 °C .....	66

FIGURE		PAGE
4.23	Difference in enthalpy values ( $-\Delta(\Delta H)$ , kcal/mol) of the enantiomers of alcohols in series 3.3 on ASiMe column .....	68
4.24	Chromatograms of (a) <b>7</b> , (b) <b>16</b> and (c) <b>20</b> on ASiMe column at 120 °C .....	68
4.25	Chromatograms of (a) <b>14</b> and (b) <b>15</b> on ASiMe column at 120 °C .....	69
4.26	Difference in enthalpy values ( $-\Delta(\Delta H)$ , kcal/mol) of the enantiomers of alcohols in series 4 on ASiMe column .....	71
4.27	Chromatograms of (a) <b>2hex</b> , (b) <b>3hex</b> and (c) <b>3hep</b> on ASiMe column at 80 °C .....	72
4.28	Difference in enthalpy values ( $-\Delta(\Delta H)$ , kcal/mol) of the enantiomers of alcohols in series 5 on ASiMe column .....	74
4.29	Chromatograms of (a) <b>2MeBen</b> , (b) <b>3MeBen</b> and (c) <b>4MeBen</b> on ASiMe column at 150 °C .....	74
4.30	Difference in enthalpy values ( $-\Delta(\Delta H)$ , kcal/mol) of the enantiomers of alcohols in series 5 (white bar) and series 1 (gray bar) on ASiMe column .....	75
4.31	Superimposed of lowest energy complexes between ASiMe and (a) <b>4Me</b> , (b) <b>4OMe</b> and (c) <b>2OMe</b> in <i>R</i> -form (green) and <i>S</i> -form (pink) in both top and side views .....	78
4.32	Superimposed of lowest energy complexes between ASiMe and (a) <b>4Bu</b> and (b) <b>4tBu</b> in <i>R</i> -form (green) and <i>S</i> -form (pink) in both top and side views .....	79

## LIST OF ABBREVIATIONS AND SIGNS

AM1	=	austin model 1
ASiMe	=	hexakis(2,3-di- <i>O</i> -methyl-6- <i>O</i> - <i>tert</i> -butyldimethylsilyl)cyclomaltohexaose
CD	=	cyclodextrin
HF	=	hartree-fock
i.d.	=	internal diameter
K	=	distribution coefficient
k'	=	retention factor or capacity factor
LGA	=	lamarckian genetic algorithm
MM+	=	molecular mechanic plus
m	=	meter
min	=	minute
mm	=	millimeter
mL	=	milliliter
N	=	number of theoretical plate
OV-1701	=	7% phenyl, 7% cyanopropyl, 86% dimethyl polysiloxane
ppm	=	part per million
R	=	universal gas constant (1.987 cal/mol·K)
R <sup>2</sup>	=	correlation coefficient
SD	=	standard deviation
T	=	absolute temperature (K)
$\alpha$	=	separation factor or selectivity
$\beta$	=	phase ratio
$\delta$	=	chemical shift
$\Delta G$	=	Gibb's free energy
$\Delta(\Delta G)$	=	difference in Gibb's free energy for an enantiomeric pair
$\Delta H$	=	enthalpy change of each enantiomer
$\Delta(\Delta H)$	=	difference in enthalpy change for an enantiomeric pair

$\Delta S$	=	entropy change of each enantiomer
$\Delta(\Delta S)$	=	difference in entropy change for an enantiomeric pair
$\mu$	=	dipole moment
$\mu\text{m}$	=	micrometer
$^{\circ}\text{C}$	=	degree celsius
$\bar{x}$	=	mean
3-21G	=	extended basis set
6-31G**	=	polarization basis set



สถาบันวิทยบริการ  
จุฬาลงกรณ์มหาวิทยาลัย

# CHAPTER I

## INTRODUCTION

Nowadays, many chiral organic compounds were used in pharmaceutical and agrochemical industries. Both enantiomeric forms of chiral compounds display identical physical and chemical properties except for the direction of rotating polarized light; however, they show different behaviors when they are in a chiral environment. Enantiomers may exhibit quite different biological activities depending on stereochemistry of each enantiomer. In many cases, only one enantiomer is responsible for the desired activity; whereas the other may have no biological activity or may cause unsuspected adverse effects. For example, (*S*)-propranolol is used for treatment of angina pectoris while (*R*)-enantiomer is inactive [1]. (*R*)-Thalidomide could be used as a sedative drug whereas (*S*)-enantiomer could cause fetal abnormality [2]. Another example is lavandulol; (*R*)-enantiomer is a constituent of French lavender oil, which is used in the perfume chemistry but (*S*)-enantiomer has been identified as the sex pheromone of the vine mealybug, which is a serious pest in vineyards [3].

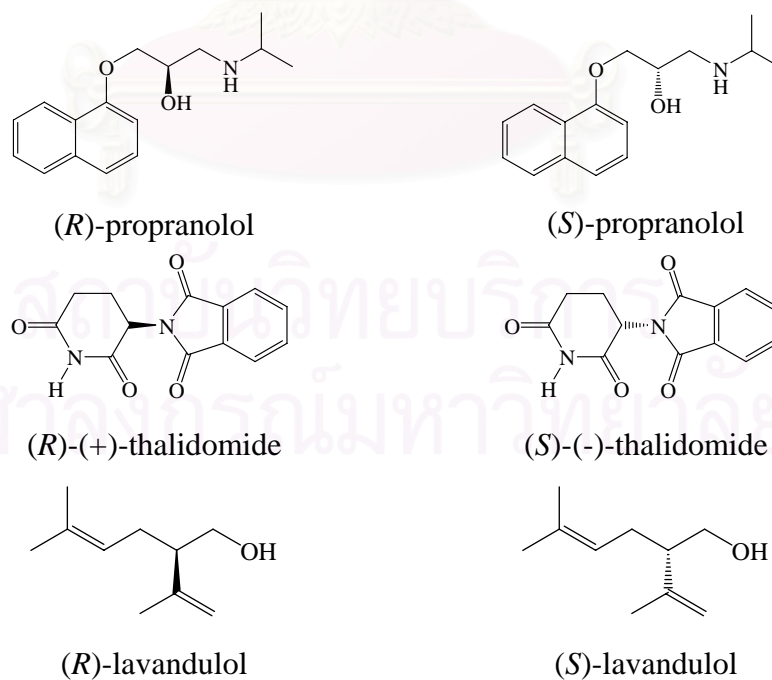


**Figure 1.1** Structures of propranolol, thalidomide and lavandulol

Because there are differences in biological activity between each enantiomeric pair, the requirement of purely single enantiomers was increased; especially in pharmaceutical market, to decrease the consumption of chemical reagent, avoid the unwanted effect and enhance the therapeutic ability. Survey of pharmaceutical data through the last two decades indicated that the use of single enantiomer drugs has been increased from 25% to 58% while the use of racemic drugs has been decreased from 32% to 8% [4].

To obtain purely single enantiomers, two approaches can be regarded [5-8]: the first is enantioselective synthesis of the desired enantiomer using stereoselective catalytic or auxiliary processes; while the other is the preparation of racemate which is subsequently resolved into the corresponding enantiomers. Thus, chiral separations have become the most important tool for separation of enantiomeric pairs and investigation the purity of chiral reagents or products. Chiral separation by chromatography can be achieved in two ways. An indirect method involves the derivatization of both enantiomers with a pure, chiral reagent resulting in diastereomers of different physical properties which are subsequently separated on an achiral environment. While the direct method resolves an enantiomeric pair via a chiral selector, as a stationary phase or a mobile phase additive, capable of forming a diastereomeric complex with one enantiomer.

Among many chromatographic techniques, gas chromatography (GC) is preferred to investigate enantiomeric composition of volatile and thermostable organic compounds because of its high efficiency, sensitivity and short analysis time. Cyclodextrins (CDs) and their derivatives are frequently used as chiral stationary phase due to its capability to form inclusion complexes with many analytes. Generally, it is perceived that the resolution of chiral analytes occurs through the reversible diastereomeric association between each enantiomer and cyclodextrin molecule [7-10]. However, the mechanism of chiral recognition is still not fully understood. Thus, more investigations of chiral separations are still needed.



There are various parameters that affect the enantiomeric separations using cyclodextrins such as types and concentration of CD derivatives, substituents on CD rings and nature of analyte structures. It is evidence that a small variation in analyte structure can cause a large change in enantiomeric separations. In the past, there are only a few studies into the relationships between enantioselectivity of CD derivatives and chiral analytes [11-15]. Therefore, this research aims to systematically examine the influence of analyte structure on the enantiomeric separation and to understand the mechanism of chiral recognition using molecular modeling.

In this research alcohols were the analytes of interest because of their importance as chiral intermediates in the asymmetric synthesis of drugs and agrochemicals. Furthermore, chiral alcohols are important components of pheromone systems of various insect species [7-8, 15-16]. Previously, 2,3-di-*O*-methyl-6-*O*-*tert*-butyldimethylsilyl derivatives of  $\beta$ - and  $\gamma$ -cyclodextrins have been used as chiral selectors in GC for the separation of chiral alcohols whereas its  $\alpha$ -derivative has not yet been explored [17, 18]. 1-Phenylethanol and their derivatives with different type and number of substituents on aromatic ring, different type and number of side chain substituents, different position of chiral center and different base structure are separated by gas chromatography using hexakis(2,3-di-*O*-methyl-6-*O*-*tert*-butyldimethylsilyl)cyclomaltohexaose (or ASiMe) dissolved in polysiloxane as chiral GC stationary phase. Moreover, thermodynamic parameters attained through van't Hoff approach are used to evaluate the interaction between analytes and stationary phase as well as the enantiodifferentiation. The results obtained from ASiMe column will be compared with those from  $\beta$ - and  $\gamma$ -derivatives. Additionally, molecular modeling is used for better understanding of the chiral recognition process between analytes and ASiMe selector. Hopefully, information obtained from this study will explain the influence of alcohols structure on enantioselectivity as well as types of interactions between alcohols and ASiMe.

## CHAPTER II

### THEORY

#### 2.1 Gas chromatographic separation of enantiomers

Gas chromatography (GC) is usually considered as an accurate and reliable technique for the separation of volatile and thermostable organic compounds. Its advantages include high efficiency, sensitivity, reproducibility and short analysis time [8]. For chiral separation using GC, two strategies can be performed: direct and indirect approaches. The indirect approach involves the conversion of the enantiomers with a chiral reagent into diastereomeric derivatives which are subsequently separated on an achiral environment. Disadvantages of this approach include the requirement of active functional group for the formation of diastereomeric derivatives and a pure form of chiral reagent. Moreover, discrimination by incomplete recovery and loss due to decomposition may occur during work-up, isolation and sample handling [9]. On the other hand, the direct approach involves the use of chiral selectors as chiral stationary phases (CSP). Chiral selector can rapidly form transient diastereomeric intermediates with racemic analytes. For GC, chiral selector is generally chemically bonded or coated on the supported material or on column surface; therefore, the chiral selectors and chromatographic column can be used several times. Furthermore, the direct approach using CSP is a single and effective method to separate enantiomers [5, 9].

Among several chiral selectors, cyclodextrins (CDs) and their derivatives are frequently used in gas chromatography because of their ability to form inclusion complexes with various types of analyte. Moreover, the wide operating temperature of CDs and their derivatives makes them one of the most versatile stationary phases for GC [19-20].

## 2.2 Cyclodextrins and their derivatives

Cyclodextrins (CDs) are cyclic oligosaccharides produced from degradation of starch by cyclodextrin glucanotransferase (CGTase) enzyme. The three most common CDs are composed of six, seven and eight D-glucose units linked by  $\alpha$ -1,4-glycosidic bond; referred as  $\alpha$ -,  $\beta$ - and  $\gamma$ -CD, respectively. Some important properties of three native CDs are summarized in table 2.1.

**Table 2.1** Some physical properties of native  $\alpha$ -,  $\beta$ - and  $\gamma$ -CDs [20-21].

CD	$\alpha$	$\beta$	$\gamma$
number of glucopyranose units	6	7	8
number of chiral centers	30	35	40
anhydrous molecular weight (g/mol)	972.85	1134.99	1297.14
internal diameter (Å)	4.7-5.3	6.0-6.5	7.5-8.3
cavity depth (Å)	7.9	7.9	7.9
cavity volume (Å) <sup>3</sup>	174	262	427
water solubility (g/100 mL, 25 °C)	14.50	1.85	73.20
decomposition temperature (°C)	278	299	267

Native CDs are torus-like macromolecules which are frequently characterized as a doughnut or wreath-shaped truncated cone. Every glucopyranose unit of CD ring has secondary hydroxyl groups at C2 and C3 positions on the large rim and the primary hydroxyl groups at C6 position on the narrow edge (figure 2.1). As a result, the exterior surface of the CD molecules is relatively hydrophilic while the interior surface shows hydrophobic property. Because of their hollow structure, CDs are able to form inclusion complex with a wide variety of analyte molecules. Furthermore, cyclodextrins can be chemically modified to improve their properties, such as decomposition temperature, solubility, chiral recognition or selectivities, by substituting various functional groups on the primary and/or secondary hydroxyl groups [19-21].

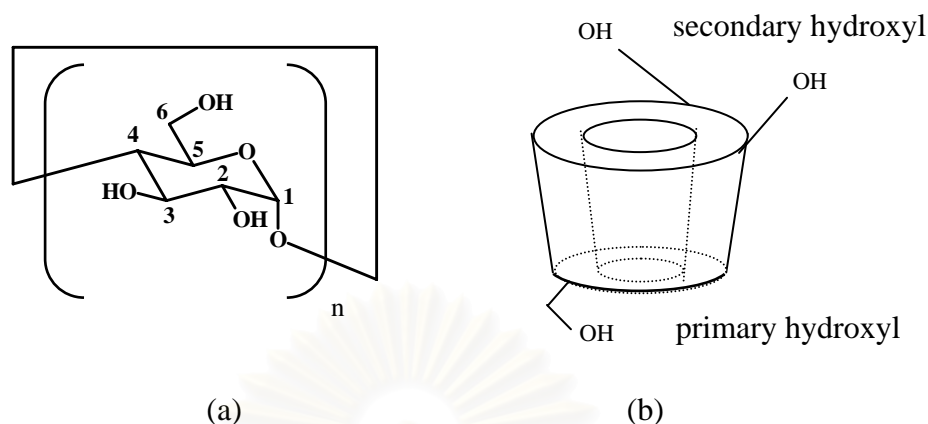


**Figure 2.1** (a) A structure of cyclodextrin molecule with  $n$  glucose units  
 (b) The side view of cyclodextrin showing primary hydroxyls on a narrow rim and secondary hydroxyls on a larger rim of a ring

Generally, the secondary hydroxyl groups at C2 and C3 positions of each glucose unit are modified with small alkyl or acyl groups to improve the enantioselectivities, whereas the primary C6 hydroxyl groups are replaced with longer alkyl or bulky groups to affect the conformation of the CDs. At room temperature, most CD derivatives are solid which can cause non-homogenous film coating problem. Therefore, they are usually diluted in achiral polysiloxane in order to improve their properties and to acquire high efficiency with wide operating temperature range [5, 8-9].

### 2.3 Parameters affecting enantioseparation

As described above, the enantiomeric separation occurs by generating a transient diastereomeric intermediate between chiral analyte and CSP. Obviously, the recognition process involves various forces such as dispersion force, dipole-dipole interaction, hydrogen bonding and other forces [5-6, 20]. Derivatization of free hydroxyls of CD molecule can change the type of interactions associated between the analyte and CSP. Thus, the chiral discriminations will be differed in each enantiomeric pair. Moreover, previous research had been demonstrated that enantioseparation by GC using CD derivatives as chiral selectors was influenced by

the CD ring size, the concentration of CDs in polysiloxane, polarity of polymer matrix, separation temperature and structure of chiral analytes [12-14, 17, 22-26].

Previous studies concerning the enantiomeric separation with gas chromatography using cyclodextrin derivatives as chiral stationary phases are summarized as follow.

Nie *et al.* [22] separated enantiomers of amines, alcohols, diols carboxylic acids, amine acids, epoxides, halohydrocarbons and ketones with three derivatized- $\beta$ -CDs as CSPs: heptakis-(2,6-di-*O*-nonyl-3-*O*-trifluoroacetyl)- $\beta$ -CD (DNTBCD); heptakis-(2,6-di-*O*-dodecyl-3-*O*-trifluoroacetyl)- $\beta$ -CD (DDTBCD) and heptakis-(2,6-di-*O*-pentyl-3-*O*-trifluoroacetyl)- $\beta$ -CD (DPTBCD). The results showed that DNTBCD could separate various types of enantiomers as broad as DPTBCD, but DNTBCD has better enantioselectivity than DPTBCD for analytes studied. In addition, thermodynamic data of racemic  $\alpha$ -phenylethylamine derivatives indicated that enantioseparations on both DNTBCD and DPTBCD was directed by the same mechanism.

Kobor and Schomburg [23] studied the influence of CD ring size on enantiomeric separation of different homologues of 1-phenylethanol using three different types of CD derivatives as CSPs: 6-*t*-butyldimethylsilyl-2,3-dimethyl derivatives of  $\alpha$ ,  $\beta$  and  $\gamma$ -cyclodextrins (TB- $\alpha$ -CD, TB- $\beta$ -CD, TB- $\gamma$ -CD, respectively). The results showed that homologous 1-phenylalkanols with short side chains, e.g. 1-phenylethanol and 1-phenylpropanol, were separated with greater enantioselectivity with TB- $\alpha$ -CD, whereas larger  $\beta$ -CD derivative offered better enantioselectivity for the analytes with longer alkyl chain length such as 1-phenyl-1-butanol and 1-phenyl-1-pentanol. Nonetheless, no enantiomeric separation of any homologous 1-phenylalkanols could be resolved on  $\gamma$ -CD derivative.

Takahisa *et al.* [24] separated enantiomers of various flavor compounds from different chemical classes with octakis-(2,3-di-*O*-methoxymethyl-6-*O*-*tert*-butyldimethylsilyl)- $\gamma$ -CD (2,3-MOM-6-TBDMS- $\gamma$ -CD) as chiral selector. It was found that 2,3-MOM-6-TBDMS- $\gamma$ -CD could resolve a very broad spectrum of

volatiles comprising various functional groups. However, this CSP is not suitable for enantiodifferentiation of tertiary alcohols (e.g. linalool) and their esters, bicyclic compounds (e.g. camphene, camphor) and less volatile esters (e.g. hexyl 2-methylbutanoate, 2-methylbutanoate). Moreover, they used the corresponding  $\beta$ -CD derivative (2,3-MOM-6-TBDMS- $\beta$ -CD) to separate the volatiles from various corresponding chemical classes [25]. Compared to the 2,3-MOM-6-TBDMS- $\gamma$ -CD, it was observed that the range of compounds for which enantiomers could be separated with 2,3-MOM-6-TBDMS- $\beta$ -CD was more limited and the enantioseparation achieved was less pronounced. Furthermore, 2,3-MOM-6-TBDMS- $\beta$ -CD was not suitable for the separation of enantiomers of secondary alcohols.

Skórka *et al.* [13] investigated both the influence of the size of CDs and structure of monoterpenoids on enantiodifferentiation. It was found that enantioseparation of monoterpenoids by  $\alpha$ - and  $\beta$ -CDs resulted from the formation of 1:2 stoichiometric complexes. Furthermore, thermodynamic data; enthalpy, entropy and free energy, displayed higher values for bicyclic than for monocyclic monoterpenoids as well as for  $\alpha$ -CD than for  $\beta$ -CD.

Tisse *et al.* [26] used four derivatized  $\beta$ -CD stationary phases, comprising of 2<sup>I-VII</sup>,3<sup>I-VII</sup>,6<sup>I-VII</sup>-heneicosa-*O*-methyl-cyclodextrin (PM-CD), 2<sup>I</sup>-*O*-methoxycarbonylmethyl-2<sup>II-VII</sup>,3<sup>I-VII</sup>,6<sup>I-VII</sup>-eicosa-*O*-methyl-cyclodextrin (20Me/P2OCH<sub>2</sub>COOMe), 6<sup>I</sup>-*O*-methoxycarbonylmethyl-2<sup>I-VII</sup>,3<sup>I-VII</sup>,6<sup>II-VII</sup>-eicosa-*O*-methyl-cyclodextrin (20Me/P6OCH<sub>2</sub>COOMe) and 6<sup>I</sup>-*O*-methoxycarbonyl-6<sup>I</sup>-deoxy-2<sup>I-VII</sup>,3<sup>I-VII</sup>,6<sup>II-VII</sup>-eicosa-*O*-methylcyclodextrin (20Me/P6COOMe), to separate enantiomers. Secondary alcohols were chosen to examine the influence of the alkyl chain length (C<sub>5</sub>-C<sub>8</sub>) on chiral recognition. The enantiomers of 2-heptanol were unresolved while the enantiomers of 2-pentanol, 2-hexanol and 2-octanol were baseline separated, except on 20Me/P6OCH<sub>2</sub>COOMe, with the same elution order. This indicated that both the presence of an ester group and the position of ester group on CD derivatives did not affect their enantioselectivity. Moreover, they separated a series of *p*-halogenated phenylethanol derivatives. The results showed that the size of the halogen atom bonded to the aromatic ring has a great influence on chiral recognition.

McGachy *et al.* [12] used permethylated  $\beta$ -cyclodextrin (Me-CD) as a chiral selector to investigate the influence of 12 pairs of *N*-trifluoroacetyl-*O*-alkyl nipecotic acid ester enantiomers. The results showed that the *n*-alkyl esters have stronger interaction with Me-CD than ester containing branched alkyl groups. However, esters with  $\alpha$ -branched alkyl groups exhibited higher enantioselectivity than the corresponding *n*-alkyl or  $\beta$ -branched isobutyl esters.

Iamsam-ang [18] separated the enantiomers of 1-phenylethanol derivatives using heptakis(2,3,6-tri-*O*-methyl)- $\beta$ -cyclodextrin and heptakis(2,3-di-*O*-methyl-6-*O*-*tert*-butyldimethylsilyl)- $\beta$ -cyclodextrin as chiral selectors. It was obvious that the enantioselectivities of alcohol derivatives on both CSPs were highly affected by the position of substituent on the aromatic ring rather than the type of substituent. Further studies were performed by Konghuirob using octakis(2,3-di-*O*-methyl-6-*O*-*tert*-butyldimethylsilyl)- $\gamma$ -cyclodextrin (GSiMe) as chiral selector [17]. The results agreed with those studied by Iamsam-ang but the enantiodifferentiation of alcohol derivatives on GSiMe were small.

## 2.4 Molecular modeling studies for enantioseparation

As previously mentioned, the chiral discriminations were influenced by various factors. However, the interactions between analytes and the cyclodextrin derivatives that lead to enantiomer separations are not yet understood in sufficient detail. Therefore, the molecular modeling calculations are performed to better understand the mechanism of chiral discrimination. Preceding researches concerning the molecular modeling by cyclodextrin derivatives as chiral selector are summarized as follow.

Kobor *et al.* [27] used the combination of molecular dynamic calculations, Monte-Carlo type docking and energy minimization to investigate the mechanism of chiral recognition of non-polar (limonene) and polar (1-phenylethanol) chiral compounds using permethyl- $\beta$ -cyclodextrin (PMCD) and (2,3-dimethyl-*tert*-butyldimethylsilyl)- $\beta$ -cyclodextrin (TBCD) as chiral selectors. It could be seen that a more rigid CD cavity like TBCD showed higher enantioselectivity for non-polar

analytes than CD with a more flexible structure like PMCD. Since the interaction between non-polar analyte and chiral stationary phases were the van der Waals forces; therefore, the size and shape of the cavity had an influence to enantiomeric separations.

Ramos *et al.* [28] separated 2-alkyl-2-keto- $\gamma$ -butyrolactone derivatives and their alcohol analogs using (2,3-di-*O*-methyl-6-*O*-*tert*-butyldimethylsilyl)- $\beta$ -cyclodextrin (DIMETBCD) as chiral selector. By molecular modeling calculations, the chiral recognition for DIMETBCD depended more on the geometry than on the polarity of the alkyl substituent on the butyrolactones. Furthermore, hydrogen bonds and alkyl group steric effect could affect the chiral recognition.

Cervelló *et al.* [29] studied the inclusion complexes of a series of *m*- and *p*-nitrophenyl alkanoates using molecular mechanics and molecular dynamics computations. Inclusion complexes were existing for the *m*-series while external complexation was important in the *p*-series.

Lipkowitz *et al.* [30] used the stochastic molecular dynamics simulations to study the mechanism of enantioselective of moderately polar chiral analytes with permethylated  $\beta$ -cyclodextrin. It was found that the major binding domain was the interior of the macrocycle rather than the exterior and most analytes had a preference to associate to the primary rim rather than to the secondary rim. Furthermore, van der Waals forces were dominating forces for enantiodifferentiation.

Beier and Hóltje [31] investigated the enantioselective binding properties of chiral dihydrofuranones on heptakis(2,3-di-*O*-methyl-6-*O*-*tert*-butyldimethylsilyl)- $\beta$ -cyclodextrin using annealed molecular dynamics and program GRID. The inclusion mechanism between the dihydrofuranones and the cyclodextrin host was important for chiral recognition. The intermediate diastereomeric complex could be stabilized by hydrogen bonds leading to strong enantioselective interaction. Moreover, the flexibility of modified  $\beta$ -cyclodextrin also played an important role in the enantioselective binding process.



Kim *et al.* [1] analyzed the enantioselectivity of propranolol on  $\beta$ -cyclodextrin ( $\beta$ -CD) by Monte Carlo (MC) docking and molecular dynamics (MD) simulations. The calculated complexation energy of (*R*)-propranolol- $\beta$ -CD complex was lower than that of (*S*)-propranolol- $\beta$ -CD complex. These calculations corresponded with experimental data. Moreover, it was found that the naphthyl moiety of (*R*)-propranolol was oriented toward the primary rim of  $\beta$ -CD, whereas naphthyl moiety of (*S*)-propranolol was oriented toward the secondary rim of  $\beta$ -CD.

Jesus *et al.* [32] studied the inclusion complexes between praziquantel (PZQ) and  $\beta$ -cyclodextrin ( $\beta$ -CD) through molecular mechanic (MM) calculations. The molecular modeling data suggested that the PZQ/ $\beta$ -CD inclusion complex had a 1:1 stoichiometry and that the isoquinoline ring system of PZQ was embedded in the large face of the  $\beta$ -CD cavity.

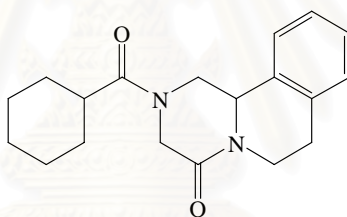


**Figure 2.2** Structure of praziquantel

## 2.5 Thermodynamic investigation of enantiomeric separation by gas chromatography

Although the understanding of mechanism of chiral recognition in chromatographic method has been still abstruse, some mechanistic aspects can be derived from thermodynamic investigation of reliable experimental parameters. Generally, it is accepted that the direct enantiomeric separation is based on the formation of transient diastereomeric complexes which are formed by intermolecular interactions of enantiomers with a chiral selector. Consequently, temperature is the importance factor influencing the retention factor, enantioselectivity and resolution.

The chemical association equilibrium between individual enantiomer and chiral stationary phase can be described by thermodynamic data using the Gibbs-Helmholtz equation [8, 11].

Due to its simplicity and short analysis time, the van't Hoff approach is used as the first method to determine thermodynamic parameters from retention factor ( $k'$ ) and separation factor ( $\alpha$ ) obtained at different temperatures on a single chiral column.

In van't Hoff approach, the difference in Gibb's free energy,  $\Delta(\Delta G)$ , is calculated from the separation factor ( $\alpha$ ) derived from chiral separation on a chiral column at a given temperature according to equation (1):

$$-\Delta(\Delta G) = RT \cdot \ln \alpha = RT \cdot \ln\left(\frac{k'_2}{k'_1}\right) \quad (1)$$

where  $\alpha$  is the separation factor or selectivity calculated from the ratio of  $k'$  of two enantiomers

$k'$  is the retention factor or capacity factor of each enantiomer calculated from solute retention time according to

$$k' = \frac{t_R - t_M}{t_M}$$

$t_R$  is the retention time of an enantiomer or analyte

$t_M$  is the time for mobile phase or an unretained compound to travel at the same distance as analyte

$R$  is the universal gas constant (1.987 cal/mol · K)

$T$  is the absolute temperature (K)

1,2 arbitrarily to the less and the more retained enantiomers, respectively

From the Gibbs-Helmholtz equation (2) and equation (1), given equation (3):

$$-\Delta(\Delta G) = -\Delta(\Delta H) + T \cdot \Delta(\Delta S) \quad (2)$$

$$RT \cdot \ln \alpha = -\Delta(\Delta H) + T \cdot \Delta(\Delta S) \quad (3)$$

Then, equation (3) can be rewritten as show below:

$$\ln \alpha = \frac{-\Delta(\Delta H)}{RT} + \frac{\Delta(\Delta S)}{R} \quad (4)$$

where  $\Delta(\Delta H)$  is the difference in enthalpy values for an enantiomeric pair

$\Delta(\Delta S)$  is the difference in entropy values for an enantiomeric pair

According to equation (4),  $\Delta(\Delta H)$  and  $\Delta(\Delta S)$  could be evaluated from the slope and y-intercept of the  $\ln \alpha$  vs.  $1/T$  plot. However, the calculations of thermodynamic parameters from these plots are not always possible because of the nonlinear behavior of chiral selector concentration in diluted stationary phase. Therefore, this method is only valid for undiluted chiral selectors.

Alternatively, thermodynamic parameters could be calculated from retention factor. The linear relationship between  $\ln k'$  and  $1/T$  could be derived from the combination of equations (5) and (6) resulted in equation (7). Thermodynamic parameters of individual enantiomers including the differences in enthalpy and entropy of an enantiomer pair can be obtained from plots of  $\ln k'$  against  $1/T$ .

$$-\Delta G = RT \cdot \ln K = RT \cdot \ln (k' \cdot \beta) \quad (5)$$

$$\Delta G = \Delta H - T \cdot \Delta S \quad (6)$$

$$RT \cdot \ln(k' \cdot \beta) = -\Delta H + T \cdot \Delta S$$

$$\ln k' = \frac{-\Delta H}{RT} + \frac{\Delta S}{R} - \ln \beta \quad (7)$$

where  $K$  is the distribution coefficient of chiral analyte between the gas and the liquid phases

$\beta$  is a constant called phase ratio (the ratio of mobile phase volume to stationary phase volume)

$\Delta H$  is enthalpy change resulting from the interaction of the enantiomer with the stationary phase.  $\Delta H$  value describes the degree of the interaction strength. The large negative  $\Delta H$  value indicates high strength of interaction between analyte and stationary phase.

$\Delta S$  is entropy change resulting from the interaction of the enantiomer with the stationary phase.  $\Delta S$  value describes the degree of which the solute structure influences the interaction.

## 2.6 Study interaction between CD and alcohol derivatives by molecular modeling

To the understanding of structural features of the chiral recognition mechanism, several molecular modeling methods are used such as molecular docking method and molecular dynamic simulation method. The molecular docking method has been widely used for some years. Its ultimate goal is to obtain the precise docking structure, which corresponds to the energetically most stable configuration. Furthermore, it provides simplicity and short calculation time.

In this work, the molecular docking and quantum mechanical calculations were applied to elucidate the complex structures between CD and alcohol derivatives (which will be now referring to as “host” and “guest”, respectively) and their corresponding energies. Some background of docking and quantum mechanical calculation will be discussed.

### 2.6.1 Molecular Docking

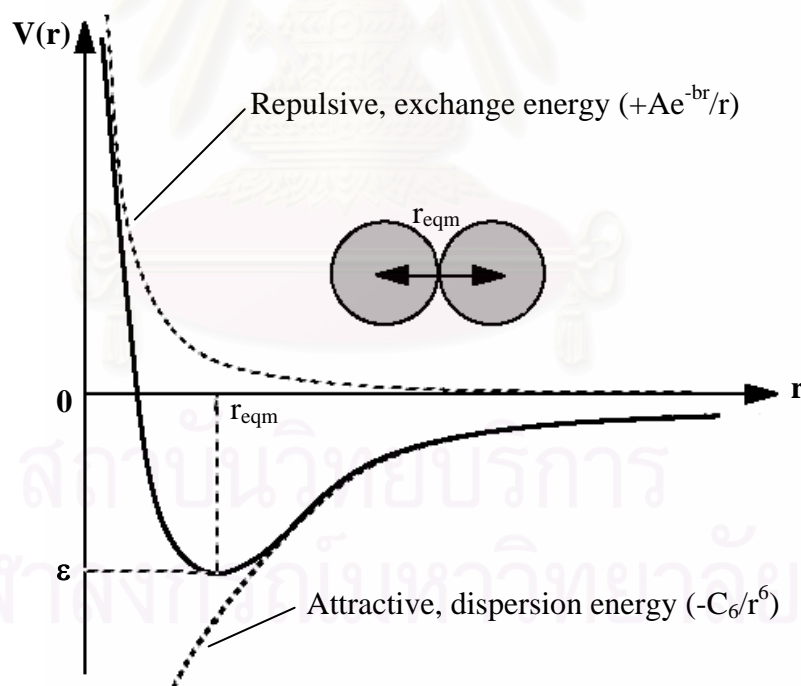
The binding energy in AutoDock3.0.5 program can be calculated by van der Waals potential and electrostatic potential terms [33-36].

#### *Van der Waals potential energy*

The pairwise potential energy,  $V(r)$ , between two non-bonded atoms can be expressed as a function of internuclear separation,  $r$ , as follows,

$$V(r) = \frac{Ae^{-br}}{r} - \frac{C_6}{r^6} \quad (8)$$

Graphically, if  $r_{\text{eqm}}$  is the equilibrium internuclear separation and  $\epsilon$  is the well depth at  $r_{\text{eqm}}$  then:



The exponential, repulsive, exchange energy is often approximated thus,

$$\frac{A}{r} e^{-br} \approx \frac{C_{12}}{r^{12}} \quad (9)$$

Hence pairwise-atomic interaction energies can be approximated using the following general equation,

$$V(r) = \frac{C_n}{r^n} - \frac{C_m}{r^m} = C_n r^{-n} - C_m r^{-m} \quad (10)$$

where  $m$  and  $n$  are integers.

$C_n$  and  $C_m$  are constants whose values depend on the depth of the energy well and equilibrium separation of the two atoms nuclei.

Typically the 12-6 Lennard-Jones parameters ( $n=12$ ,  $m=6$ ) are used to model the van der Waals forces experienced between two instantaneous dipoles. However, the 12-10 form of this expression ( $n = 12$ ,  $m = 10$ ) can be used to model hydrogen bonds.

A revised set of parameters has been calculated, which uses the same van der Waals radius of a given atom for all pairwise distances, no matter what the other atom. Likewise, the well-depths are consistently related. Let  $r_{eqm,xx}$  be the equilibrium separation between the nuclei of two like atoms, X, and let  $\epsilon_{xx}$  be their pairwise potential energy or well depth. The combining rules for the van der Waals radius,  $r_{eqm}$ , and the well depth,  $\epsilon$ , for two different atoms X and Y, are:

$$r_{eqm,XY} = \frac{1}{2}(r_{eqm,XX} + r_{eqm,YY}) \quad (11)$$

$$\epsilon_{XY} = \sqrt{\epsilon_{XX} \epsilon_{YY}} \quad (12)$$

A derivation for the Lennard-Jones potential sometimes seen in text books invokes the parameter,  $\sigma$ , thus,

$$r_{eqm,XY} = 2^{\frac{1}{6}} \sigma \quad (13)$$

Then, the Lennard-Jones 12-6 potential becomes:

$$V_{12-6}(r) = 4\varepsilon_{XY} \left[ \left( \frac{\sigma}{r} \right)^{12} - \left( \frac{\sigma}{r} \right)^6 \right] \quad (14)$$

Thus, the coefficient  $C_{12}$  and  $C_6$  are given by:

$$C_{12} = \varepsilon_{XY} r_{eqm,XY}^{12} \quad (15)$$

$$C_6 = 2\varepsilon_{XY} r_{eqm,XY}^6 \quad (16)$$

General relationship between the coefficients, equilibrium separation and well depth are derived as follows. At the equilibrium separation,  $r_{eqm}$ , the potential energy is a minimum and equal to the well depth. The derivative of the potential with respect to separation will be zero at the minimum potential:

$$\frac{dV}{dr} = \frac{nC_n}{r^{n+1}} + \frac{mC_m}{r^{m+1}} = 0 \quad (17)$$

Therefore:

$$\frac{nC_n}{r^{n+1}} = \frac{mC_m}{r^{m+1}} \quad (18)$$

So:

$$C_m = \frac{nC_n r^{m+1}}{m r^{n+1}} = \frac{n}{m} C_n r^{(m-n)} \quad (19)$$

Substituting  $C_m$  (equation (19)) into the original equation for  $V(r)$ , then at equilibrium distance we obtain,

$$V(r) = -\varepsilon = \frac{C_n}{r_{eqm}^n} - \frac{nC_n r_{eqm}^{(m-n)}}{m r_{eqm}^m}$$

Rearranging:

$$C_n \left( \frac{m-n}{m r_{eqm}^n} \right) = -\varepsilon \quad (20)$$

Therefore, the coefficient  $C_n$  can be expressed in terms of  $n$ ,  $m$ ,  $\varepsilon$  and  $r_{eqm}$  thus:

$$C_n = \frac{m}{n-m} \varepsilon r_{eqm}^n \quad (21)$$

And, substituting into equation (19),

$$C_m = \frac{n}{n-m} \varepsilon r_{eqm}^m \quad (22)$$

In summary, the general equation for any  $n$ ,  $m$  will be:

$$V(r) = \frac{\varepsilon}{n-m} \left[ m \left( \frac{r_{eqm}}{r} \right)^n - n \left( \frac{r_{eqm}}{r} \right)^m \right] \quad (23)$$

### ***Electrostatic potential grid maps***

In addition to the atomic affinity (van der Waals potential) grid maps, AutoDock requires an electrostatic potential grid maps. Polar hydrogens must be added, if hydrogen-bonds are being modeled explicitly. Partial atomic charges must be assigned to the macromolecule. The electrostatic grid can be generated by



**AutoGrid**, or by other programs such as MEAD14 or DELPHI15, which solve the linearized Poisson-Boltzmann equation. AutoGrid calculates Coulombic interactions between the macromolecule and a probe of charge  $e$ ,  $+1.60219 \times 10^{-19}$  C; there is no distance cutoff used for electrostatic interactions. A sigmoidal distance-dependent dielectric function is used to model solvent screening, based on the work of Mehler and Solmajer,

$$\varepsilon(r) = A + \frac{B}{1 + ke^{-\lambda Br}} \quad (24)$$

where  $B = \varepsilon_r - A$

$\varepsilon_r$  = the relative dielectric constant of bulk water at 25 °C = 78.4

$A = -85525$

$\lambda = 0.003627$

$k = 7.7839$

$r$  = distance

Therefore, Coulombic interaction is derived according to equation (25)

$$V_{ij}(r) = -\frac{q_i q_j}{4\pi\varepsilon_0 \varepsilon_r r_{ij}} \quad (25)$$

where  $\varepsilon_0$  = permittivity in vacuum =  $8.858 \times 10^{-12} \text{ C}^2 \cdot \text{J}^{-1} \cdot \text{m}^{-1}$

### 2.6.2 Quantum mechanics for molecular system

Quantum mechanics are applied using the Schrödinger equation and the function of the coordinates called the wave function ( $\psi$ ) [37-38]. For molecular system, Schrödinger equation is obtained according to equation (26)

$$\hat{H}_{tot}\psi_{tot}(x_1, \dots, x_N; \vec{R}_1, \dots, \vec{R}_M) = E_{tot}\psi_{tot}(x_1, \dots, x_N; \vec{R}_1, \dots, \vec{R}_M) \quad (26)$$

where  $\psi_{tot}$  is the total wave function.

$E_{tot}$  is the total energy or the energy eigenvalue.

$x_i$  is the spin coordinate which depends on the position and spin composition of electron at  $i$  ( $i = 1, \dots, N$ )

$\vec{R}_A$  is the position of nuclei  $A$  ( $A = 1, \dots, M$ )

$\hat{H}_{tot}$  is the summation of operator according to

$$\hat{H}_{tot} = \hat{T}_e + \hat{T}_n + \hat{V}_{ee} + \hat{V}_{en} + \hat{V}_{nn} \quad (27)$$

where  $\hat{T}_e$  is the kinetic energy operator of electrons

$\hat{T}_n$  is the kinetic energy operator of nuclei

$\hat{V}_{ee}$  is the electron-electron repulsion operator

$\hat{V}_{en}$  is the electron-nuclear attraction operator

$\hat{V}_{nn}$  is the nuclear-nuclear repulsion operator

Since the Schrödinger equation cannot be solved exactly for any molecular systems; thus, the approximation methods, such as variational theory, are applied. Hartree-Fock method is the variation-based approximation and in this research the Hartree-Fock method was used to calculate the energy of the molecule.

### ***Hartree-Fock method***

The energy of system are minimized by adjust the molecular orbitals (MO). Subsequently, the Hartree-Fock equation is obtained according to

$$f|x_i\rangle = \varepsilon_i|x_i\rangle \quad (28)$$

where  $f$  is the Fock operator  
 $\varepsilon_i$  is the molecular orbital energy

The Hartree-Fock equation could be solved by introduction of functions (equation (29))

$$x_i = \sum_{\mu}^K c_{\mu i} \phi_{\mu} \quad (29)$$

Substituting equation (29) into equation (28), the Roothaan-Hall equation is given as:

$$\sum_{\nu=1}^K (F_{\mu\nu} - \varepsilon_i S_{\mu\nu}) c_{\nu i} \quad (30)$$

The Roothaan-Hall equation can be conveniently written as a matrix equation:

$$F c = S c \varepsilon \quad (31)$$

where  $S_{\mu\nu}$  is the elements of the overlap matrix =  $\int \phi_{\mu}^*(1) \phi_{\nu}(1) d\bar{r}_1$   
 $F_{\mu\nu}$  is the elements of the Fock matrix which calculate from equation (32)

$$F_{\mu\nu} = H_{\mu\nu}^{core} + \sum_{\lambda=1}^N \sum_{\sigma=1}^N P_{\lambda\sigma} \left[ (\mu\nu|\lambda\sigma) - \frac{1}{2}(\mu\nu|\lambda\sigma) \right] \quad (32)$$

where  $H_{\mu\nu}^{core}$  is the combined kinetic and electron-nuclear attraction intervals or the “core” Hamiltonian

$$H_{\mu\nu}^{core} = \int \phi_{\mu}^*(1) \left( -\frac{1}{2} \nabla_1^2 - \sum_{A=1}^M \frac{Z_A}{r_{1A}} \right) \phi_{\nu}(1) d\vec{r}_1 \quad (33)$$

$(\mu\nu|\lambda\sigma)$  is the two-electron integrals

$$(\mu\nu|\lambda\sigma) = \iint \phi_{\mu}^*(1) \phi_{\nu}(1) \left( \frac{1}{r_{12}} \right) \phi_{\lambda}^*(2) \phi_{\sigma}(2) d\vec{r}_1 d\vec{r}_2 \quad (34)$$

$P_{\lambda\sigma}$  is the density matrix

$$P_{\lambda\sigma} = 2 \sum_{i=1}^{occ} c_{\lambda i}^* c_{\sigma i} \quad (35)$$

The total energy is calculated from the summation of the electronic energy (equation (36)) and the electrostatic repulsion between the positively charged nuclei (equation (37)).

$$E^{ee} = \frac{1}{2} \sum_{\mu=1}^N \sum_{\nu=1}^N P_{\mu\nu} (F_{\mu\nu} + H_{\mu\nu}^{core}) \quad (36)$$

$$E^{nr} = \sum_{A<B}^M \frac{Z_A Z_B}{R_{AB}} \quad (37)$$

The Roothaan-Hall equation is not the linear relationship because of the Fock matrix depend on the molecular orbital coefficients. Thus, the Roothaan-Hall equation must be solved by an iterative procedure, called Self-Consistent-Field (SCF) method.

For molecular system, the basis sets are suitable choiced to the quantum mechanical calculation. The basis sets most commonly used in quantum mechanical calculation are composed of atomic orbital functions. The basis set can are devised according to:

1. Minimal basis set contains the number of functions that are equaled to the filled orbitals in each atom, such as STO-3G.
2. Extended basis set contains the number of functions which are greater than the number of atomic orbital; such as 3-21G, 6-31G.
3. Polarization basis set adds functions with angular momentum quantum number higher than the last occupied orbitals. This functions is indicated by an asterisk (\*) such as 3-21G\* or 3-21G (d), 6-31G\* or 6-31G (d).



สถาบันวิทยบริการ  
จุฬาลงกรณ์มหาวิทยาลัย

## CHAPTER III

### EXPERIMENTAL

#### 3.1 Preparation of alcohol derivatives

All chemicals and solvents were purchased from Fluka, Aldrich, and J.T. Baker and were used as received. Most of alcohol racemates used in this study were obtained from previous syntheses by Konghurob [17] and Iamsam-ang [18]. Some alcohols were achieved commercially. Additionally, some chiral alcohols were synthesized from reduction of their corresponding ketones with sodium borohydride in ethanol. The progress of the synthesis was followed by thin layer chromatography (TLC) on TLC aluminum sheets, silica gel F<sub>254</sub> (Merck) and visualized under ultraviolet light at 254 nm. The structure of alcohol products were confirmed by <sup>1</sup>H-NMR spectroscopy (Varian Mercury Plus 400 at 400 MHz) using deuterated chloroform (CDCl<sub>3</sub>, 99.8% D, Aldrich) as solvent. Chiral alcohols and ketones used in this work are:

chiral alcohols:

- 2-butanol, 99.5% (Fluka)
- 2-pentanol, 98% (Fluka)
- 2-hexanol, 98% (Fluka)
- 3-hexanol, 98% (Fluka)
- 2-heptanol, 99% (Fluka)
- 3-heptanol, 98% (Fluka)
- 2-octanol, 96% (Fluka)
- 3-octanol, 95% (Fluka)
- 4-octanol, 98% (Fluka)
- 2-nonanol, 99% (Aldrich)
- 3-nonanol, 95% (Fluka)
- 2-undecanol, 98% (Fluka)

ketones:

- 4-bromobenzophenone, 98% (Aldrich)
- 2-chlorobenzophenone, 99% (Aldrich)
- 3-chlorobenzophenone, 97% (Aldrich)
- 4-chlorobenzophenone, 99% (Aldrich)
- cyclohexyl phenyl ketone, 98% (Aldrich)
- 4-fluorobenzophenone, 97% (Aldrich)
- 4-methoxybenzophenone, 97% (Aldrich)
- 2-methylbenzophenone, 98% (Aldrich)
- 3-methylbenzophenone, 99% (Aldrich)
- 4-methylbenzophenone, 99% (Aldrich)
- 4-acetylbiphenyl, 99% (Aldrich)

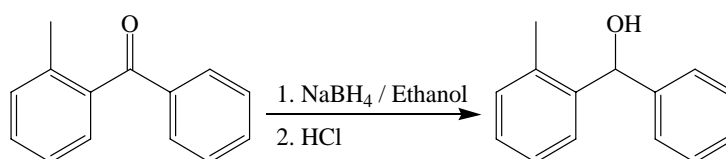
solvents:

- acetone (J.T. Baker)
- dichloromethane (J.T. Baker)
- hexane (J.T. Baker)
- pentane (J.T. Baker)
- ethanol (Merck)

other chemicals:

- anhydrous sodium sulfate (Fluka)
- hydrochloric acid (J.T. Baker)
- sodium borohydride (Aldrich)

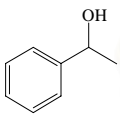
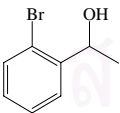
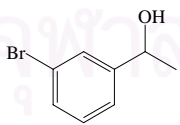
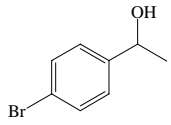
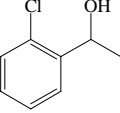
The general procedure for the synthesis of phenyl-*o*-tolyl-methanol is explained as follow:



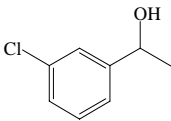
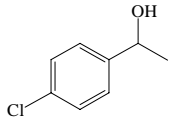
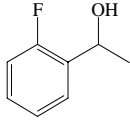
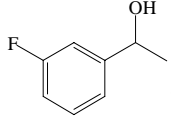
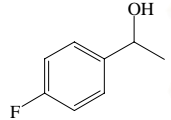
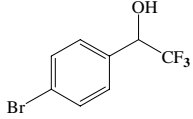
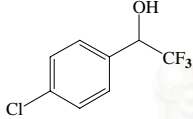
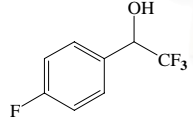
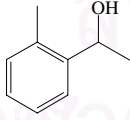
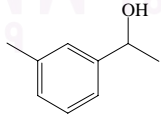
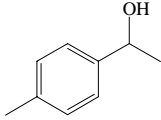
Phenyl-*o*-tolyl-methanol (2MeBen): 2-methylbenzophenone (0.507 g, 2.5 mmol) and sodium borohydride (NaBH<sub>4</sub>, 0.116 g, 3.0 mmol) were dissolved in 5 mL absolute ethanol. The mixture was refluxed for 3 hours before cooling down. The solvent was then removed by rotary evaporator to obtain white precipitate. The precipitate was redissolved in 2 M hydrochloric acid. The aqueous phase was then extracted with dichloromethane. All organic layers were combined, dried with anhydrous sodium sulfate, and evaporated to attain white solid of phenyl-*o*-tolyl-methanol with 72.3 % yield; R<sub>f</sub> = 0.68 (hexane-CH<sub>2</sub>Cl<sub>2</sub> 1:2); <sup>1</sup>H NMR (CDCl<sub>3</sub>, 400 MHz): δ 1.70 (1H, s, CHOH), 2.19 (3H, s, ArCH<sub>3</sub>), 5.93 (1H, s, CHOH), 7.05-7.24 (4H, m, ArMeH), 7.26 (4H, d, ArH), 7.45 (1H, d, ArH).

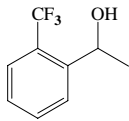
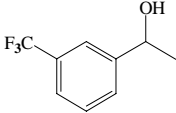
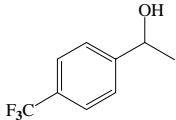
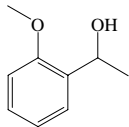
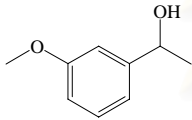
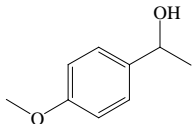
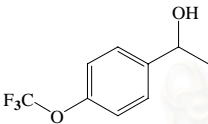
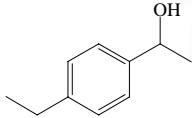
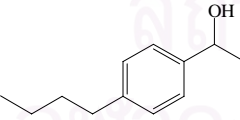
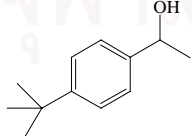
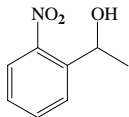
Other alcohols were prepared using the above-mentioned method. The structure, abbreviations and compound names of all alcohols used in this study are shown in table 3.1.

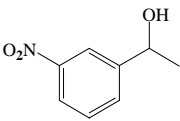
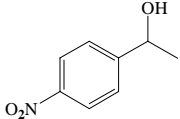
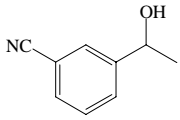
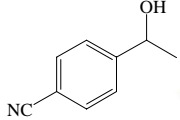
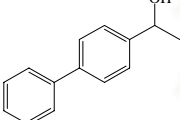
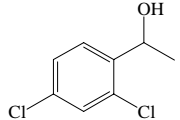
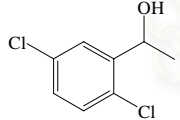
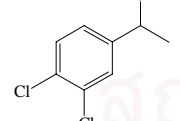
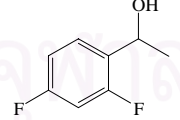
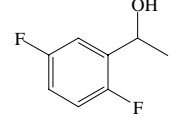
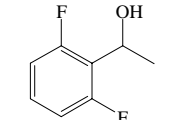
**Table 3.1** Structure and abbreviation of all alcohol derivatives used in this study

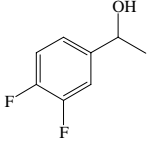
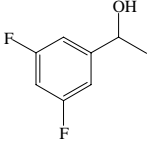
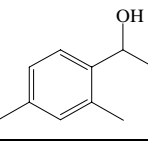
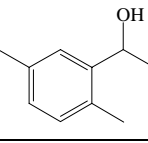
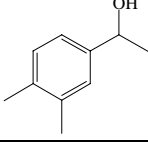
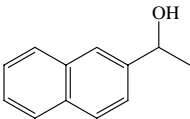
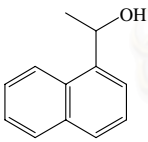
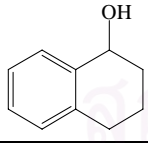
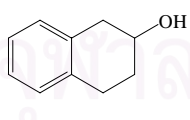
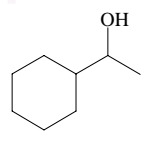
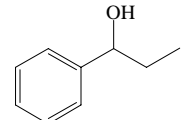
structure	abbreviation	compound
	<b>1</b>	1-phenylethanol (reference compound)
1-Phenylethanols with mono-substitution on aromatic ring		
	<b>2Br</b>	1-(2-bromophenyl)ethanol
	<b>3Br</b>	1-(3-bromophenyl)ethanol
	<b>4Br</b>	1-(4-bromophenyl)ethanol
	<b>2Cl</b>	1-(2-chlorophenyl)ethanol

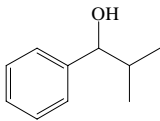
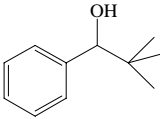
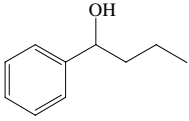
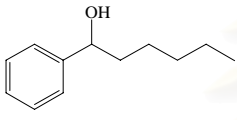
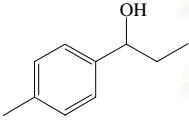
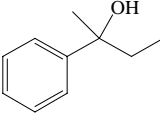
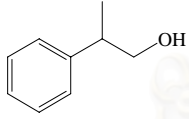
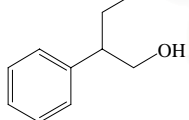
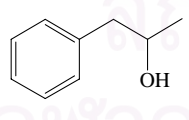
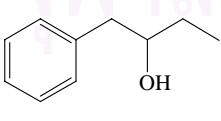
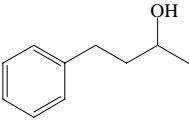


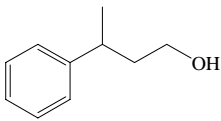
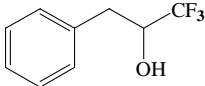
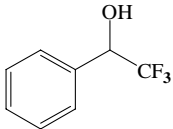
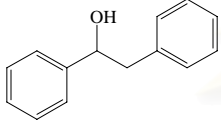
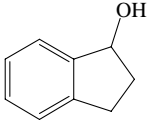
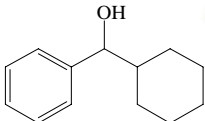
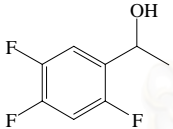
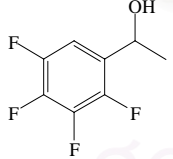
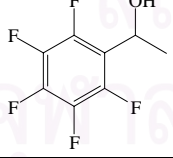
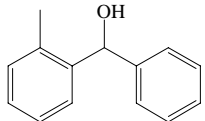
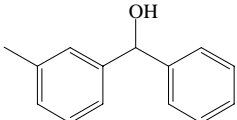
structure	abbreviation	compound
	<b>3Cl</b>	1-(3-chlorophenyl)ethanol
	<b>4Cl</b>	1-(4-chlorophenyl)ethanol
	<b>2F</b>	1-(2-fluorophenyl)ethanol
	<b>3F</b>	1-(3-fluorophenyl)ethanol
	<b>4F</b>	1-(4-fluorophenyl)ethanol
	<b>F4Br</b>	2,2,2-trifluoro-1-(4-bromophenyl)ethanol
	<b>F4Cl</b>	2,2,2-trifluoro-1-(4-chlorophenyl)ethanol
	<b>F4F</b>	2,2,2-trifluoro-1-(4-fluorophenyl)ethanol
	<b>2Me</b>	1-(2-methylphenyl)ethanol
	<b>3Me</b>	1-(3-methylphenyl)ethanol
	<b>4Me</b>	1-(4-methylphenyl)ethanol

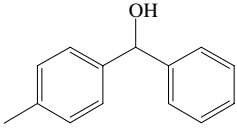
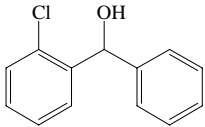
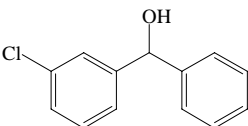
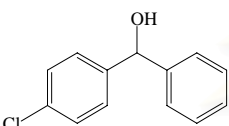
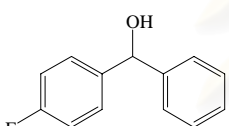
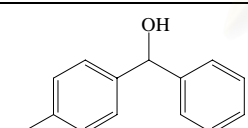
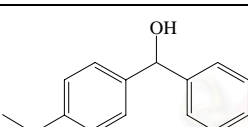
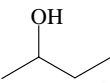
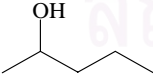
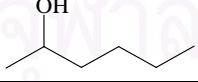
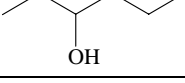
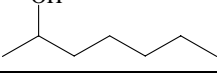
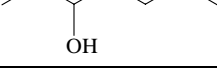
structure	abbreviation	compound
	<b>2CF3</b>	1-(2-trifluoromethylphenyl)ethanol
	<b>3CF3</b>	1-(3-trifluoromethylphenyl)ethanol
	<b>4CF3</b>	1-(4-trifluoromethylphenyl)ethanol
	<b>2OMe</b>	1-(2-methoxyphenyl)ethanol
	<b>3OMe</b>	1-(3-methoxyphenyl)ethanol
	<b>4OMe</b>	1-(4-methoxyphenyl)ethanol
	<b>4OCF3</b>	1-(4-trifluoromethoxyphenyl)ethanol
	<b>4Et</b>	1-(4-ethylphenyl)ethanol
	<b>4Bu</b>	1-(4-butylphenyl)ethanol
	<b>4tBu</b>	1-(4- <i>tert</i> -butylphenyl)ethanol
	<b>2NO2</b>	1-(2-nitrophenyl)ethanol

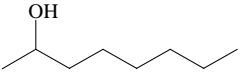
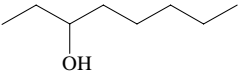
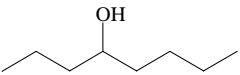
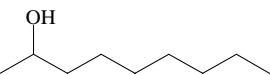
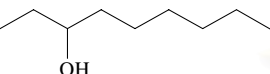
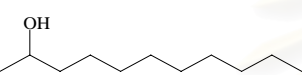
structure	abbreviation	compound
	<b>3NO2</b>	1-(3-nitrophenyl)ethanol
	<b>4NO2</b>	1-(4-nitrophenyl)ethanol
	<b>3CN</b>	1-(3-cyanophenyl)ethanol
	<b>4CN</b>	1-(4-cyanophenyl)ethanol
	<b>4Phe</b>	1-(4-diphenyl)ethanol
<b>1-Phenylethanols with di-substitution on aromatic ring</b>		
	<b>24Cl</b>	1-(2,4-dichlorophenyl)ethanol
	<b>25Cl</b>	1-(2,5-dichlorophenyl)ethanol
	<b>34Cl</b>	1-(3,4-dichlorophenyl)ethanol
	<b>24F</b>	1-(2,4-difluorophenyl)ethanol
	<b>25F</b>	1-(2,5-difluorophenyl)ethanol
	<b>26F</b>	1-(2,6-difluorophenyl)ethanol

structure	abbreviation	compound
	<b>34F</b>	1-(3,4-difluorophenyl)ethanol
	<b>35F</b>	1-(3,5-difluorophenyl)ethanol
	<b>24Me</b>	1-(2,4-dimethylphenyl)ethanol
	<b>25Me</b>	1-(2,5-dimethylphenyl)ethanol
	<b>34Me</b>	1-(3,4-dimethylphenyl)ethanol
<b>Other alcohols</b>		
	<b>2</b>	1-(2-naphthyl)ethanol
	<b>3</b>	1-(1-naphthyl)ethanol
	<b>4</b>	1,2,3,4-tetrahydro-1-naphthol
	<b>5</b>	1,2,3,4-tetrahydro-2-naphthol
	<b>6</b>	1-cyclohexylethanol
	<b>7</b>	1-phenyl-1-propanol

structure	abbreviation	compound
	<b>8</b>	2-methyl-1-phenyl-1-propanol
	<b>9</b>	2,2-dimethyl-1-phenyl-1-propanol
	<b>10</b>	1-phenyl-1-butanol
	<b>11</b>	1-phenyl-1-hexanol
	<b>12</b>	1-(4-methylphenyl)propanol
	<b>13</b>	2-phenyl-2-butanol
	<b>14</b>	2-phenyl-1-propanol
	<b>15</b>	2-phenyl-1-butanol
	<b>16</b>	1-phenyl-2-propanol
	<b>17</b>	1-phenyl-2-butanol
	<b>18</b>	4-phenyl-2-butanol

structure	abbreviation	compound
	<b>19</b>	3-phenyl-1-butanol
	<b>20</b>	1,1,1-trifluoro-3-phenyl-2-propanol
	<b>21</b>	2,2,2-trifluoro-1-phenylethanol
	<b>22</b>	1,2-diphenylethanol
	<b>23</b>	1-indanol
	<b>24</b>	cyclohexyl-phenyl-methanol
	<b>triF</b>	1-(2,4,5-trifluorophenyl)ethanol
	<b>tetraF</b>	1-(2,3,4,5-tetrafluorophenyl)ethanol
	<b>pentaF</b>	1-(pentafluorophenyl)ethanol
<b>Diphenylmethanols with mono-substitution on an aromatic ring</b>		
	<b>2MeBen</b>	phenyl- <i>o</i> -tolyl-methanol
	<b>3MeBen</b>	phenyl- <i>m</i> -tolyl-methanol

structure	abbreviation	compound
	<b>4MeBen</b>	phenyl- <i>p</i> -tolyl-methanol
	<b>2ClMen</b>	(2-chlorophenyl)phenyl-methanol
	<b>3ClMe</b>	(3-chlorophenyl)phenyl-methanol
	<b>4ClBen</b>	(4-chlorophenyl)phenyl-methanol
	<b>4FBen</b>	(4-fluorophenyl)phenyl-methanol
	<b>4BrBen</b>	(4-bromophenyl)phenyl-methanol
	<b>4OMeBen</b>	(4-methoxyphenyl)phenyl-methanol
<i>n</i> -alkyl alcohols		
	<b>2but</b>	2-butanol
	<b>2pen</b>	2-pentanol
	<b>2hex</b>	2-hexanol
	<b>3hex</b>	3-hexanol
	<b>2hep</b>	2-heptanol
	<b>3hep</b>	3-heptanol

structure	abbreviation	compound
	<b>2oc</b>	2-octanol
	<b>3oc</b>	3-octanol
	<b>4oc</b>	4-octanol
	<b>2non</b>	2-nonanol
	<b>3non</b>	3-nonanol
	<b>2unde</b>	2-undecanol

### 3.2 Gas chromatographic analyses

All chromatographic separations were performed on a Hewlett-Packard 5890 system equipped with a split/splitless injector and a flame ionization detector (FID). Temperatures of both injector and detector were set at 250 °C. Hydrogen was used as carrier gas with an average linear velocity of 50 cm/s. Two types of stationary phases were used in this research:

- polysiloxane OV-1701 (7% phenyl, 7% cyanopropyl, 86% dimethyl polysiloxane, Supelco) was used as a reference stationary phase and diluent for solid cyclodextrin derivative in a chiral column
- 26.8% hexakis(2,3-di-*O*-methyl-6-*O*-*tert*-butyldimethylsilyl) cyclomaltohexaose (or ASiMe) in OV-1701

Before injection, alcohol derivative was dissolved in acetone at a concentration ~ 10-20 mg/mL. Approximately 0.2-0.6  $\mu$ L of solution was injected with a split ratio of 150:1. Each solution of analyte was injected at least in duplicate. All temperature studies were performed isothermally between 60 and 240 °C in steps of 10 °C. Retention factors and enantioselectivities of all analytes were calculated



from chromatogram. Finally, thermodynamic parameters were determined by means of van't Hoff approach.

### 3.3 Methods of molecular modeling calculations

#### 3.3.1 Optimization of the ASiMe (host) conformation

The molecular structure of ASiMe was generated from the x-ray crystallographic data of the permethylated  $\alpha$ -CD by the substitution of methyl groups at the primary oxygen in position 6 with *tert*-butyldimethylsilyl groups. Subsequently, the obtained geometry was optimized at the HF/3-21G level.

#### 3.3.2 Optimization of the alcohols (guest) conformations

Some analytes which included *R*- and *S*-forms of **1**, **4MeBen**, **4Me**, **4Et**, **4Bu**, **4tBu**, **2OMe**, **3OMe** and **4OMe** were selected for investigation of the interaction between analytes and CD molecule. The structures of both *R*- and *S*-forms were constructed by GaussView program (version 2.1) and were then optimized at the HF/6-31G\*\* level using Gaussian03. The optimization structures were further used for the molecular docking calculations.

#### 3.3.3 Docking calculations

The docking calculations were performed using the automated docking program, AutoDock 3.0.5 software [33]. The AutoDock employs a Lamarckian genetic algorithm (LGA) in combination with a rapid grid-based energy evaluation method. The rapid energy evaluation is achieved by precalculating atomic affinity potentials for each atom type present in the alcohol molecule. For example, 1-phenylethanol has only three atom types in the molecule (carbon, oxygen and hydrogen); therefore, three atomic affinity potentials, i.e., ASiMe-carbon, ASiMe-oxygen and ASiMe-hydrogen interaction energies, are required. To create these potentials, a grid map of dimension 22.5 x 22.5 x 22.5 Å<sup>3</sup> with a grid spacing of 0.375 Å, is placed covering the ASiMe (figure 3.1).

Considering the C atomic affinity potential, a probe atom, which is the same atom type used to create the atomic affinity potential (in this case is carbon), is placed at the edge of every lattice points. For each lattice point, the interaction energy between the probe atom and CD atoms is calculated using the Lennard-Jones 12-6 potential and is assigned to that lattice point. The O and H atomic affinity potentials are calculated in the same manner as that of the carbon.

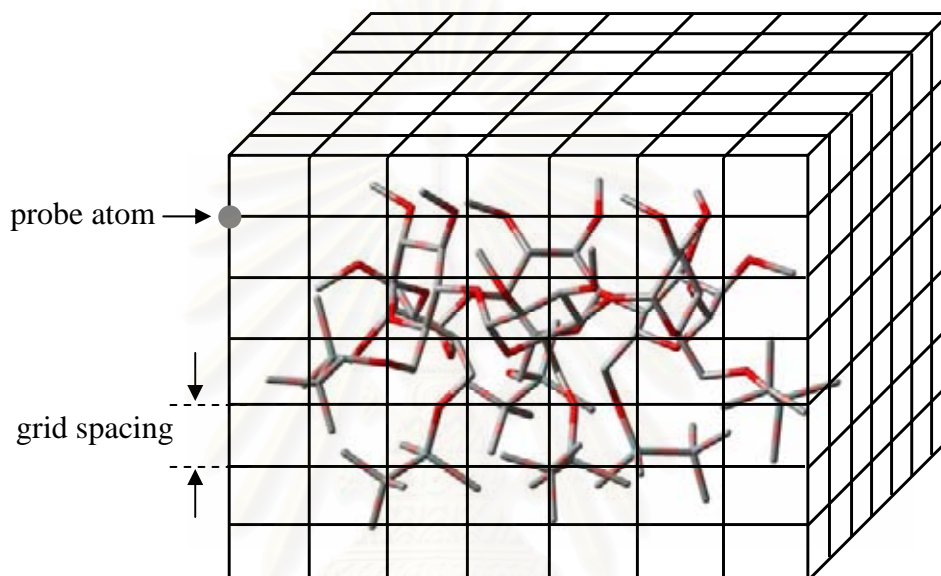


**Figure 3.1** Grid base energy evaluation

In addition to the atomic affinity grid maps, an electrostatic potential grid map of the CD molecule is created. The electrostatic interaction energy between the CD and a guest molecule is calculated using a Coulomb potential.

For the docking calculation, 100 LGA runs with 50 numbers of individuals in population were performed. The run was terminated if either 250000 numbers of energy evaluations or 270000 numbers of generations was reached. The number of the best individuals in the current population that automatically survive into the next generation was set as 1. The rate of gene mutation and the rate of gene crossover were given as 0.02 and 0.80, respectively. The number of generations for picking the worst individual was set at 10. The maximum number of local search iterations was set to 300. The maximum number of consecutive successes or failures

were both typically 4. The size of the local search space to sample was 1.0. The lower bound on rho set the smallest step size that a move can make before terminating the local search, and was 0.01. The probability that an individual in the population will experience local search was set at 0.06.

Since the LGA is based on random movements, the final docked configuration depends on the starting configuration. In order to avoid any bias and to generate as many final docked configurations as possible, the starting configuration was assigned in random manner for each docking calculation. A cluster analysis was used to categorize all 100 docked configurations into groups. Configurations with root-mean-square-deviation (rmsd) values of less than 1 Å were grouped together. In each group, the lowest energy configuration was selected as the representative of that group. The “% frequency” was used to represent the number of members (configurations) in each group. Our attention was focused to the group with the highest % frequency or “the dominating configuration”.

### **3.3.4 Binding energy and entropy calculations**

The docking configurations were re-optimized at MM+ level [39] using HyperChem. Then, the binding energy calculation of optimized complex structures was carried out at the AM1 level [39], using HyperChem program, and at the 3-21G level, using Gaussian03. Entropy change values of reference analyte were also calculated using AM1 method. The entropy change was combined with the binding energy to predict the free energy of binding.

## CHAPTER IV

### RESULTS AND DISCUSSION

#### 4.1 Synthesis of alcohol derivatives

Some alcohol derivatives used in this research were prepared by reduction of their corresponding ketones with sodium borohydride. Most synthesized products were acquired in approximately 60 % yield or higher. The identity of all synthesized products was confirmed by  $^1\text{H-NMR}$ .

#### 4.2 Gas chromatographic separation of alcohol derivatives

All separations on ASiMe column was performed isothermally, at least in duplicate, at 10 °C intervals in the temperature range of 60-240 °C. Considering the chromatographic results at the same operating temperature, the retention factor ( $k'$ ) and separation factors ( $\alpha$ ) of selected alcohol racemates on OV-1701 and ASiMe columns were compared at 160 °C and presented in figures 4.1-4.3.

The retention factor ( $k'$ ) of analytes on each column varied significantly depending on their molecular weight, boiling point, type, number and position of substituents. On both OV-1701 and ASiMe columns, mono-substitution at *para*-position on aromatic ring is likely to increase retention of analytes than *ortho*- or *meta*-position. Additionally, it is apparently noticed that most analytes display higher retention on ASiMe column than on polysiloxane OV-1701 column, even though ASiMe column employed polysiloxane as a major component in the stationary phase with identical film thickness. Therefore, the additional interactions would be derived from the cyclodextrin derivative diluted in the stationary phase.

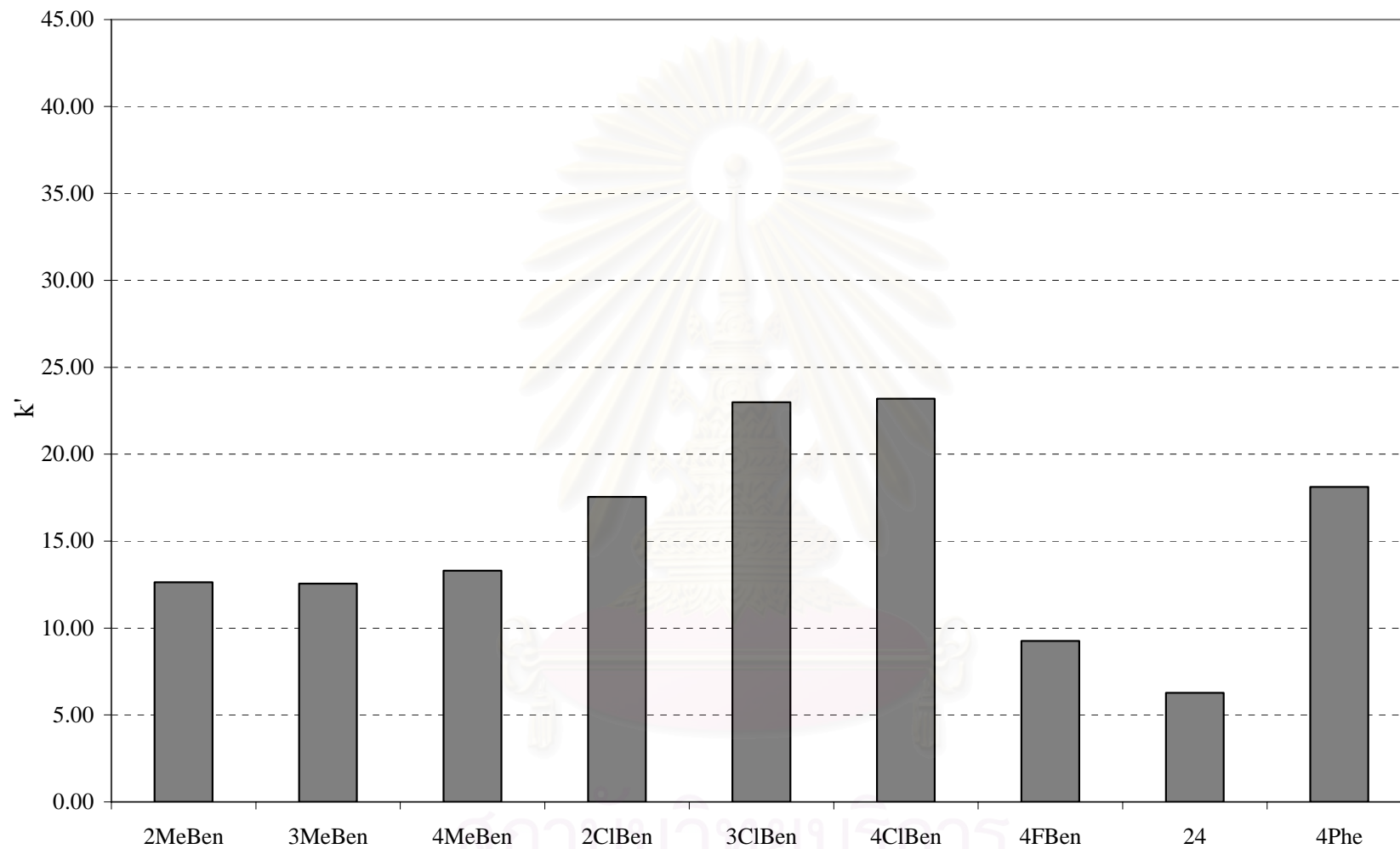


**Figure 4.1** Retention factors ( $k'$ ) of selected alcohols on OV-1701 column at 160 °C.

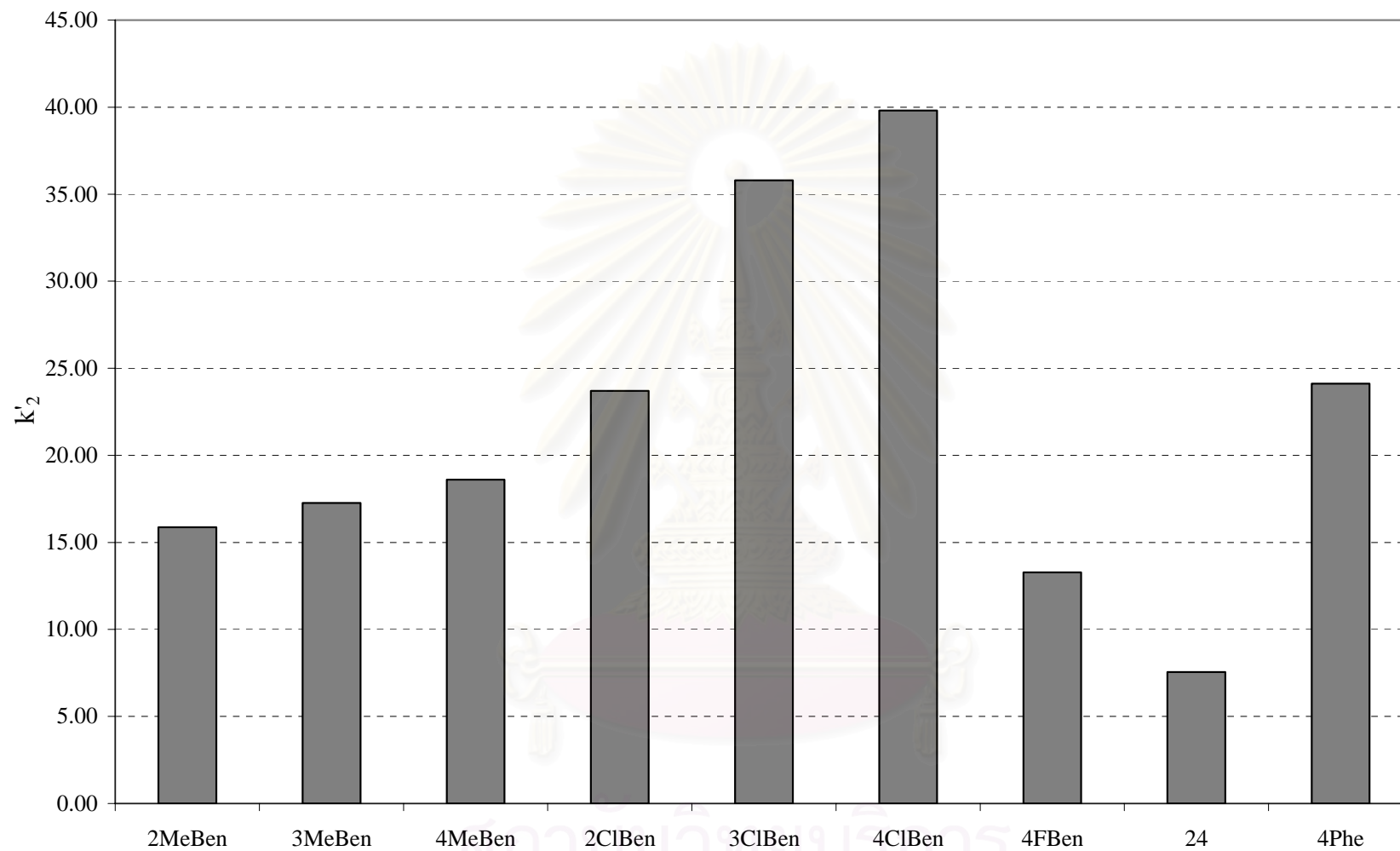


**Figure 4.2** Retention factors ( $k'_2$ ) of the more retained enantiomers of selected alcohols on ASiMe column at 160 °C.

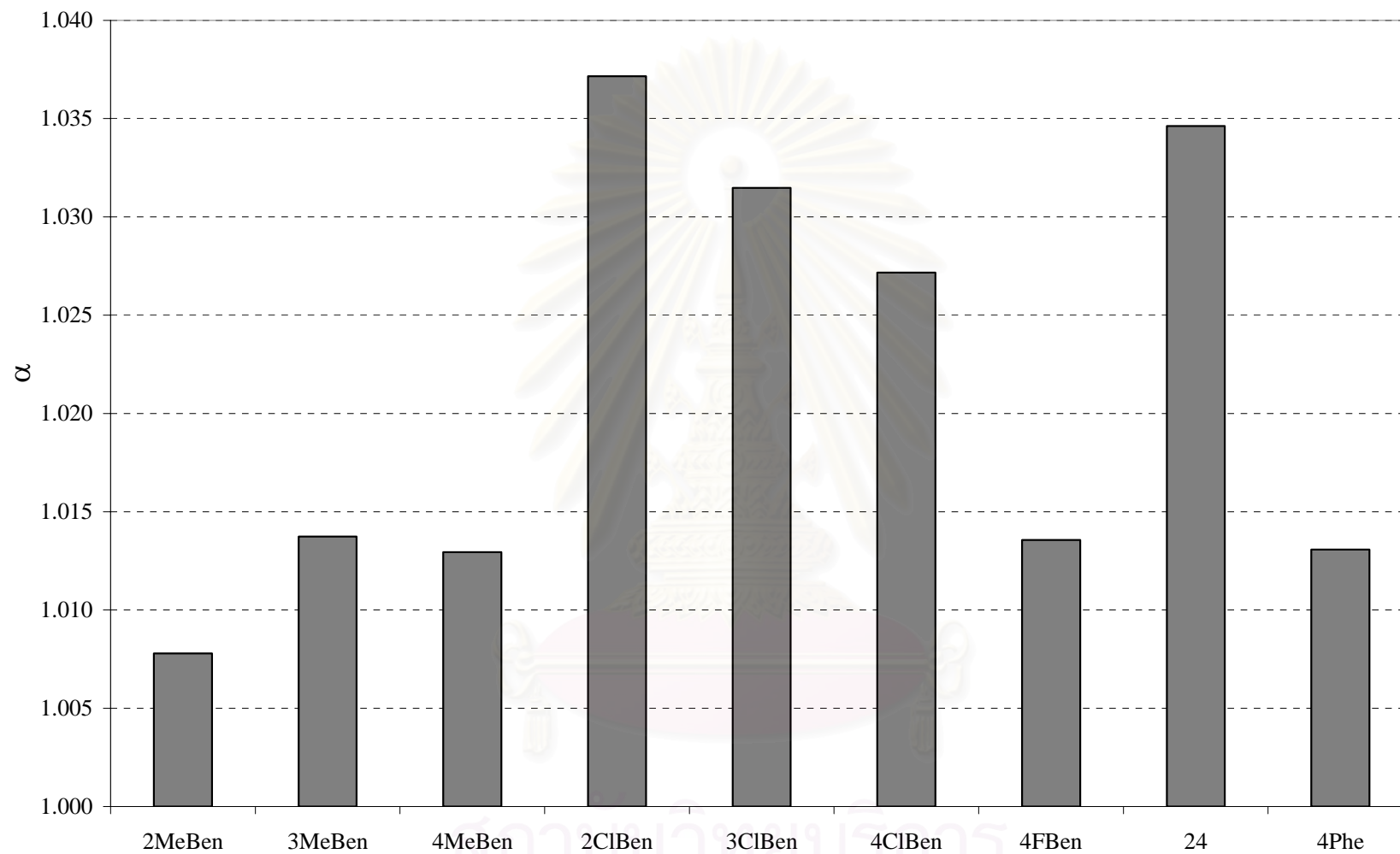


**Figure 4.3** Separation factors ( $\alpha$ ) of the enantiomeric pairs of selected alcohols on ASiMe column at 160 °C.

All racemic alcohols, except for **4OMe**, **12**, **15**, **17**, **4OMeBen** and **2but**, could be resolved into their enantiomers on ASiMe column. The separation factors of selected alcohol analytes on ASiMe at 160 °C are compared in figure 4.3. It seems that the type of substituent have a stronger effect on selectivity than the position. Nonetheless, due to the physical properties of analytes, such as boiling point and vapor pressure, are substantially different, information from retention factors and enantioselectivities at specific temperature could not be directly compared. Therefore, thermodynamic parameters over a temperature range should be determined to provide better understanding of the interactions between analytes and gas chromatographic stationary phases.

### 4.3 Thermodynamic investigation by van't Hoff approach

To examine the influence of analyte structure on the strength of interaction and enantioresolution, thermodynamic parameters affiliated with the interaction between alcohol analytes and stationary phase were achieved through van't Hoff plot of  $\ln k'$  versus  $1/T$ . Almost all  $\ln k'$  versus  $1/T$  plots show linear relationship with correlation coefficient value ( $R^2$ ) greater than 0.998. From these plots, enthalpy ( $\Delta H$ ) and entropy ( $\Delta S$ ) values could be calculated from slope and y-intercept, respectively. When enantiomeric pairs were separated, the enthalpy and entropy differences ( $\Delta(\Delta H)$  and  $\Delta(\Delta S)$ , respectively) could be determined from the relationship between  $\ln \alpha$  and  $1/T$ . Theoretically, the  $\ln \alpha$  and  $1/T$  plot should be linear; however, the curvatures were observed in the temperature range examined for many analytes and caused errors in calculated thermodynamic values. The nonlinearity may be an indicator for a change in the interaction mechanism between analytes and chiral stationary phase as the temperature changed. The determination of  $\Delta(\Delta H)$  and  $\Delta(\Delta S)$  values in this research were; therefore, calculated from the differences in  $\Delta H$  and  $\Delta S$  values of two enantiomers derived from van't Hoff plot.

Additionally, the thermodynamic values of alcohols obtained from ASiMe column in this study were compared to those previously achieved by Konghuirob on the corresponding  $\beta$ - and  $\gamma$ -CD derivatives, referred to as BSiMe and



GSiMe, respectively [17]. These results would reveal the effect of size of cyclodextrin ring on the enantioseparation.

#### 4.3.1 Enthalpy change ( $-\Delta H$ ) and entropy change ( $-\Delta S$ ) values

The enthalpy value ( $-\Delta H$ ) indicated the strength of interaction between an analyte and a stationary phase: the larger the value (more negative value), the stronger the interaction. While the entropy value ( $-\Delta S$ ) symbolized the loss of degree of freedom associated with the interaction between an analyte and a stationary phase.

From Konghuirob's study [17], the enthalpy and entropy values of most aromatic alcohols on the reference OV-1701 column showed very similar values. It is likely that the major contribution of analytes towards the interaction would come from the hydroxyl group. Two groups of alcohols were newly included in this study: mono-substituted diphenylmethanols and *n*-alkyl alcohols. Their enthalpy and entropy values on the reference OV-1701 column are shown in figures 4.4-4.5. It can be seen that the  $-\Delta H$  values of *n*-alkyl alcohols are lower than those of diphenylmethanols. In addition, the  $-\Delta H$  values of *n*-alkyl alcohols tend to increase with the chain length. The effect of number of carbon in an analyte molecule is less pronounced for the  $-\Delta S$  values.

Enthalpy and entropy values of the more retained enantiomers ( $-\Delta H_2$  and  $-\Delta S_2$ ) of all analytes on ASiMe (figures 4.6-4.7) were higher than those obtained on OV-1701 column. These results indicated the enhancement of interaction between analytes and cyclodextrin derivative. Nevertheless, the  $-\Delta H$  and  $-\Delta S$  values of all analytes on ASiMe were not significantly different, except for aliphatic alcohols which showed low  $-\Delta H$  and  $-\Delta S$  values. For the position isomers of mono-substituted aromatic alcohols, the  $-\Delta H$  and  $-\Delta S$  values slightly decreased in the order of *meta* > *para* > *ortho*. The results suggested that *meta*-substituent may cause an appropriate analyte conformation to form a more stable complex intermediate with ASiMe phase.

The  $-\Delta H_2$  and  $-\Delta S_2$  values of aromatic alcohols obtained from three cyclodextrin derivatives (ASiMe, BSiMe, and GSiMe) were also compared [17]. It was found that the average  $-\Delta H_2$  and  $-\Delta S_2$  values increased in the order of GSiMe < ASiMe < BSiMe. This indicated that the size and structure of  $\beta$ -cyclodextrin derivative was probably the most suitable for complexing with analytes.



สถาบันวิทยบริการ  
จุฬาลงกรณ์มหาวิทยาลัย

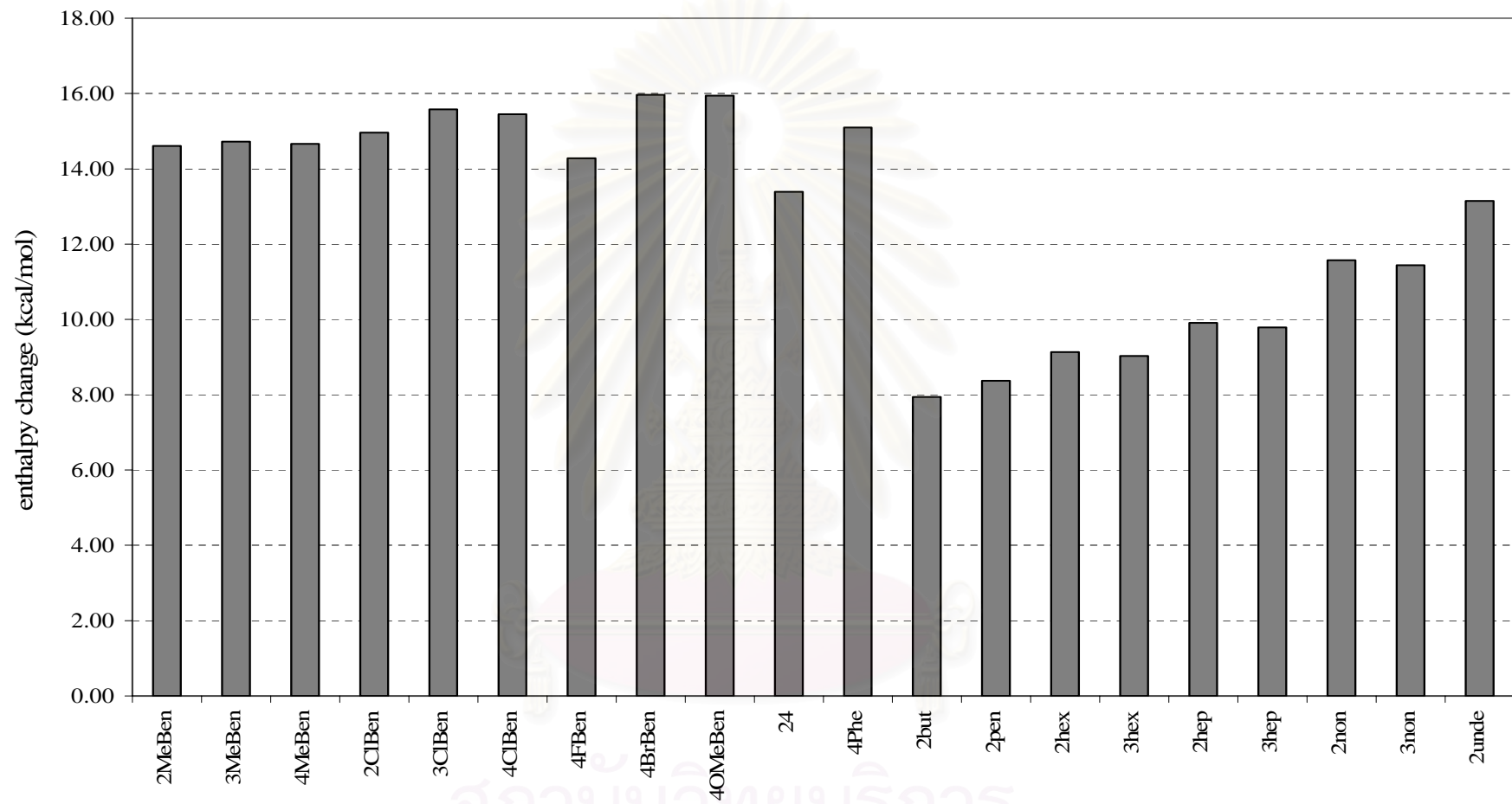


**Figure 4.4** Enthalpy change ( $-\Delta H$ , kcal/mol) of alcohol analytes on OV-1701 column obtained from van't Hoff approach ( $\bar{x} = 12.75$ ;  $SD = 2.73$ ).

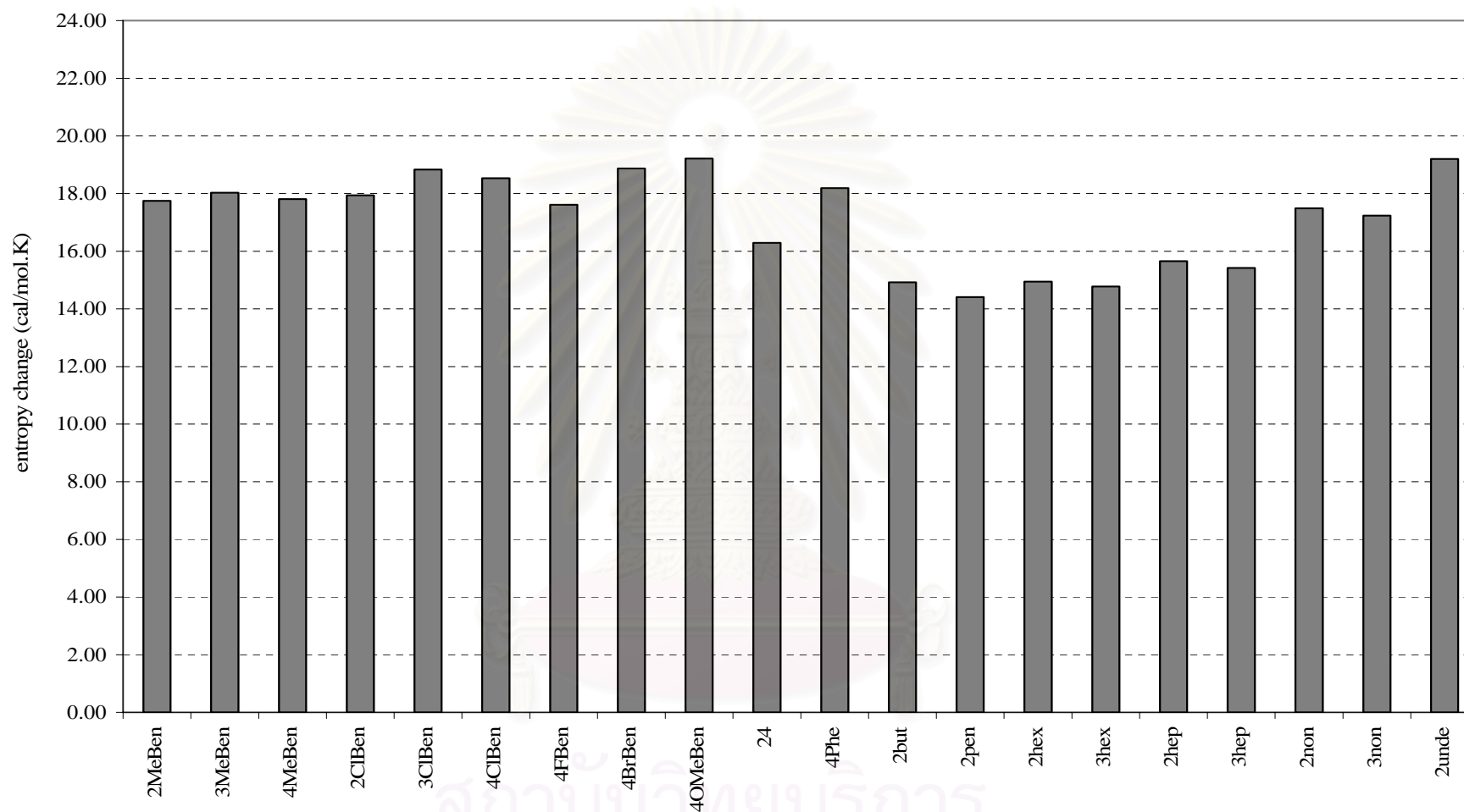


**Figure 4.5** Entropy change ( $-\Delta S$ , cal/mol.K) of alcohol analytes on OV-1701 column obtained from van't Hoff approach ( $\bar{x} = 17.15$ ; SD = 1.56).

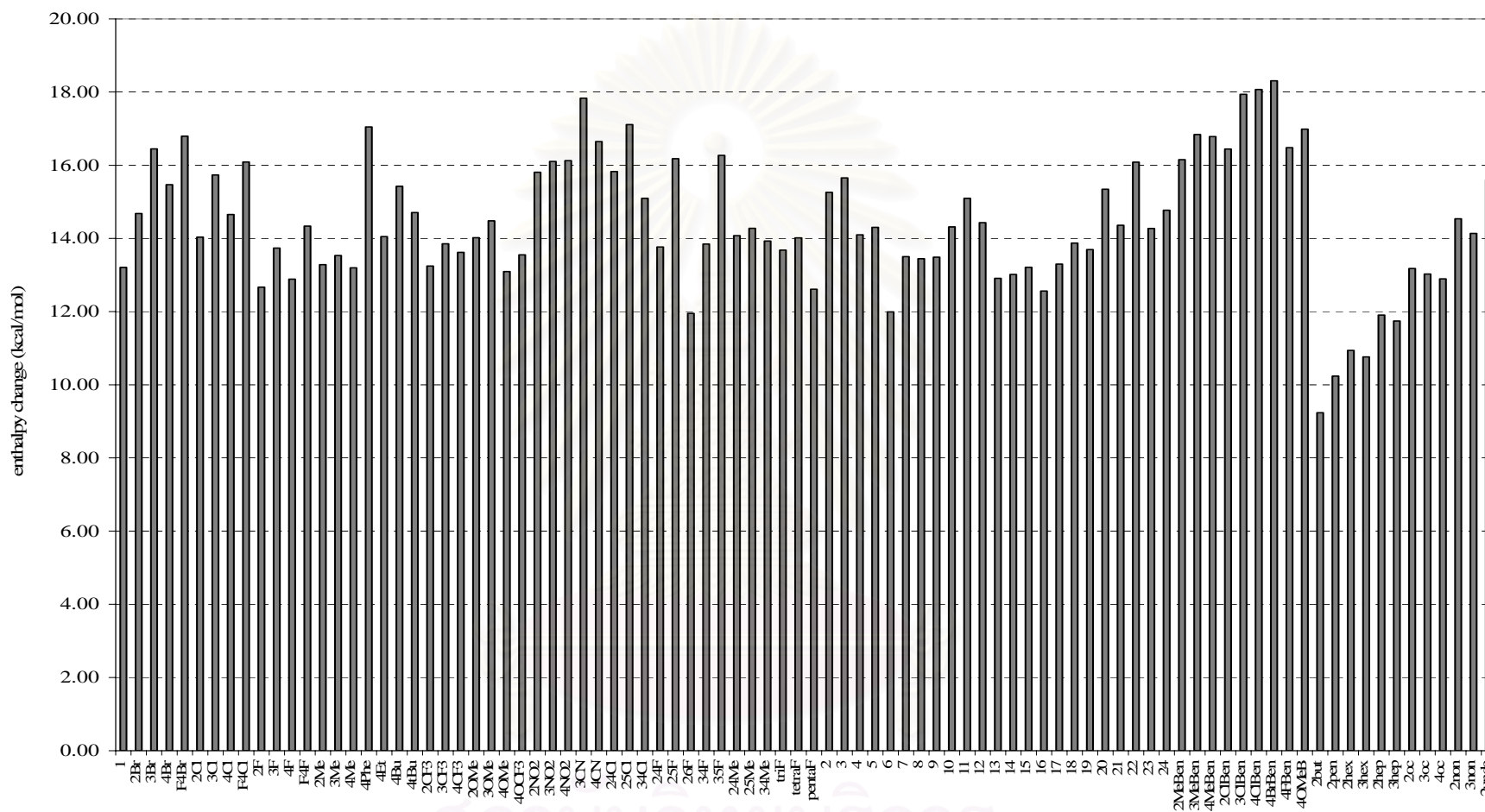


**Figure 4.6** Enthalpy change ( $-\Delta H_2$ , kcal/mol) of the more retained enantiomers of alcohol analytes on ASiMe column obtained from van't Hoff approach ( $\bar{x} = 14.42$ ;  $SD = 1.78$ ).

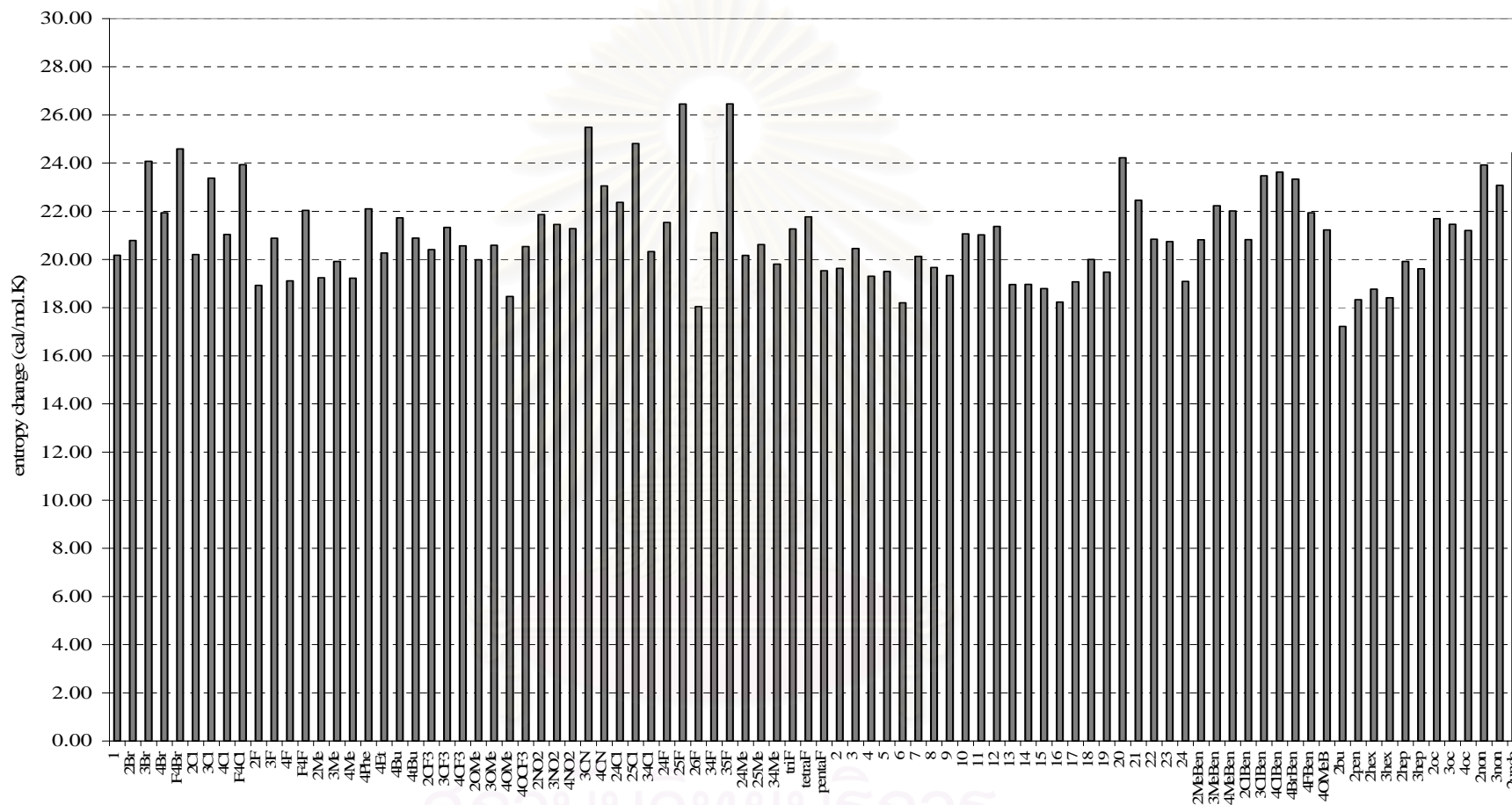


**Figure 4.7** Entropy change ( $-\Delta S_2$ , cal/mol·K) of the more retained enantiomers of alcohol analytes on ASiMe column obtained from van't Hoff approach ( $\bar{x} = 21.02$ ; SD = 1.92).

### 4.3.2 Enthalpy difference ( $-\Delta(\Delta H)$ ) and entropy difference ( $-\Delta(\Delta S)$ )

In this research, 1-phenylethanol (**1**) was regarded as a reference analyte and the influence of analyte structure and substituents on enantioseparation were systematically examined and discussed through the thermodynamic values. Additionally, the thermodynamic values responsible for enantioseparation on ASiMe column were compared to those previously attained from BSiMe and GSiMe columns [17].

The  $-\Delta(\Delta H)$  and  $-\Delta(\Delta S)$  values shown in this research derived from the difference in  $-\Delta H$  and  $-\Delta S$  of enantiomer pairs through van't Hoff plot of  $\ln k'$  versus  $1/T$ . The  $-\Delta(\Delta H)$  and  $-\Delta(\Delta S)$  values of 1-phenylethanol derivatives on ASiMe column were exhibited on figures 4.8-4.9. The  $-\Delta(\Delta S)$  values of the same enantiomers on ASiMe column displayed similar trend as their corresponding  $-\Delta(\Delta H)$  values. Therefore, discussion concerning enantioseparation on ASiMe column will be mentioned through  $-\Delta(\Delta H)$  values only. The  $-\Delta(\Delta H)$  values representing the enantioseparation of analytes on ASiMe column were significantly different depending on the analyte structure, including type, position, and number of substituents. Approximately 25% of all analytes displayed higher enantioseparation than a reference analyte (**1**) on ASiMe column. Detailed discussion will be classified according to the similarity of analyte structure.

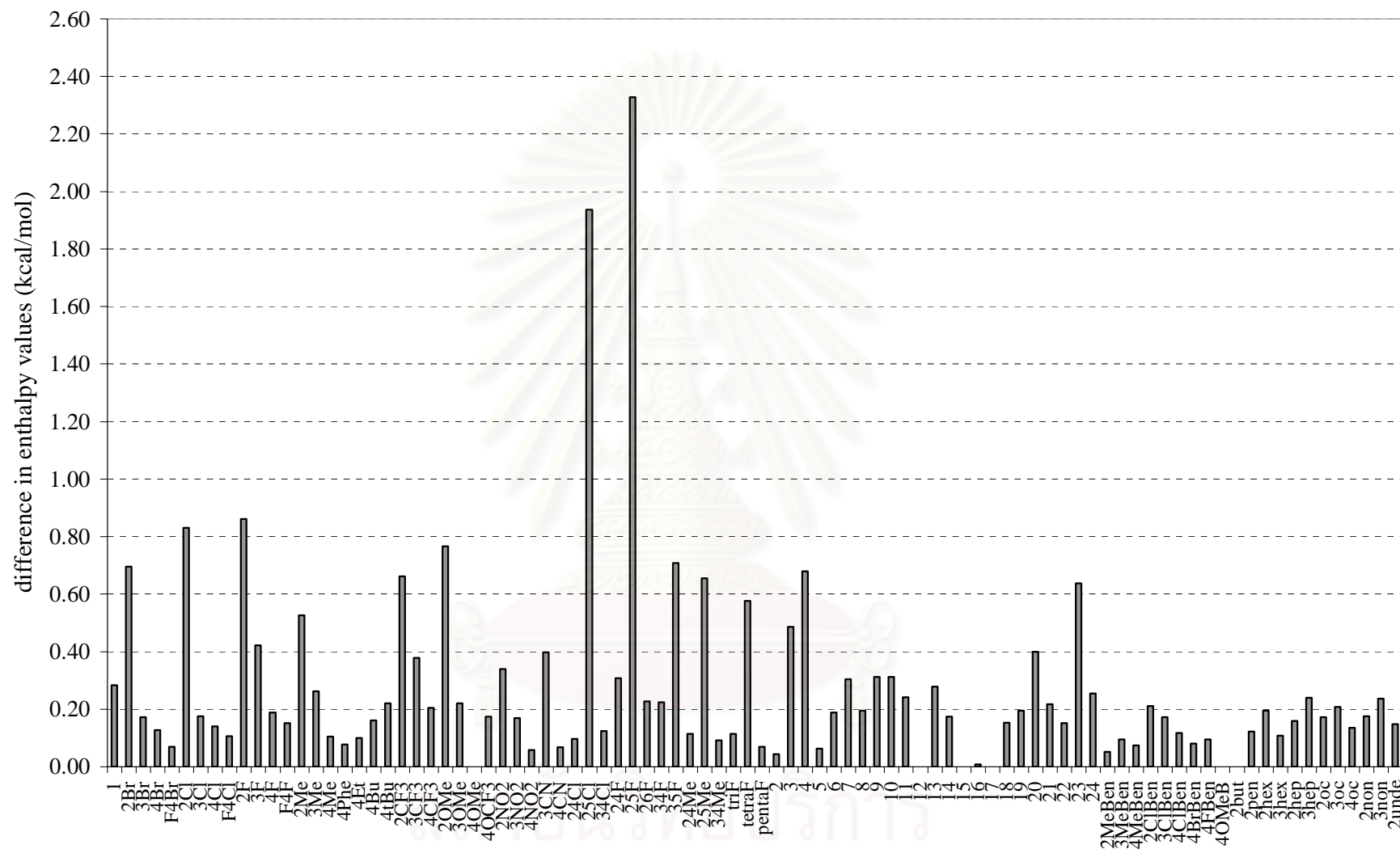


**Figure 4.8** Difference in enthalpy values ( $-\Delta(\Delta H)$ , kcal/mol) of the enantiomers of alcohol analytes on ASiMe column.



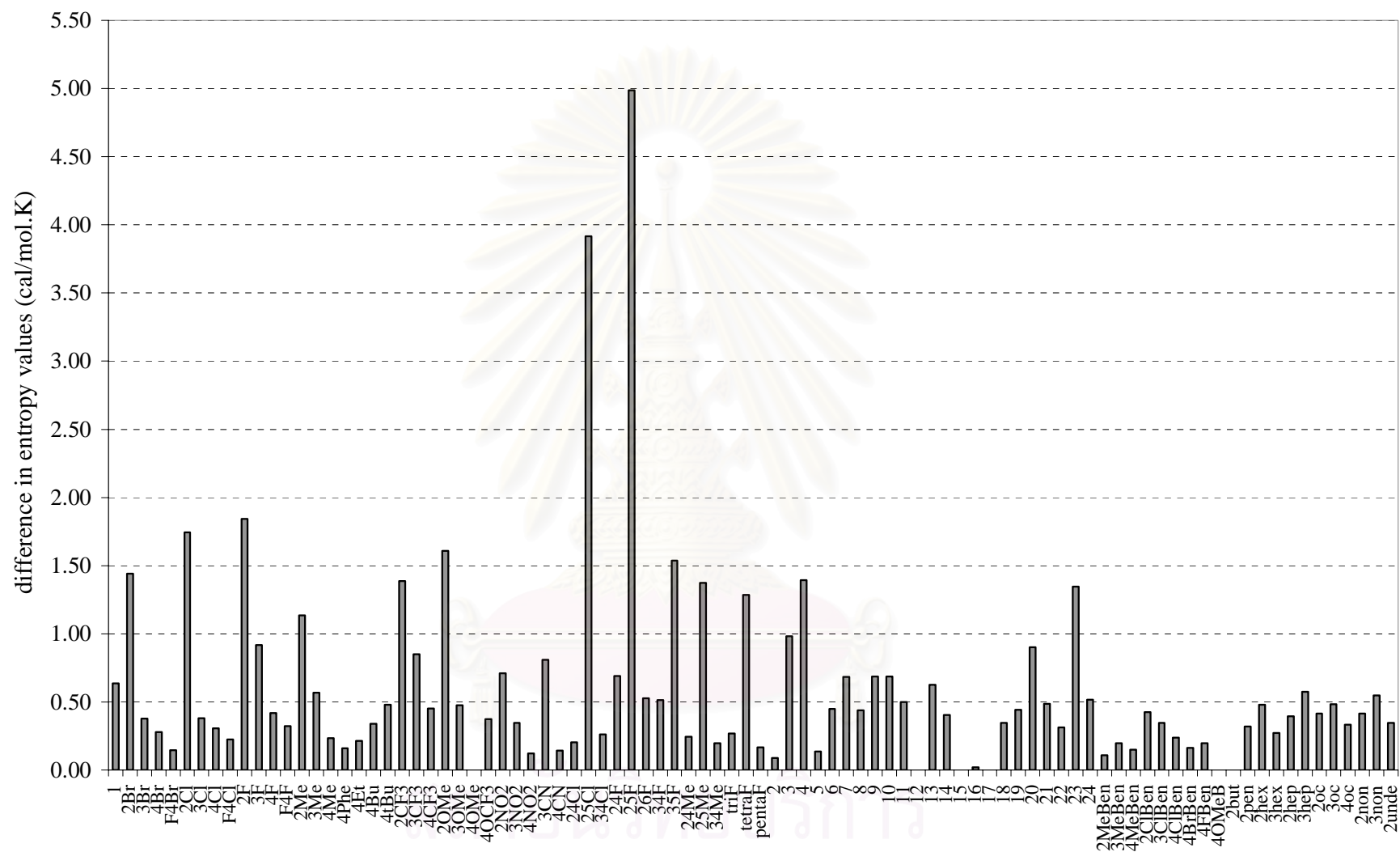
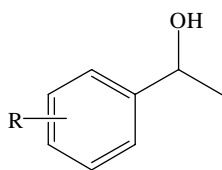
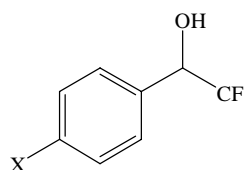


**Figure 4.9** Difference in entropy values ( $-\Delta(\Delta S)$ , cal/mol.K) of the enantiomers of alcohol analytes on ASiMe column.

*Series 1: Alcohols with mono-substitution on the aromatic ring*



R = Br, Cl, F, Me,  
Et, Bu, *t*Bu, Phe,  
OMe, CN, NO<sub>2</sub>,  
CF<sub>3</sub>, OCF<sub>3</sub>



X = Br, Cl, F

Racemic alcohols in this series are 1-phenylethanol derivatives with mono-substitution on the aromatic ring as shown above. The type of substituent includes bromo, chloro, fluoro, methyl, ethyl, butyl, *tert*-butyl, phenyl, methoxy, cyano, nitro, trifluoromethyl and trifluoromethoxy at *ortho*-, *meta*- or *para*-position. The enthalpy difference ( $-\Delta(\Delta H)$ ) values, representing the enantioselectivity, for the separation of enantiomers of alcohols in series 1 on ASiMe are compared in figure 4.10.

It can be seen that the  $-\Delta(\Delta H)$  values are obviously different but a trend is detected. Considering the effect of substituent position, the  $-\Delta(\Delta H)$  values of substituted analytes are in the order of *ortho*  $\gg$  *meta*  $>$  *para*. The  $-\Delta(\Delta H)$  values of *ortho*-substituted analytes are also much larger than that of 1-phenylethanol, whereas those of *meta*- or *para*-position are closed to or lower than that of 1-phenylethanol. The relationships between  $\ln \alpha$  versus  $1/T$  of chloro-substituted alcohols, as in **2Cl**, **3Cl** and **4Cl**, are shown as example in figure 4.11. It is clear that **2Cl** has superior enantioselectivity ( $\alpha$ ) at all temperatures. Furthermore, **2Cl** also displayed the highest slope, indicating that the enantioseparation of **2Cl** could be easily increased with a slight decrease in temperature (figure 4.12). These results demonstrated the importance of substitution position on enantioseparation. Among solutes in series 1, the best enantioseparation was observed on *ortho*-substituted 1-(4-fluorophenyl) ethanol (**4F**).

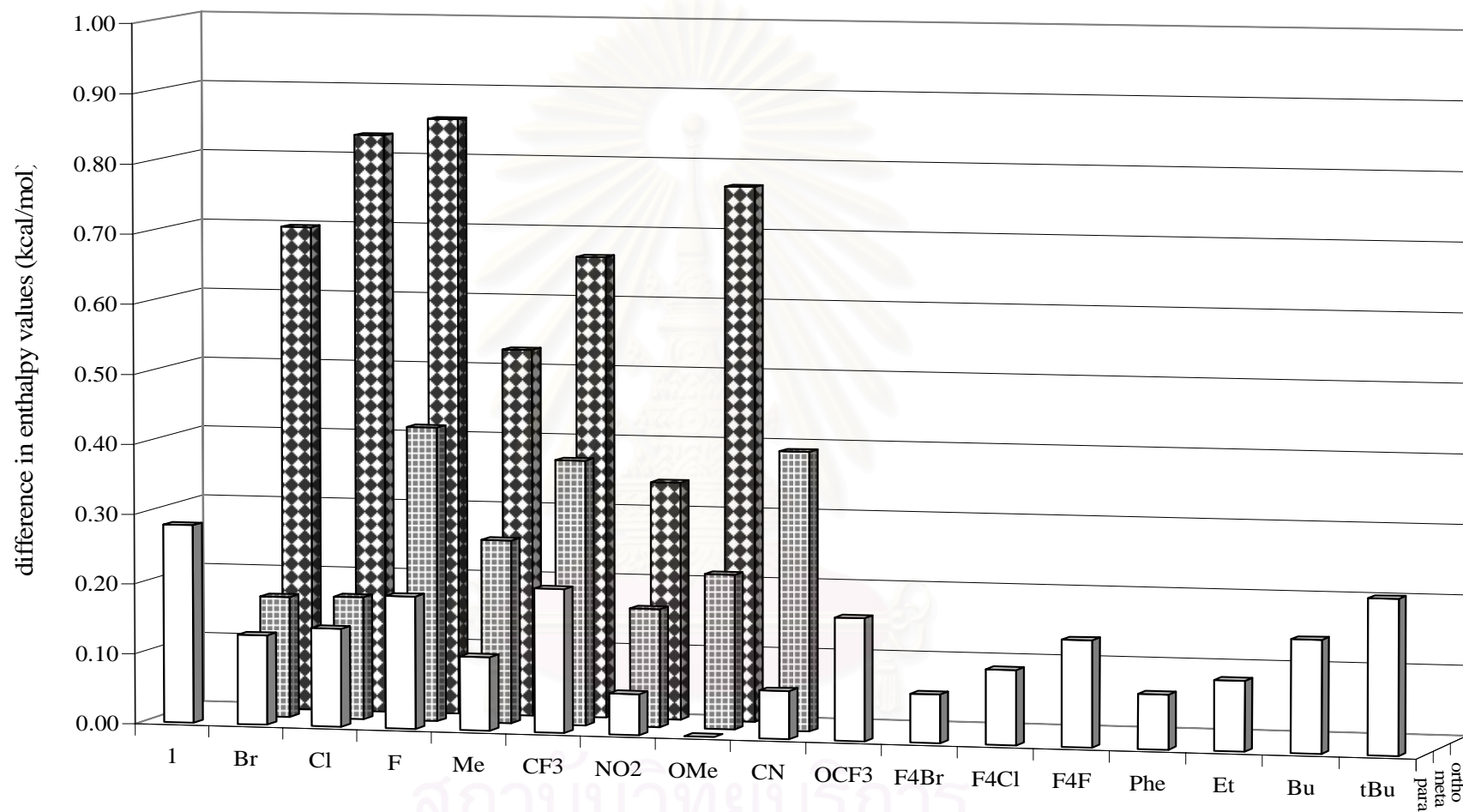


**Figure 4.10** Difference in enthalpy values ( $-\Delta(\Delta H)$ , kcal/mol) of the enantiomers of mono-substituted 1-phenylethanol derivatives on ASiMe column.

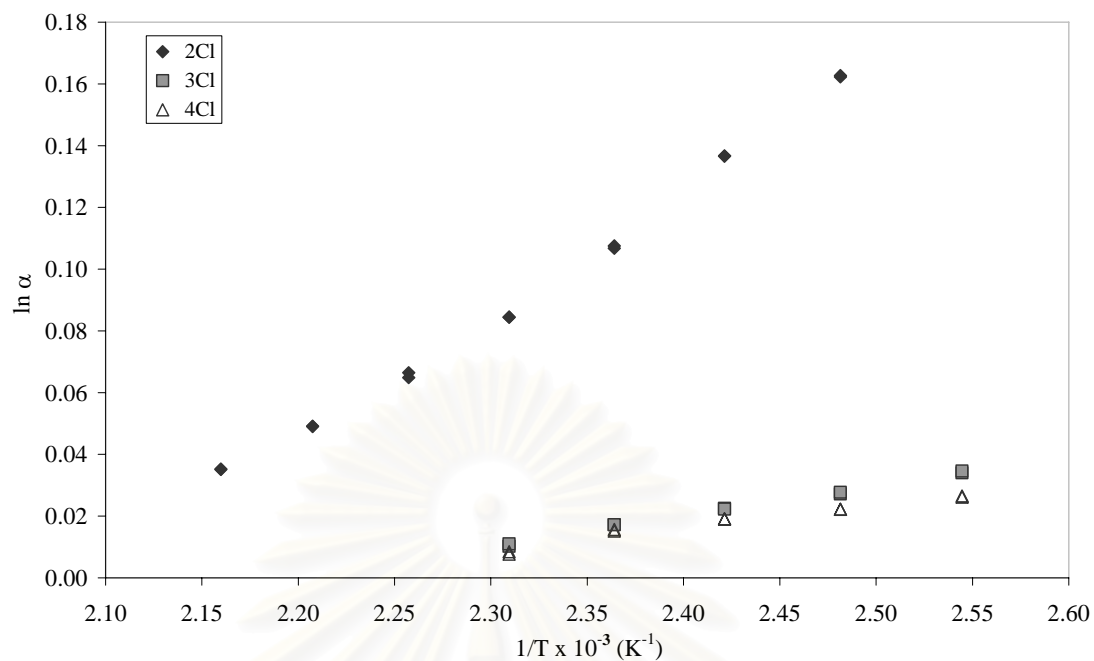


**Figure 4.11** Plots of  $\ln \alpha$  versus  $1/T$  of **2Cl**, **3Cl** and **4Cl** on ASiMe column.

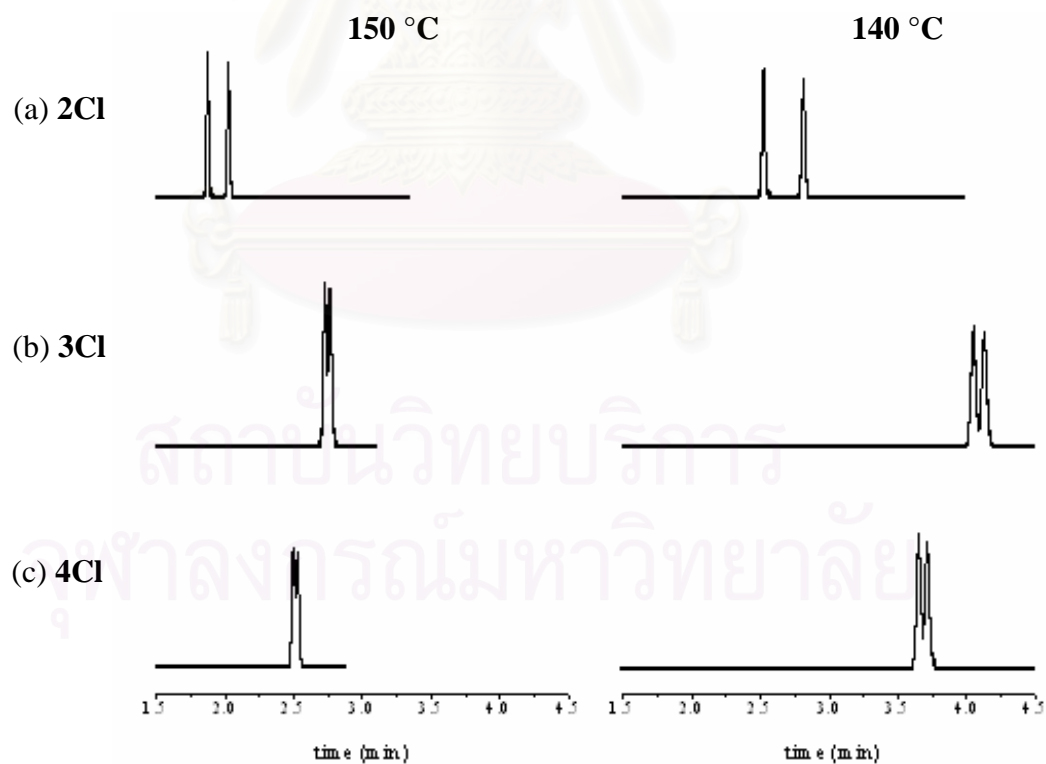


**Figure 4.12** Chromatograms of (a) **2Cl**, (b) **3Cl**, (c) **4Cl** on ASiMe column at (left) 150 °C and (right) 140 °C.

From figure 4.10, it can be seen that the type of substituent could affect enantioselectivity as seen from 1-(4-methoxyphenyl)ethanol (**4OMe**). Among alcohols in series 1, only **4OMe** could not be separated in the temperature range examined for ASiMe column. When the substitution is changed from methoxy to trifluoromethoxy as in **4OCF3** (figure 4.13) or to methyl as in **4Me**, the enantioseparation is observed. However, the type of substituent has lower influence on enantioseparation towards *meta*- and *para*-substituted analytes than towards *ortho*-substituted analytes.

The effect of alkyl chain length or bulkiness of substituent was also demonstrated. For *para*-substituted alcohols, longer or bulkier alkyl substituents (as in **4Et**, **4Bu**, **4tBu**) tend to increase enantioseparation on ASiMe column (figures 4.10 and 4.14). Nevertheless, the results are reversed on BSiMe and GSiMe columns [17]. In case of halogen-substituted analytes, it was observed that  $-\Delta(\Delta H)$  values increased in the order of  $\text{Br} < \text{Cl} < \text{F}$ , according to the increasing electronegativity of substituent ( $\text{EN}_{\text{Br}} = 2.7$ ,  $\text{EN}_{\text{Cl}} = 2.8$ ,  $\text{EN}_{\text{F}} = 4.0$  [40]) and to the decreasing of substituent size ( $r_{\text{Br}} = 1.96$  pm,  $r_{\text{Cl}} = 1.81$  pm,  $r_{\text{F}} = 1.31$  pm [41]).

The average  $-\Delta(\Delta H)$  values of series 1 alcohols obtained from ASiMe were also compared to those from BSiMe and GSiMe. It was found that the average  $-\Delta(\Delta H)$  values decreased in the order of  $\text{BSiMe} > \text{ASiMe} > \text{GSiMe}$ . Although the average  $-\Delta(\Delta H)$  values acquired from BSiMe phase were higher than those from ASiMe phase, some analytes showed better enantioselectivity on ASiMe than on BSiMe as for 2,2,2-trifluoro-1-(4-bromophenyl)ethanol (**F4Br**) and 2,2,2-trifluoro-1-(4-chlorophenyl)ethanol (**F4Cl**). Furthermore, it was evident that the GSiMe was not suitable for the enantioseparation of alcohols in series 1 since only a few can be resolved with the lowest degree of separation. Noticeably, all three columns showed the highest enantioseparation (high  $-\Delta(\Delta H)$  values) when analytes possessing substituents at *ortho*-position.

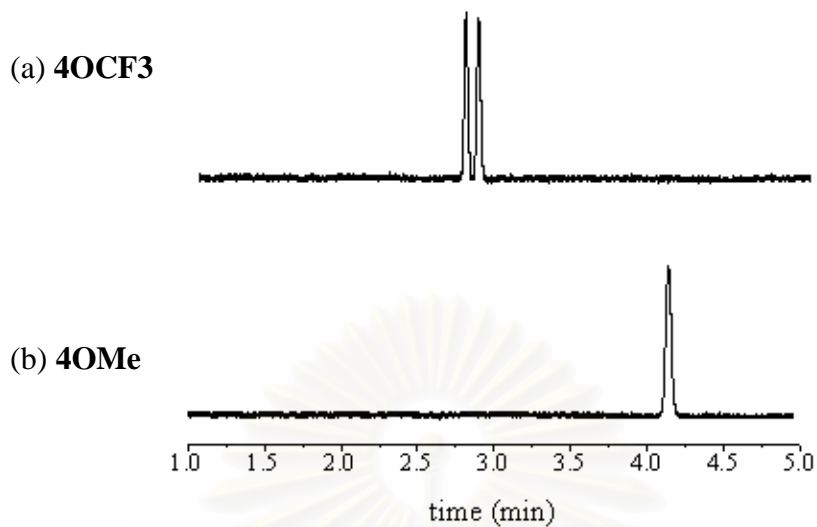


**Figure 4.13** Chromatograms of (a) **4OCF3** and (b) **4OMe** on ASiMe column at 120 °C.

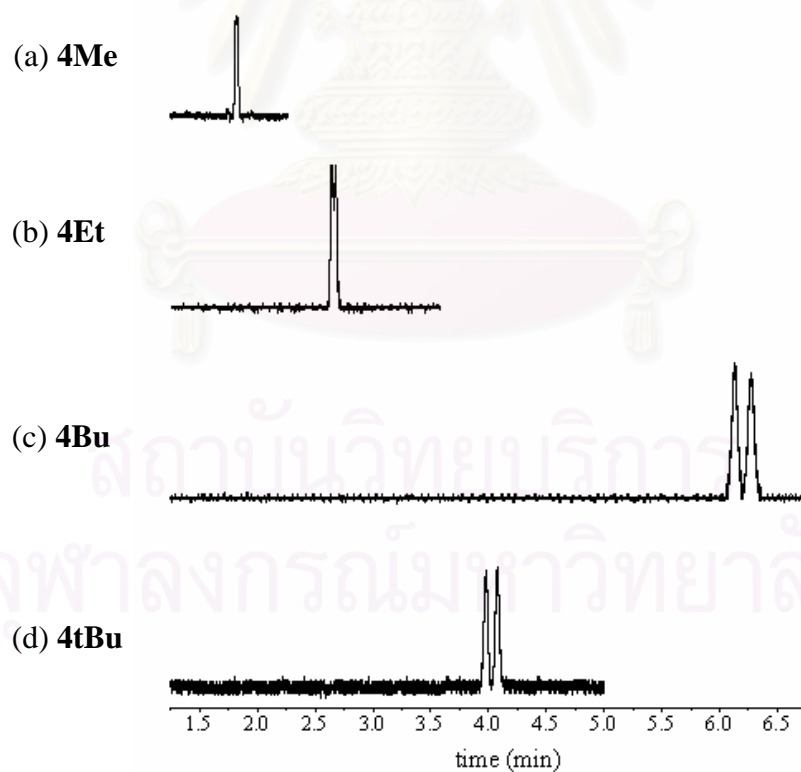
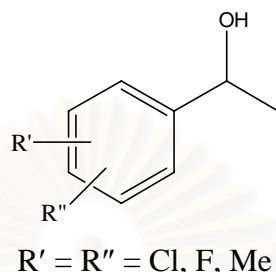


**Figure 4.14** Chromatograms of (a) **4Me**, (b) **4Et**, (c) **4Bu** and (d) **4tBu** on ASiMe column at 140 °C.

**Series 2: Alcohols with di-substitution on the aromatic ring**

Racemic alcohols in series 2 comprise of 1-phenylethanol derivatives with dichloro-, difluoro and dimethyl-substitutions at different position of the aromatic ring, as shown below.



The  $-\Delta(\Delta H)$  values representing the enantioseparation of di-substituted alcohols were illustrated in figure 4.15. The  $-\Delta(\Delta S)$  values also exhibited similar trends as their corresponding  $-\Delta(\Delta H)$  values as seen in figures 4.9.

According to figures 4.15-4.16, the substituent position on the aromatic ring still played an important role as the highest enantioseparation was observed with the 2,5-substitution. Considering the effect of type of substituent, a small trend could be observed. The  $-\Delta(\Delta H)$  values have a tendency to decrease in the order of  $F > Cl > Me$ . It was possible that the small-sized,  $\alpha$ -cyclodextrin would be suitable to the small and less steric substituents, as difluoro-substituted alcohols. However, when comparing results with previous work by Konghurob [17], it was found that ASiMe phase exhibited the lowest  $-\Delta(\Delta H)$  values whereas BSiMe phase gave the highest values. Nevertheless, the separation of all di-substituted analytes was achieved on ASiMe phase while some analytes were not resolved on BSiMe and GSiMe phases.

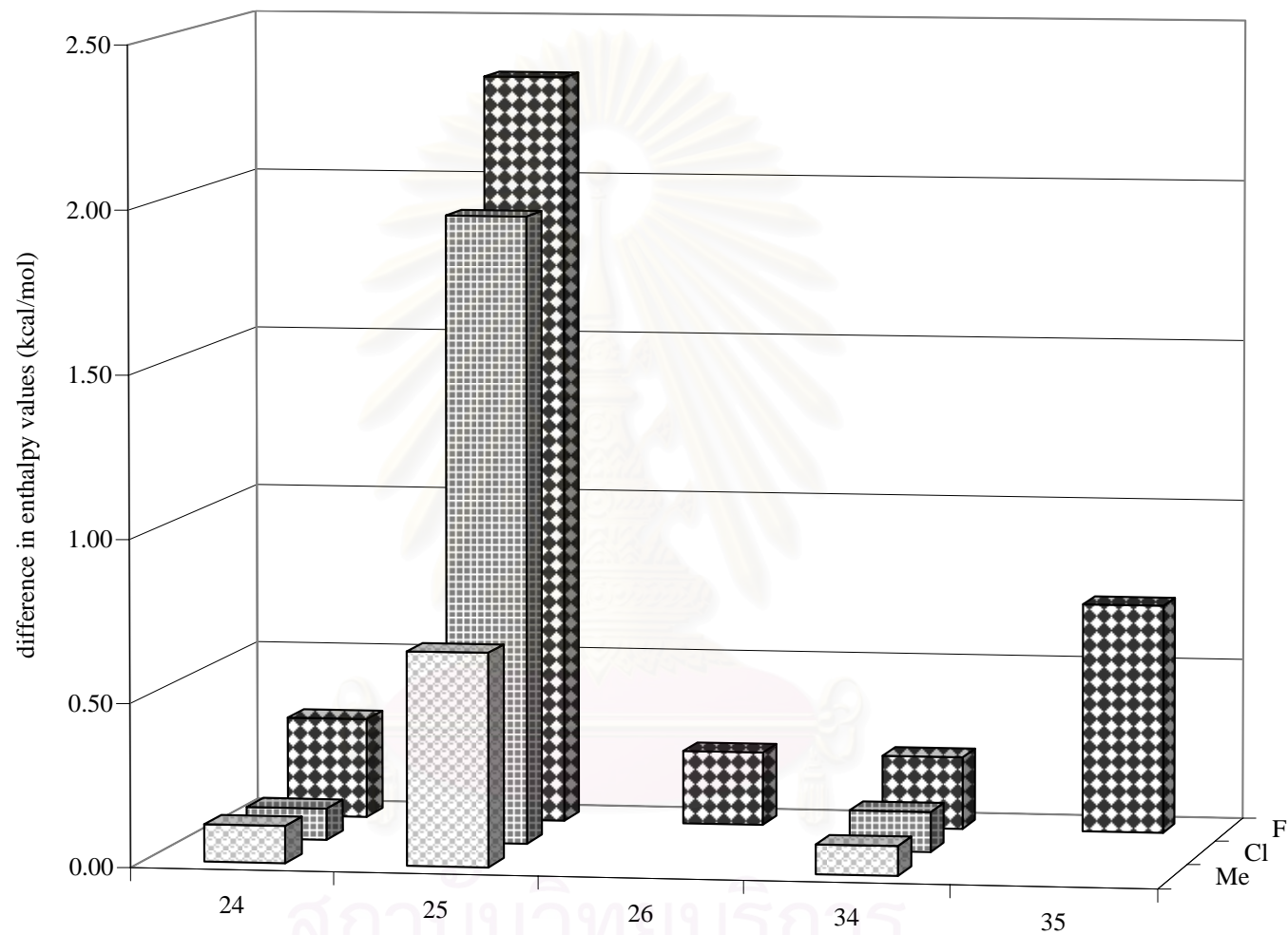


**Figure 4.15** Difference in enthalpy values ( $-\Delta(\Delta H)$ , kcal/mol) of the enantiomers of di-substituted 1-phenylethanol derivatives on ASiMe column.



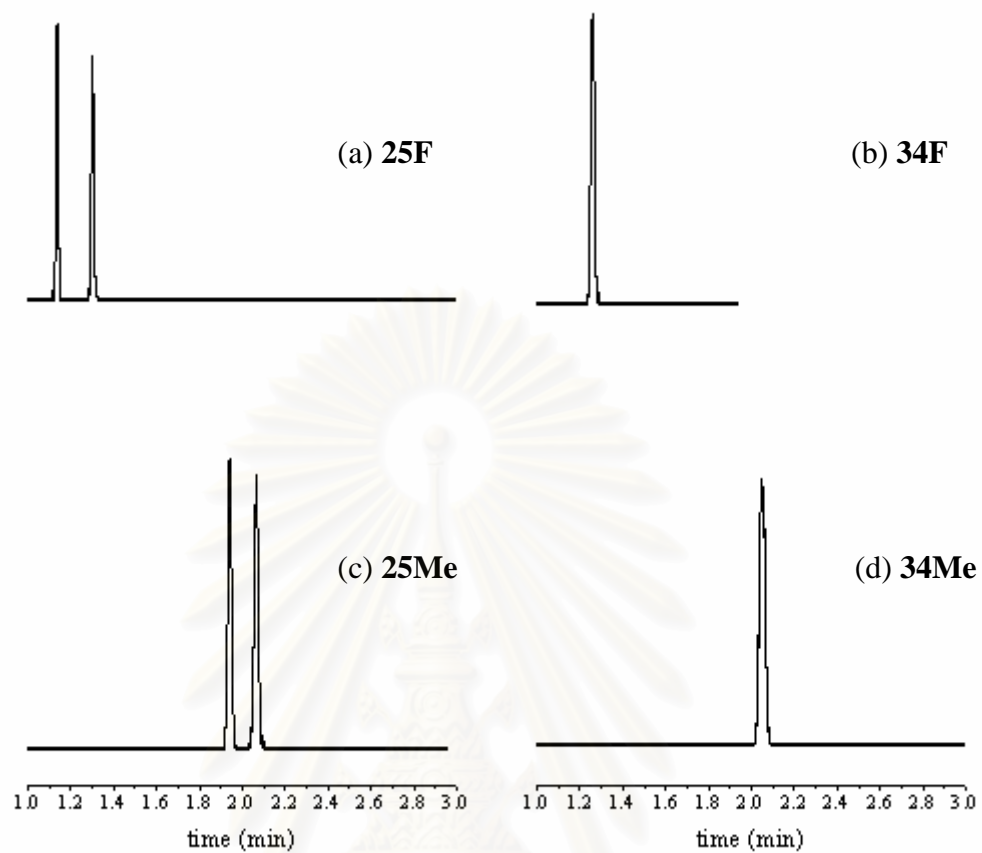


**Figure 4.16** Chromatograms of (a) 25F, (b) 34F, (c) 25Me and (d) 34Me on ASiMe column at 150 °C

สถาบันวิทยบริการ  
จุฬาลงกรณ์มหาวิทยาลัย

*Series 3: Other alcohols*

Other alcohols with various types of substitution and structures were also investigated. The  $-\Delta(\Delta H)$  values of alcohols in series 3 were compared to reference alcohol (1) in figure 4.17. The  $-\Delta(\Delta H)$  values were notably different. For the simplicity of discussion, alcohols in series 3 are further subdivided into 3 subgroups according to the similarity of their structures.



สถาบันวิทยบริการ  
จุฬาลงกรณ์มหาวิทยาลัย

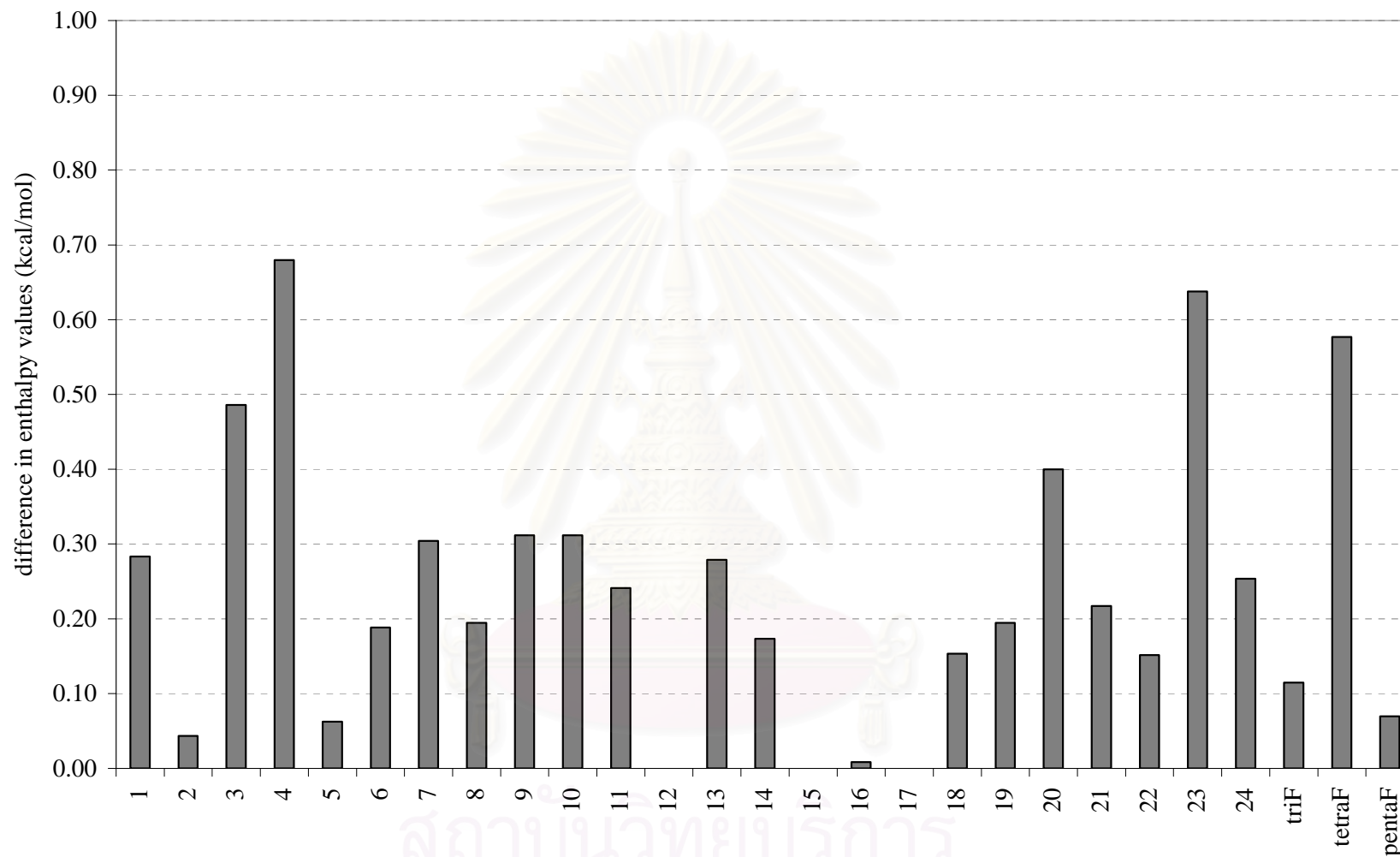
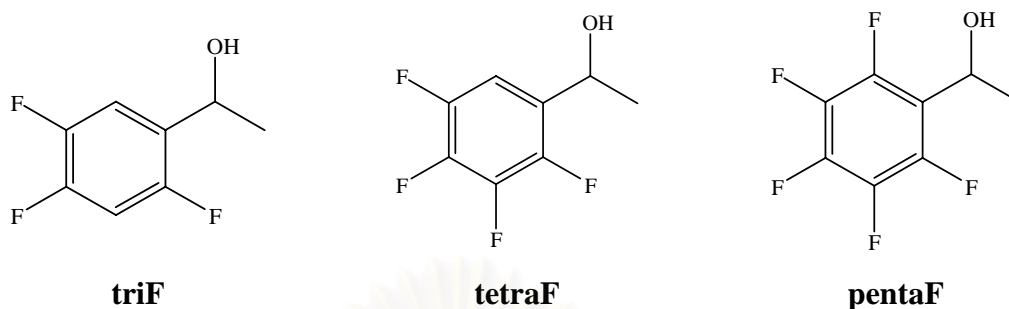


**Figure 4.17** Difference in enthalpy values ( $-\Delta(H)$ , kcal/mol) of the enantiomers of alcohols in series 3 on ASiMe column.

**Series 3.1: Polyfluoro-substituted 1-phenylethanols**



Alcohols in this subgroup are 1-(2,4,5-trifluorophenyl)ethanol (**triF**), 1-(2,3,4,5-tetrafluorophenyl)ethanol (**tetraF**) and 1-(pentafluorophenyl)ethanol (**pentaF**), as shown above. Their thermodynamic data were compared with other monofluoro- and difluoro-substituted 1-phenylethanols in figure 4.18.

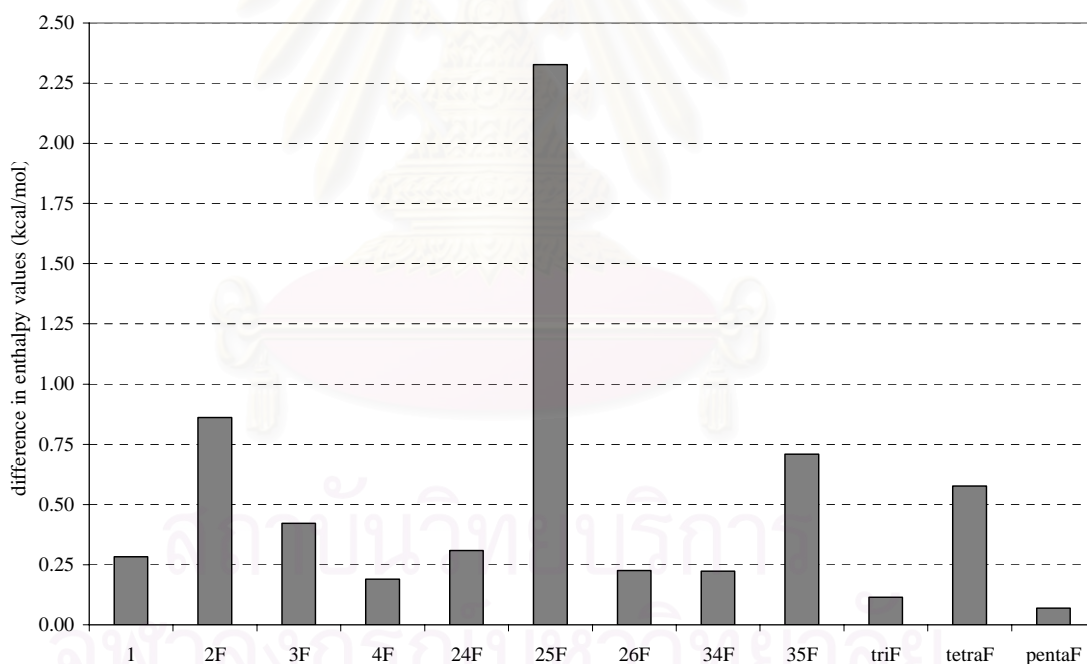


**Figure 4.18** Difference in enthalpy values ( $-\Delta(\Delta H)$ , kcal/mol) of the enantiomers of alcohols in series 3.1 on ASiMe column.

The  $-\Delta(\Delta H)$  values of fluoro-substituted analytes are definitely different but a trend is detected. The analytes containing *para*-substitution show reduced enantioseparation, as in **4F**, **24F**, **34F**, **triF** and **pentaF**, compared to alcohol **1**, except for **tetraF**. Among three polyfluoro-substituted 1-phenylethanols examined, **tetraF** presents the best enantioseparation on ASiMe (figure 4.19). Conversely, **triF** displayed the greatest enantioseparation on both BSiMe and GSiMe [17]. These results show that the degree of enantioseparation varies depending on the number and position of fluoro-substitution as well as the size of cyclodextrin ring. Unfortunately, not all isomers of trifluoro-substituted 1-phenylethanol are available to study the effect of position of fluoro-substituent.

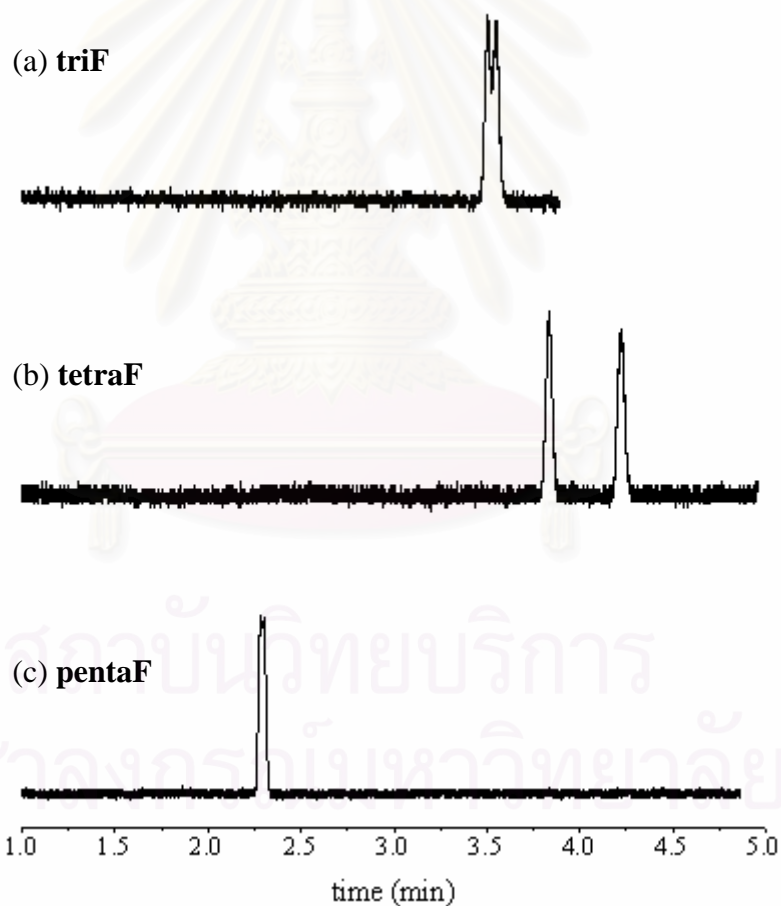
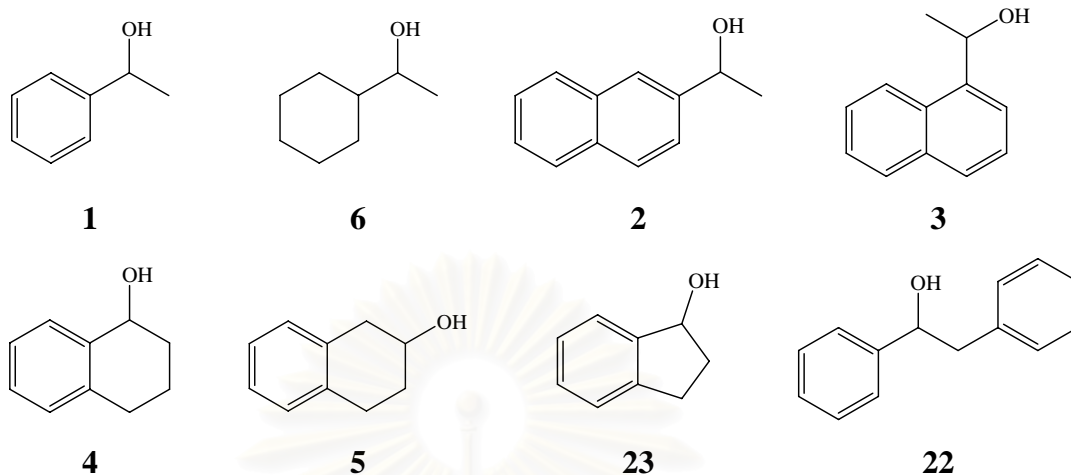


**Figure 4.19** Chromatograms of (a) **triF**, (b) **tetraF** and (c) **pentaF** on ASiMe column at 110 °C.

**Series 3.2: Alcohols with different structures**



This subgroup is composed of alcohols with different structure based on 1-phenylethanol (**1**), as seen above. Their thermodynamic values for the separation are compared in figure 4.20.

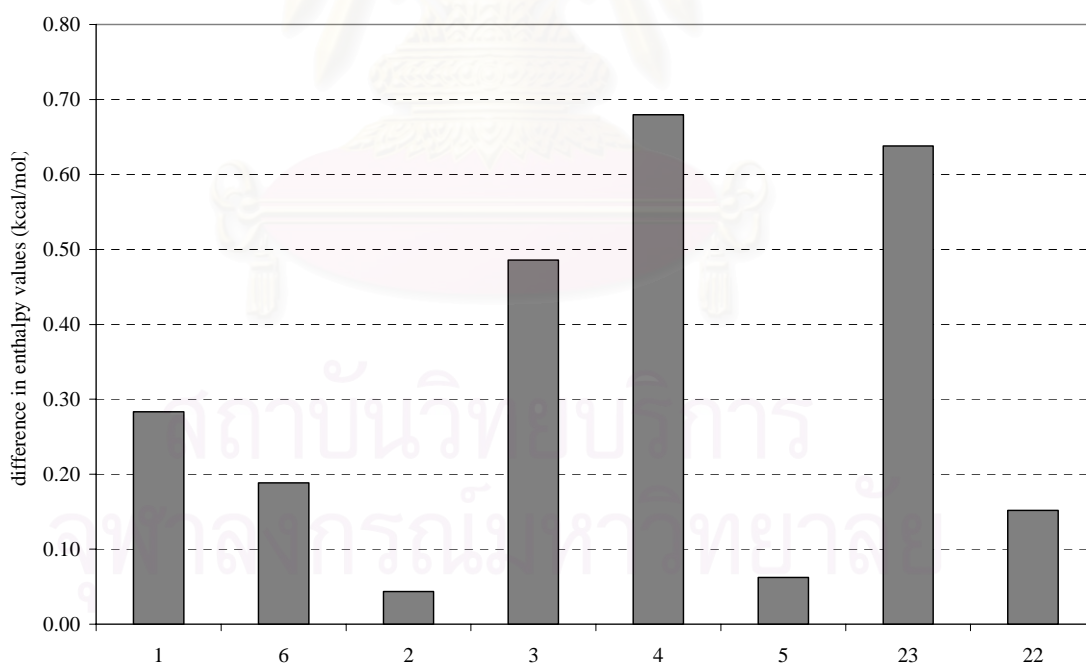


**Figure 4.20** Difference in enthalpy values ( $-\Delta(\Delta H)$ , kcal/mol) of the enantiomers of alcohols in series 3.2 on ASiMe column.

Comparing the enantioseparation of analytes **1** and **6**, the selectivity of ASiMe was higher for enantiomers of alcohols containing an aromatic moiety (as in **1**) than for alcohols that had a cyclohexyl group (as in **6**). The enantioseparation was markedly affected by the position of chiral center as the separations of enantiomers of **4** and **23** (chiral centers closed to the aromatic ring) were much better than **5** (figure 4.21). Similar results were detected for alcohols **2** and **3**. The enantioseparations of both isomers were considerably different as the position of 1-ethanoyl substituent was changed (figure 4.22).

Similar enantioseparation of alcohols in series 3.2 were also observed on BSiMe and GSiMe phases [17]. Interestingly, it was found that all large alcohols in series 3.2 (**2**, **3**, **4**, **5**, **22**, **23**) could be separated on the small ASiMe phase but some could not be resolved on BSiMe and GSiMe phases.

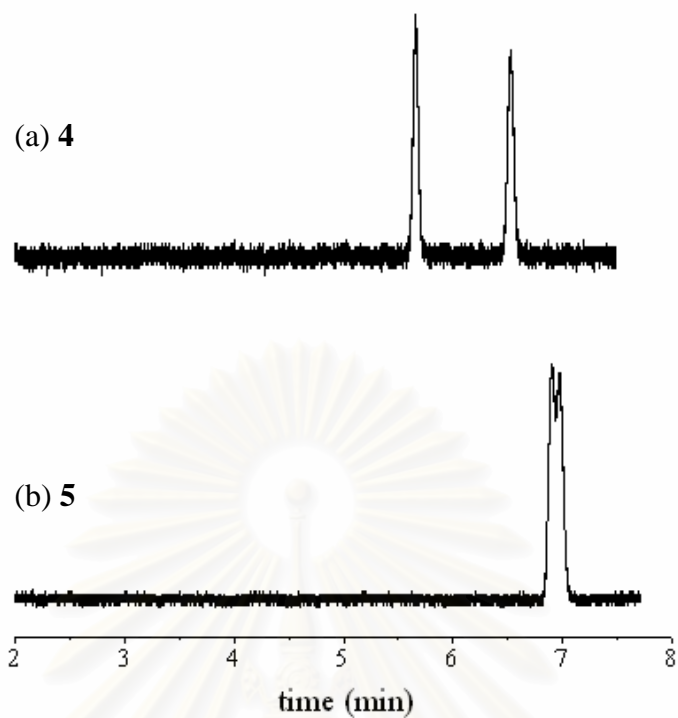


**Figure 4.21** Chromatograms of (a) **4** and (b) **5** on ASiMe column at 130 °C.

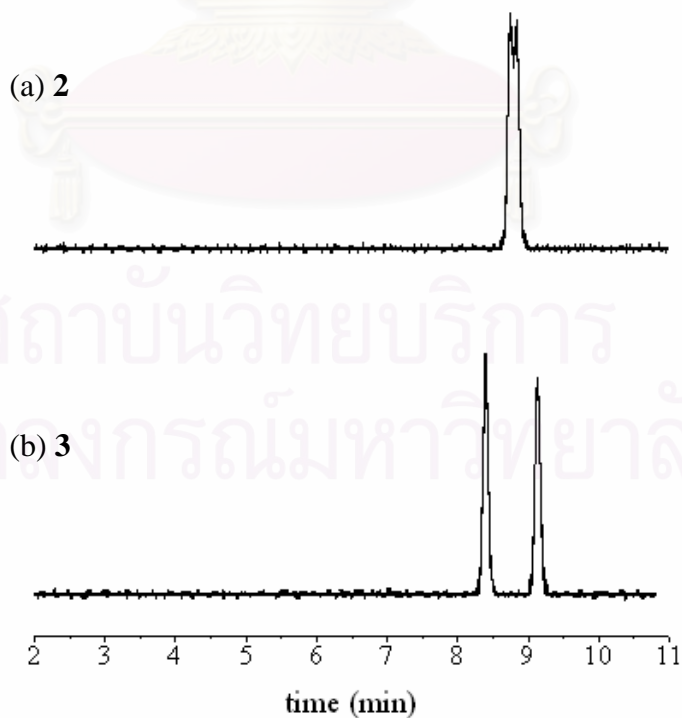
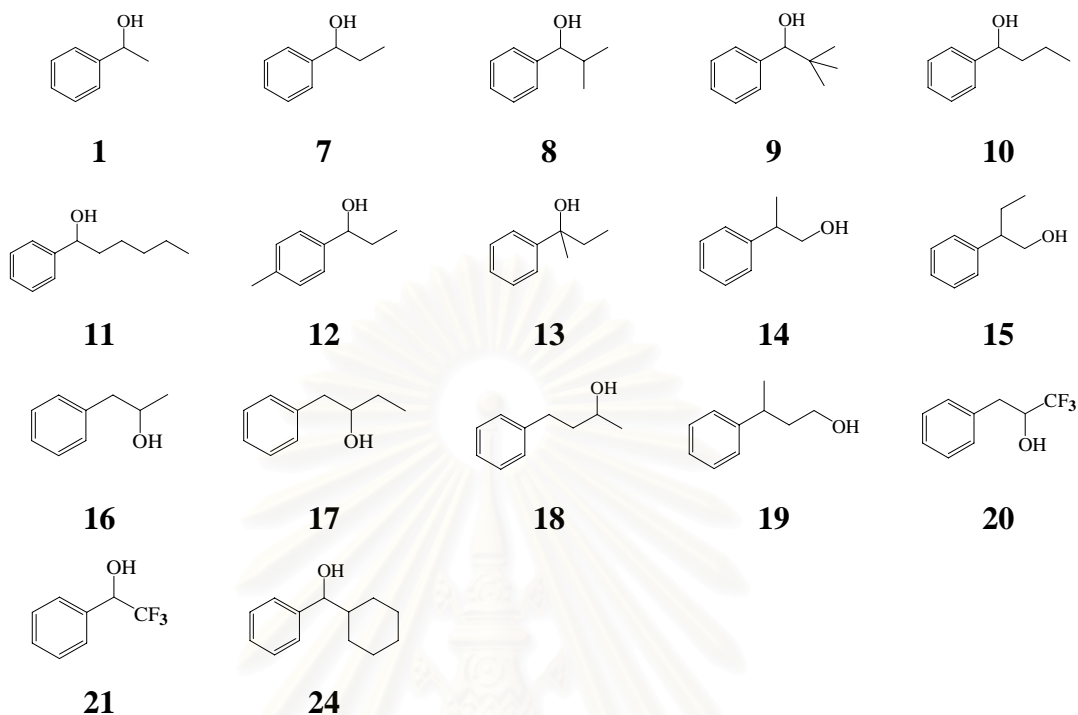


**Figure 4.22** Chromatograms of (a) **2** and (b) **3** on ASiMe column at 150 °C.



**Series 3.3: Alcohols with different alkyl chain**



Alcohols in series 3.3 include derivatives of 1-phenylethanols with different alkyl substituent on the  $\alpha$ -carbon (as in **7**, **8**, **9**, **10**, **11**, **12**, **13**, **24**); aromatic alcohols with different position of chiral center or hydroxyl group (as in **14**, **15**, **16**, **17**, **18**, **19**, **20**); and aromatic alcohols with trifluoromethyl substituent at the chiral center (as in **20**, **21**). The  $-\Delta(\Delta H)$  values of alcohols in series 3.3 are illustrated in figure 4.23.

Among all alcohols in this series, analyte **20** displayed the greatest enantioseparation, while analytes **12**, **15**, and **17** could not be resolved on ASiMe column. It was found that the  $-\Delta(\Delta H)$  values seemed to be higher if the position of chiral center was closer the aromatic ring, as seen from **7** and **16** (as shown in figure 4.24) and **10**, **17** and **18**. There were many evidences to support that any small differences in the analyte structure could lead to an enormous change in enantioseparation. A change from trifluoromethyl substitution of alcohol **20** to methyl substitution (as in **16**) could diminish enantioselectivity (figure 4.24), while a similar change between alcohols **21** and **1** showed a minor difference in enantioseparation.

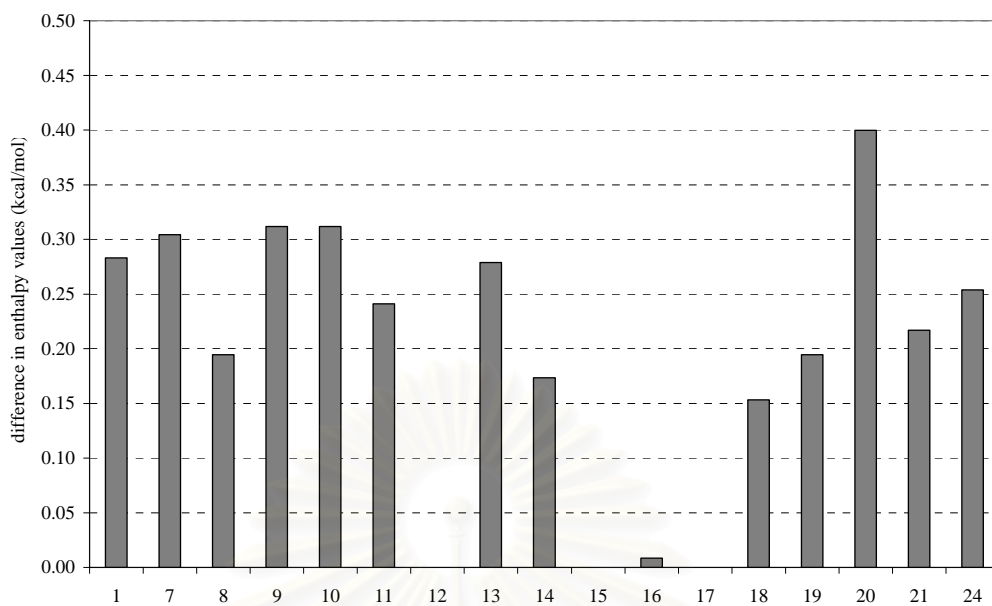


**Figure 4.23** Difference in enthalpy values ( $-\Delta(\Delta H)$ , kcal/mol) of the enantiomers of alcohols in series 3.3 on ASiMe column.

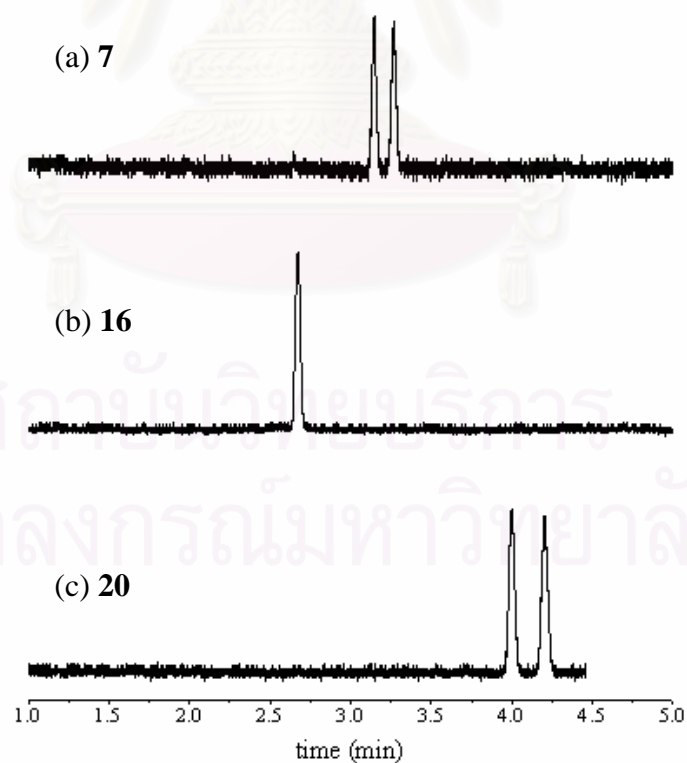


**Figure 4.24** Chromatograms of (a) 7, (b) 16 and (c) 20 on ASiMe column at 120 °C.

A change of side-chain substitution from methyl (**14**) to ethyl (**15**) could lead to no separation (figure 4.25). A change of methyl group from side-chain substitution (**8**) to aromatic substitution (**12**) could also lead to no enantioseparation. On the contrary, analyte **12** showed better enantioseparation than **8** on both BSiMe and GSiMe [17].

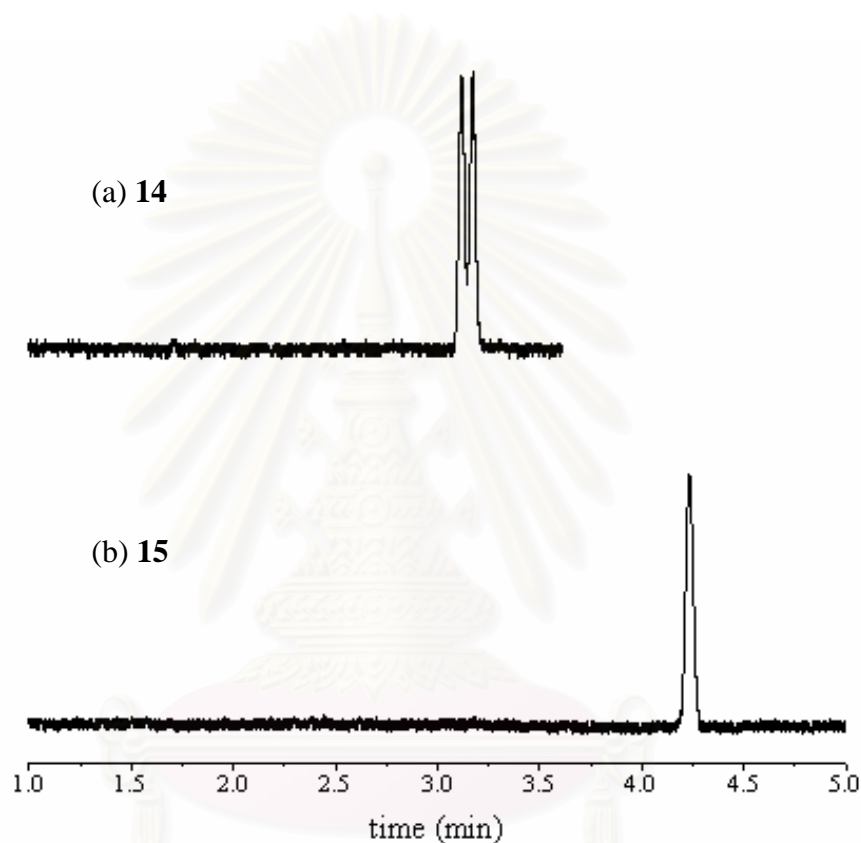
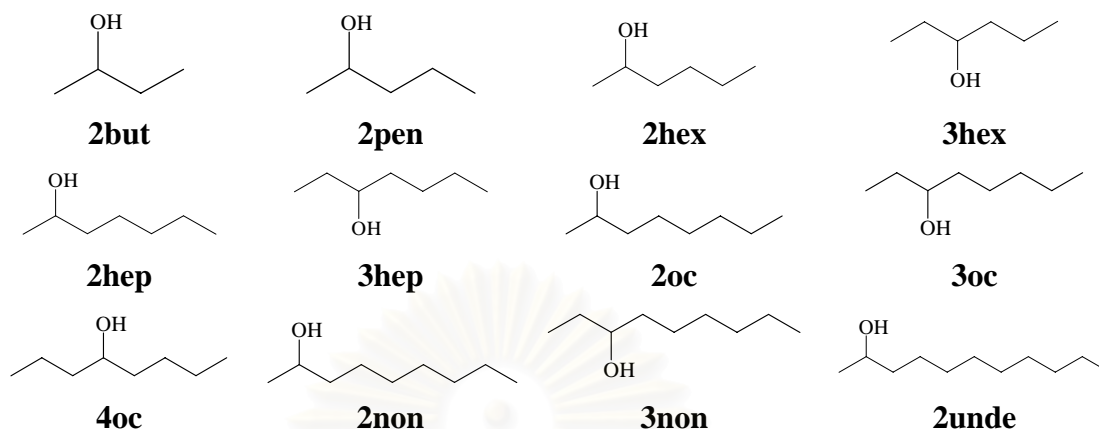


**Figure 4.25** Chromatograms of (a) **14** and (b) **15** on ASiMe column at 120 °C.

*Series 4: Aliphatic alcohols*



Alcohols in series 4 compose of aliphatic alcohols with different number of carbon (C<sub>4</sub>-C<sub>11</sub>) and different position of chiral center, as shown above. The  $-\Delta(\Delta H)$  values of analytes in series 4 are compared in figure 4.26.

All alcohols in series 4 exhibit lower enantiodifferentiation than reference alcohol **1**. Additionally, **2but** could not be separated on ASiMe phase within temperature range examined. Considering the effect of position of chiral center, the  $-\Delta(\Delta H)$  values of analytes with chiral center at C3 position were larger than those with chiral center at C2 position, except for hexanol. Among all 2-alkyl alcohols studied, 2-hexanol (**2hex**) displays the highest  $-\Delta(\Delta H)$  values. However, when the position of chiral center was changed from C2 to C3 as in 3-hexanol (**3hex**), the  $-\Delta(\Delta H)$  values was the lowest among the 3-alkyl alcohols (figure 4.27). The opposite trend was detected for other isomers of alkyl alcohols. Among all alcohols in series 4, **3hep** exhibited the highest enantioseparation (figure 4.27). The number of carbon also played an important role on enantioseparation as seen from **2but** where no separation was observed and **3hex** where enantioseparation was the lowest among the 3-alkyl alcohols.

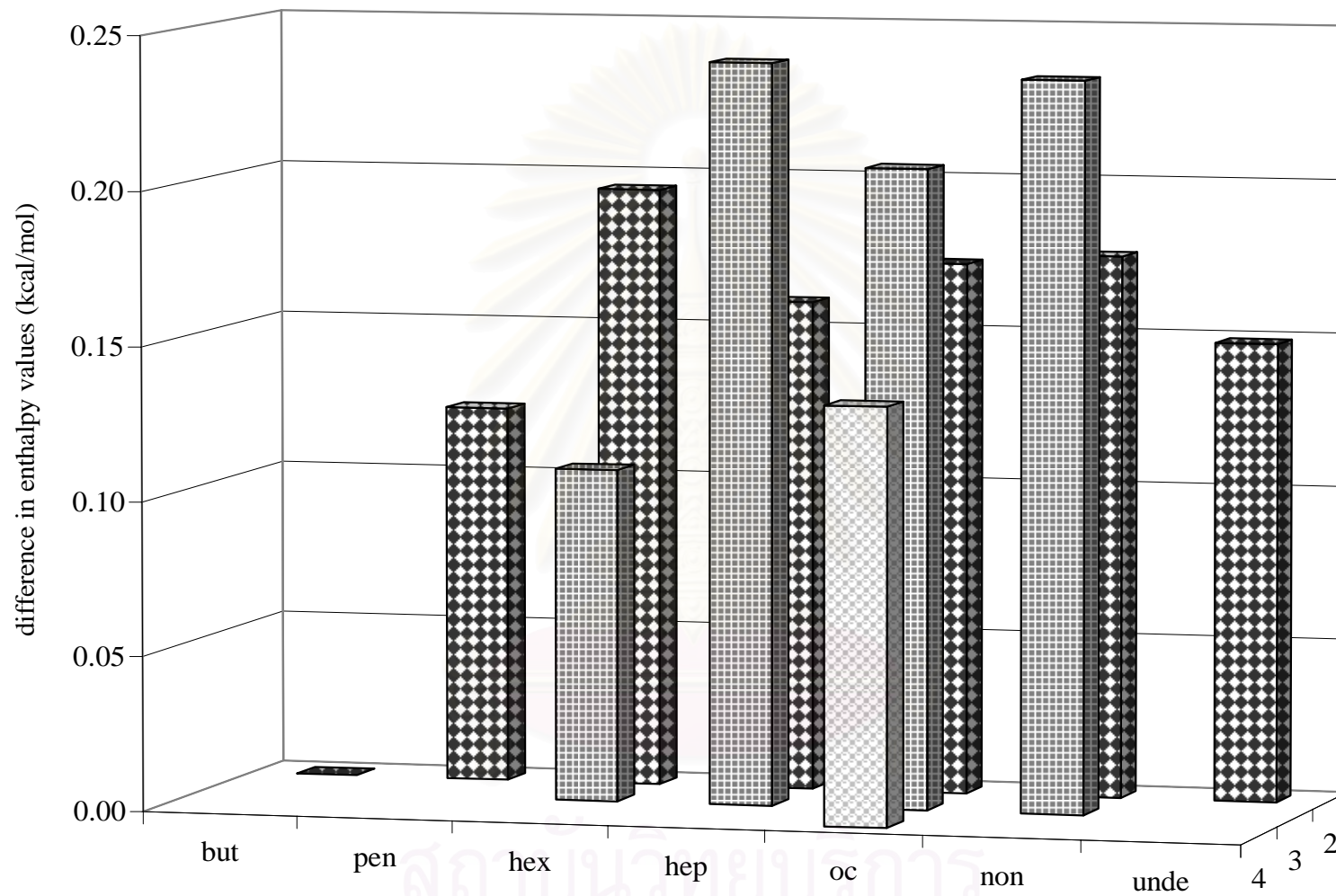


**Figure 4.26** Difference in enthalpy values ( $-\Delta(\Delta H)$ , kcal/mol) of the enantiomers of alcohols in series 4 on ASiMe column.

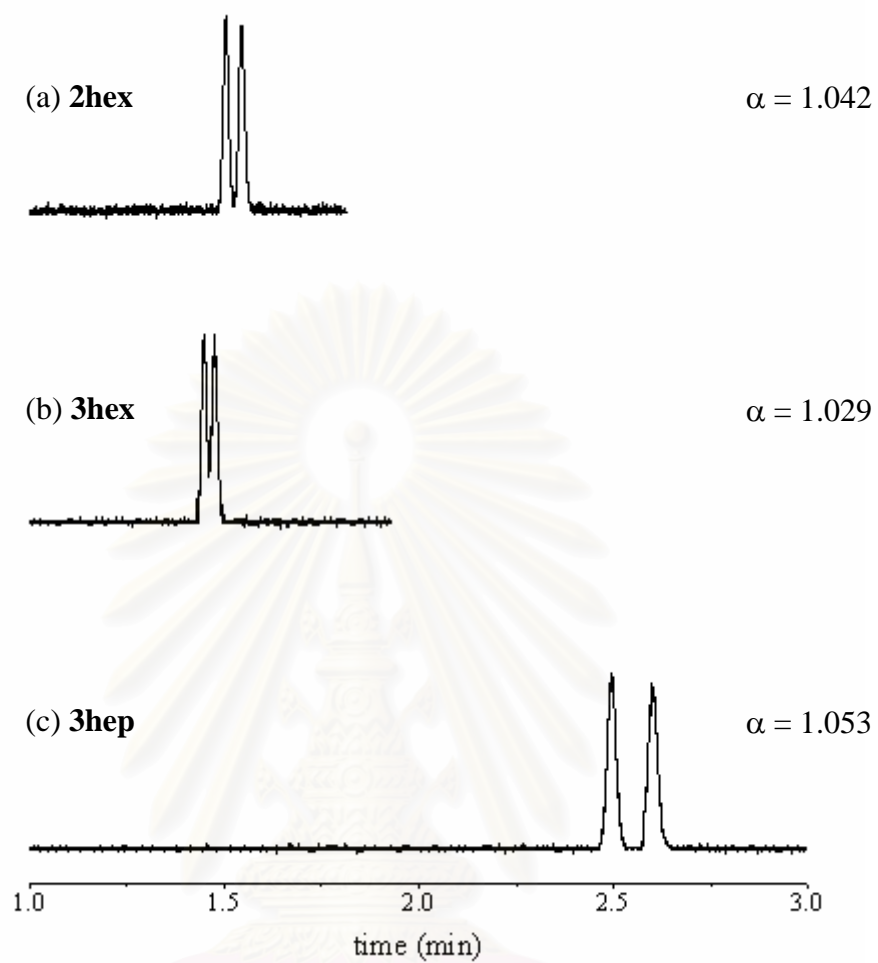
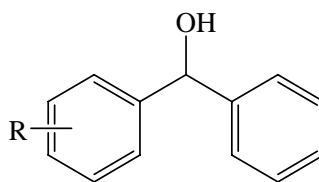


**Figure 4.27** Chromatograms of (a) **2hex**, (b) **3hex** and (c) **3hep** on ASiMe column at 80 °C.

สถาบันวิทยบริการ  
จุฬาลงกรณ์มหาวิทยาลัย

**Series 5: Diphenylmethanol with mono-substitution on an aromatic ring**



Racemic alcohols in series 5 are derivatives of diphenylmethanol with mono-substitution on an aromatic ring, as shown above. The substituent types are fluoro, chloro, bromo, methyl and methoxy at *ortho*-, *meta*- or *para*-position. Enthalpy differences responsible for chiral discrimination of alcohols in series 5 are depicted in figure 4.28. The effect of substituent position on separation could still be seen in phenyl chlorophenyl methanol. The greatest  $-\Delta(\Delta H)$  value was observed for *ortho*-substituted alcohol (**2ClBen**) and the values decreased in the order of *ortho* > *meta* > *para*, similar to results obtained from series 1. An exception was found for **2MeBen** where the enantioseparation was the lowest among three isomers (figure 4.29). Unfortunately, not all substituent type and isomer of alcohols in series 5 could be acquired; thus, a common trend on the effect of substituent type and position on enantioseparation could not be proposed.

In addition, the  $-\Delta(\Delta H)$  values of alcohols in series 5 were compared to alcohols in series 1 having similar substituent, as shown in figure 4.30. The  $-\Delta(\Delta H)$  values of alcohols in series 5 were generally lower than those of series 1, especially for *ortho*-substituted analytes. A significant reduction of  $-\Delta(\Delta H)$  values of **2MeBen** and **2ClBen** was noticed. This was probably caused by the increased steric hindrance of the aromatic moiety that obstructed the interaction between analytes and ASiMe phase.

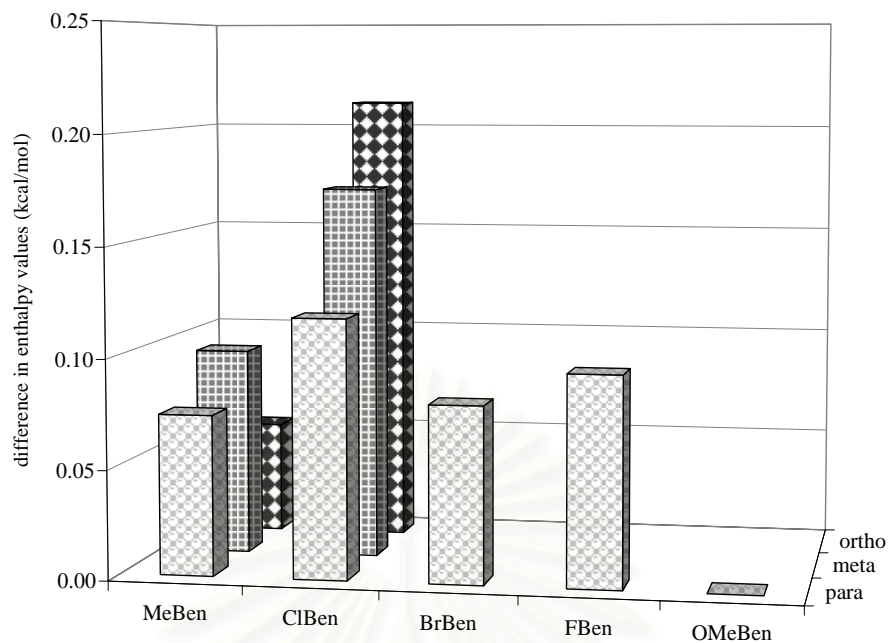


**Figure 4.28** Difference in enthalpy values ( $-\Delta(\Delta H)$ , kcal/mol) of the enantiomers of alcohols in series 5 on ASiMe column.

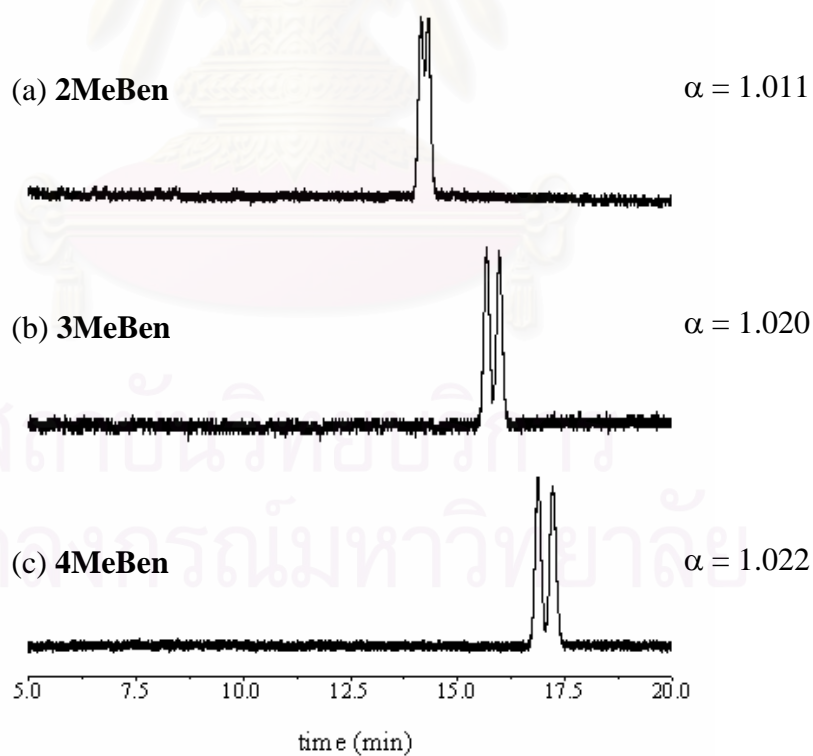


**Figure 4.29** Chromatograms of (a) **2MeBen**, (b) **3MeBen** and (c) **4MeBen** on ASiMe column at 150 °C.



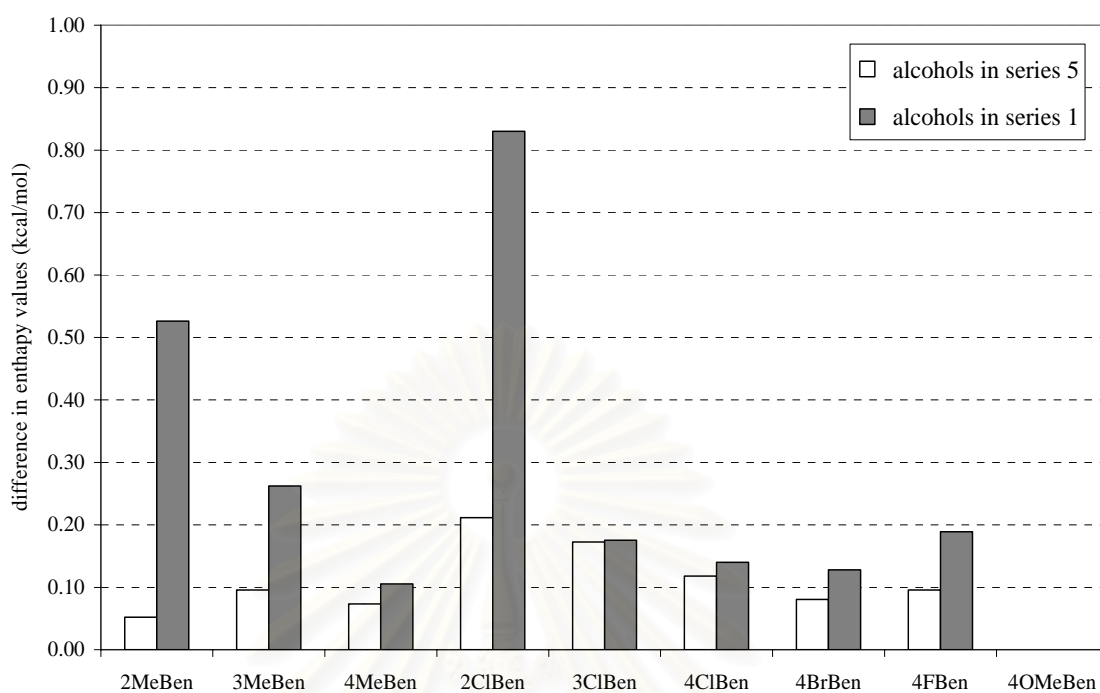


**Figure 4.30** Difference in enthalpy values ( $-\Delta(\Delta H)$ , kcal/mol) of the enantiomers of alcohols in series 5 (white bar) and series 1 (gray bar) on ASiMe column.

#### 4.4 Molecular modeling of the interaction between chiral solute and selector

The docking results were summarized in table 4.1. This study considered only the minimum binding energies acquired from the most probable configuration, indicating by the % frequency. Apart from information regarding binding energies, docking calculations also provided structural information. Both *R*- and *S*-enantiomers of each analytes can be partially interacted in a similar fashion with the cavity of ASiMe at the larger rim. Comparing the effect of substituent type, as in **4Me** and **4OMe**, it was found that analytes were likely to orient their aromatic rings outward of ASiMe cavity (figure 4.31). Considering the effect of substituent position, as seen from three methoxy-substituted analytes, the two different orientations for the analyte were observed when the substituent position was changed. The aromatic moiety of **2OMe** was pointing toward into the ASiMe cavity while the aromatic moiety of **3OMe** and **4OMe** were directed outside. These results indicated that the position of substituent had much stronger influence to orientation than the type of substituent (figure 4.31). It could be seen that when the structure of substituent was changed from straight-chain (as **4Bu**) to branch chain (as **4tBu**), the complex structures were very much different as seen from figure 4.32. This result was probably caused by appropriate configuration of *tert*-butyl substituent for interaction with ASiMe more than *n*-butyl substituent.

**Table 4.1** The docking results of selected analytes and ASiMe.

analyte		binding energy <sup>(a)</sup> ( $\Delta H$ , kcal/mol)	% frequency	$-\Delta(\Delta H) = -(\Delta H_{\text{low}} - \Delta H_{\text{high}})^{(b)}$ (kcal/mol)
<b>1</b>	<i>R</i>	-6.16 (-5.88)	75 (23)	0.32
	<i>S</i>	-6.48	93	
<b>4MeBen</b>	<i>R</i>	-6.23 (-6.26/-6.14)	43 (26/18)	0.31
	<i>S</i>	-6.54 (-6.56/-6.17)	46 (29/16)	
<b>4Me</b>	<i>R</i>	-5.75 (-5.59)	78 (21)	0.08
	<i>S</i>	-5.83	88	
<b>4Et</b>	<i>R</i>	-5.54 (-5.15)	74 (10)	0.36
	<i>S</i>	-5.90	89	
<b>4Bu</b>	<i>R</i>	-4.66 (-5.19/-4.74)	32 (18/11)	0.21
	<i>S</i>	-4.87 (-4.84/-5.54)	48 (16/12)	
<b>4tBu</b>	<i>R</i>	-6.13 (-5.83)	66 (30)	0.08
	<i>S</i>	-6.21	88	
<b>2OMe</b>	<i>R</i>	-6.27 (-6.00)	87 (12)	0.33
	<i>S</i>	-5.94 (-5.91)	67 (31)	
<b>3OMe</b>	<i>R</i>	-5.32 (-5.30)	70 (29)	0.34
	<i>S</i>	-5.66 (-5.30)	46 (40)	
<b>4OMe</b>	<i>R</i>	-5.70 (-5.56)	77 (18)	0.10
	<i>S</i>	-5.60	81	

**Note** (a) values for the 2<sup>nd</sup> and the 3<sup>rd</sup> most probable configurations shown in parenthesis

(b) difference of binding energy between low energy and high energy complexes

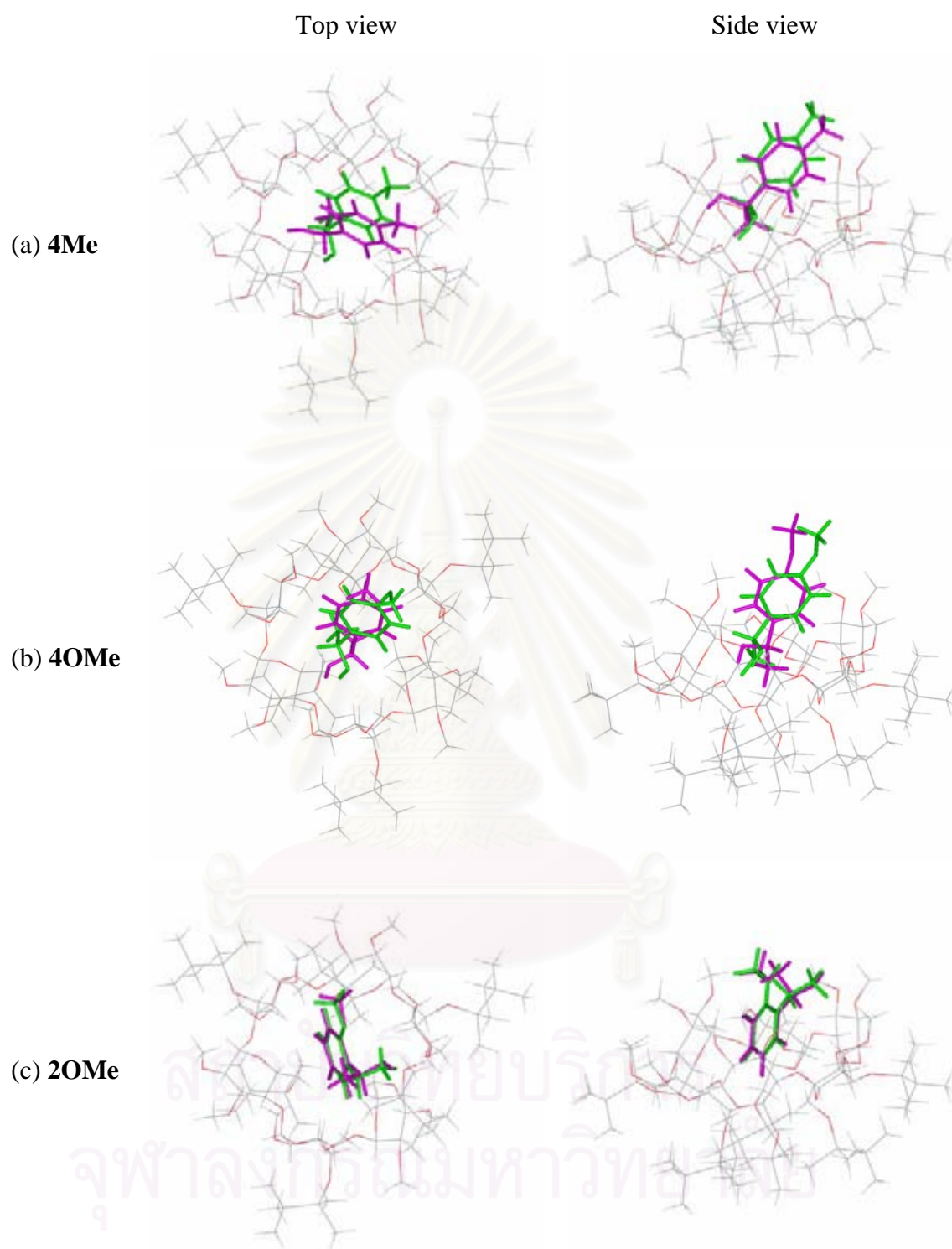


**Figure 4.31** Superimposed of lowest energy complexes between ASiMe and (a) **4Me**, (b) **4OMe** and (c) **2OMe** in *R*-form (green) and *S*-form (pink) in both top and side views.

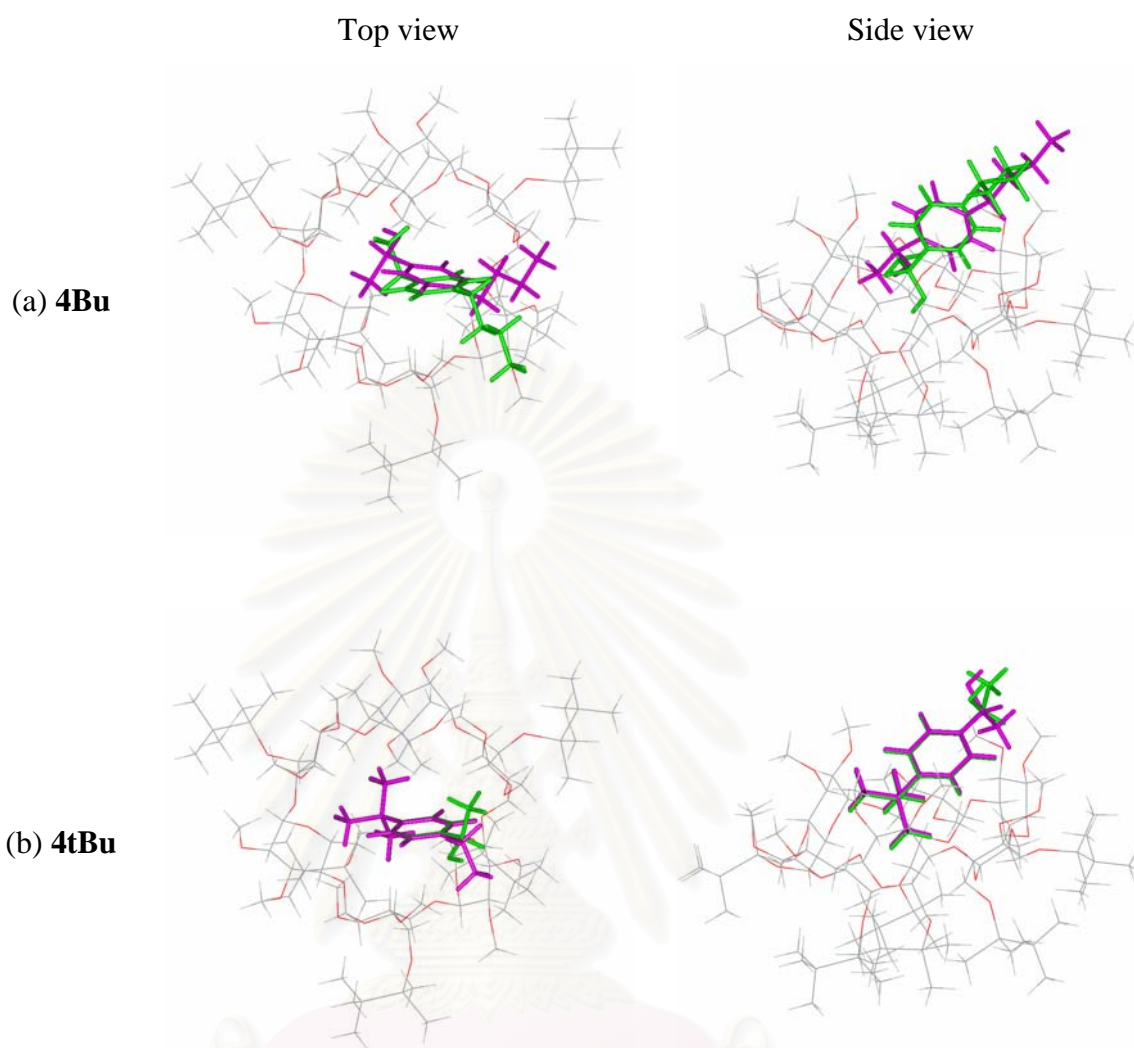


**Figure 4.32** Superimposed of lowest energy complexes between ASiMe and (a) **4Bu** and (b) **4tBu** in *R*-form (green) and *S*-form (pink) in both top and side views.

ศูนย์หน่วยบริการ  
จุฬาลงกรณ์มหาวิทยาลัย

From the docking configuration, most analytes generated more than one preferable configuration, except for *S*-forms of **1**, **4Me**, **4Et**, **4tBu** and **4OMe** (table 4.1). This might affect the selection of the appropriated docking configuration for the study of the formation of analytes/ASiMe complex. Other factors which might affect the docking calculation are as followed:

1. The Lennard-Jones 12-6 parameters of carbon atom were used for silicon atom since the Lennard-Jones 12-6 parameters for silicon atom were not available.
2. Although temperature played an important role in separation, it was not considered in the docking calculations with LGA.
3. The flexibility of ASiMe structure cannot be performed.

According to table 4.1, it can be seen from binding energy values that the *S*-form of most analytes, except for **2OMe** and **4OMe**, has a preference to associate with ASiMe rather than the *R*-form. The experimental results of reference analyte (**1**) obtained from gas chromatographic method displayed the elution sequence of *S*-form before *R*-form, demonstrating the stronger interaction between *R*-form and ASiMe. The difference in the binding preference is worth for further investigation.

The entropy parameter may also affect the elution sequence of enantiomeric pairs. The entropic calculation of reference analyte (**1**) was performed since the elution order of **1** was known from GC experiment (*S* before *R*). The entropy values of *R*-form/ASiMe and *S*-form/ASiMe complexes acquired from calculation at AM1 level were +651.88 and +668.65 cal/mol·K, respectively; therefore, the difference of entropy between *R*-form/ASiMe and *S*-form/ASiMe complexes was -16.77 cal/mol·K. The elution order of **1** was then re-evaluated from the obtained difference of entropy value together with the binding energy difference. The order of *R* before *S* was still obtained, at both low and high temperatures, which was not in agreement with the GC experiment.

Additionally, the binding energy difference of analytes with closely related structure, such as alkyl- or methoxy-substituted analytes, did not correspond with the experimental results. For the methoxy-substituted analytes, the enantioseparation values obtained from the experiment were in order of **2OMe** > **3OMe** > **4OMe** whereas results from the docking calculation did not show a similar trend. However, the second and third most probable configurations were not used to calculate the binding energy difference.

Since both host and guest structures are rigid in the docking calculations and energy determination is empirical, the docking configurations might not be the good representative for minimum structure. The docking configurations of all analytes were re-optimized at MM+ level and the binding energies were more accurately determined using AM1 and 3-21G calculations. The binding energy difference of enantiomeric pairs is summarized in table 4.2. Considering the **4MeBen** and **4Me**, calculated results were in agreement with the experiments (figure 4.8). However, the binding energy difference of alkyl- or methoxy-substituted analytes did not agree with the experimental results. Interestingly, the elution sequence alternation of enantiomer pairs was also observed when different calculation methods were performed. It should be pointed out that only the most probable configurations from the docking calculation were re-optimized and recalculated at higher level. Results might be different if other preferable structures were investigated.

**Table 4.2** Comparison of the binding energy difference ( $-\Delta(\Delta H)$ ) obtained for the analyte and ASiMe complex.

analyte	methods		
	MM+	AM1	3-21G
<b>1</b>	0.11	2.80	6.94
<b>4MeBen</b>	0.82	0.70	3.30
<b>4Me</b>	1.13	1.70	4.02
<b>4Et</b>	1.64	3.80	1.27
<b>4Bu</b>	2.49	3.00	1.19
<b>4tBu</b>	0.12	1.40	1.09
<b>2OMe</b>	0.82	0.10	5.62
<b>3OMe</b>	1.35	5.20	0.10
<b>4OMe</b>	2.11	1.60	4.44



## CHAPTER V

### CONCLUSION

Ninety chiral alcohol analytes with closely related structure were enantioseparated with hexakis(2,3-di-*O*-methyl-6-*O*-*tert*-butyldimethylsilyl)- $\alpha$ -cyclodextrin (or ASiMe) column. Approximately 93% of chiral analytes could be successfully enantioseparated with ASiMe column.

To derive more information about the influence of analyte structure on the enantioseparation on ASiMe phases systematically, several groups of analytes with closely related structure were selected and thermodynamic investigation was performed using van't Hoff approach. As expected, the interactions of analytes towards ASiMe column are greater than interactions towards a nonchiral polysiloxane column, as indicated by larger  $-\Delta H$  and  $-\Delta S$  values on chiral column. The  $-\Delta H_2$  and  $-\Delta S_2$  values obtained from ASiMe column exhibited similar trend. Furthermore, these values of all analytes are relatively comparable demonstrating that the main analyte contributions to the interaction arise from the hydroxyl group. Nonetheless, the interaction strength does not necessarily correlate with the discrimination of enantiomers, since some analytes showing strong interaction with stationary phase do not exhibit high enantioseparation.

On ASiMe phase, the position of substituent has great effect to enantioseparation than the type of substituent, as seen from the mono-substituted analytes. The substitution at *ortho*-position of the aromatic ring seems to enhance the enantioselectivity than substitution at *meta*- or *para*-position. However, type of substituent also plays an important role in enantioseparation, such as the halogen-substituted analytes. The small and highly electronegative substituents, such as fluoro, on an aromatic ring of analytes tend to promote enantioresolution.

To understand the mechanism of chiral recognition, the molecular docking method using the Lamarckian genetic algorithm (LGA), including binding energy calculation, were employed. From calculation results, the differences of binding energies were not corresponding with the experimentally determined thermodynamic values. Although molecular docking calculations provide the unexpected results, some information involving complex formation is generated. Both *R*- and *S*-enantiomers of each analyte can be partially combined to the cavity of ASiMe at the large rim in a similar fashion. The docking configurations were affected by the position, type and structure of substituent.

All the above results demonstrated that the differences in retention and degree of separation of all of alcohol enantiomers on ASiMe column depended on several factors, such as type, position and number of substituent on the aromatic ring. Hopefully, further study with larger number of analytes with various substitution patterns as well as appropriate molecular modeling calculation, such as molecular dynamics simulation, will lead to precise assumption about analyte-stationary phase interaction and better understanding of enantiorecognition mechanism.

## REFERENCES

1. Kim, H., Jeong, K., Lee, S., and Jung, S. Molecular modeling of the chiral recognition of propranolol enantiomers by a  $\beta$ -cyclodextrin. Bull. Korean Chem. Soc. 24 (2003): 95-98.
2. Franks, M. E., Macpherson, G. R., and Figg, W. D. Thalidomide. Lancet 363 (2004): 1802-1811.
3. Zada, A., and Harel, M. Enzymatic transesterification of racemic lavandulol: preparation of the two enantiomeric alcohols and of the two enantiomers of lavandulyl senecioate. Tetrahedron: Asymmetry 15 (2004): 2339-2343.
4. Caner, H., Groner, E., and Levy, L. Trends in development of chiral drugs. DDT 9 (2004): 105-110.
5. Schurig, V. Chiral separations using gas chromatography. Trends Anal. Chem. 21 (2002): 647-661.
6. Francotte, E. R. Enantioselective chromatography as a powerful alternative for the preparation of drug enantiomers. J. Chromatogr. A 906 (2001): 379-397.
7. Maier, N. M., Franco, P., and Lindner, W. Separation of enantiomers: needs, challenges, perspectives. J. Chromatogr. A 906 (2001): 3-33.
8. Schurig, V. Separation of enantiomers by gas chromatography. J. Chromatogr. A 906 (2001): 275-299.
9. Schurig, V. Enantiomer separation by gas chromatography on chiral stationary phases. J. Chromatogr. A 666 (1994): 111-129.

10. König, W. A. Enantioselective gas chromatography. Trends Anal. Chem. 12 (1993): 130-137.
11. Spanik, I., Krupcik, J., and Schurig, V. Comparison of two methods for the gas chromatographic determination of thermodynamic parameters of enantioselectivity. J. Chromatogr. A 843 (1999): 123-128.
12. McGachy, N. T., Grinberg, N., and Variankaval, N. Thermodynamic study of *N*-trifluoroacetyl-*O*-alkyl nipecotic acid ester enantiomer on diluted permethylated  $\beta$ -cyclodextrin stationary phase. J. Chromatogr. A 1064 (2005): 193-204.
13. Skórka, M., Asztemborska, M., and Żukowski, J. Thermodynamic studies of complexation and enantiorecognition processes of monoterpenoids by  $\alpha$ - and  $\beta$ -cyclodextrin in gas chromatography. J. Chromatogr. A 1078 (2005): 136-143.
14. Shitangkoon, A., Yanchinda, J., and Shiowatana, J. Thermodynamic study on the gas chromatographic separation of the enantiomers of aromatic alcohols using heptakis(2,3-di-*O*-methyl-6-*O*-*tert*-butyldimethylsilyl)- $\beta$ -cyclodextrin as a stationary phase. J. Chromatogr. A 1049 (2004): 223-226.
15. König, W. A., Francke, W., and Benecke, I. Gas chromatographic enantiomer separation of chiral alcohols. J. Chromatogr. 239 (1982): 227-231.
16. King, A. O., Corley, E. G., Anderson, R. K., Larsen, R. D., Verhoeven, T. R., Reider, P. J., Xiang, Y. B., Belley, M., Leblanc, Y., Labelle, M., Prasit, P., and Zamboni, R. J. An Efficient Synthesis of LTD an Antagonist L-699,392. J. Org. Chem. 58 (1993): 3731-3735.

17. Konghuirob, O. Enantiomeric separation of alcohols by gas chromatography using cyclodextrin derivatives as stationary phases. Master's Thesis, Department of Chemistry, Faculty of Science, Chulalongkorn University, 2004.
18. Iamsam-ang, W. Enantiomeric separation of aromatic alcohols by gas chromatography using derivatized  $\beta$ -cyclodextrins as stationary phases. Master's Thesis, Department of Chemistry, Faculty of Science, Chulalongkorn University, 2002.
19. Juvancz, Z. The role of cyclodextrins in chiral selective chromatography. Trends Anal. Chem. 21 (2002): 379-388.
20. Valle, E. M. M. D. Cyclodextrins and their uses: a review. Process Biochemistry 39 (2004): 1033-1046.
21. Szejtli, J. Introduction and general overview of cyclodextrin chemistry. Chem. Rev. 98 (1998): 1743-1753.
22. Nie, M. Y., Zhou, L. M., Liu, X. L., Wang, Q. H., and Zhu, D. Q. Gas chromatographic enantiomer separation on long-chain alkylated  $\beta$ -cyclodextrin chiral stationary phases. Anal. Chim. Acta 408 (2000): 279-284.
23. Kobor, F., and Schomburg, G. 6-*tert*-Butyldimethylsilyl-2,3-dimethyl- $\alpha$ -,  $\beta$ -, and  $\gamma$ -cyclodextrin, dissolved in polysiloxanes, as chiral selectors for gas chromatography: Influence of selector concentration and polysiloxane matrix polarity on enantioselectivity. J. High Resolut. Chromatogr. 16 (1993): 693-699.

24. Takahisa, E. and Engel, K.-H. 2,3-Di-*O*-methoxymethyl-6-*O*-*tert*-butyldimethylsilyl- $\gamma$ -cyclodextrin: a new class of cyclodextrin derivatives for gas chromatographic separation of enantiomers. J. Chromatogr. A 1063 (2005): 181-192.
25. Takahisa, E. and Engel, K.-H. 2,3-Di-*O*-methoxymethyl-6-*O*-*tert*-butyldimethylsilyl- $\beta$ -cyclodextrin, a useful stationary phase for gas chromatographic separation of enantiomers. J. Chromatogr. A 1076 (2005): 148-154.
26. Tisse, S., Peulon-Agasse, V., Cardinaël, P., Bouillon J.-P., and Combret, J.-C. Capillary gas chromatographic properties of three new mono-ester permethylated  $\beta$ -cyclodextrin derivatives. Anal. Chim. Acta 560 (2006): 207-217.
27. Kobor, F., Angermund, K., and Schomburg, G. Molecular modelling experiments on chiral recognition in GC with specially derivatized cyclodextrins as selectors. J. High Resolut. Chromatogr. 16 (1993): 299-311.
28. Ramos, M. C. K. V., Teixeira, L. H. P., Neto, F. R. A., Barreiro, E. J., Rodrigues, C. R., and Fraga, C. A. M. Chiral separation of  $\gamma$ -butyrolactone derivatives by gas chromatography on 2,3-di-*O*-methyl-6-*O*-*tert*-butyldimethylsilyl- $\beta$ -cyclodextrin. J. Chromatogr. A 985 (2003): 321-331.
29. Cervelló, E., Mazzucchi, F., and Jaime, C. Molecular mechanics and molecular dynamics calculations of the  $\beta$ -cyclodextrin inclusion complexes with *m*-, and *p*-nitrophenyl alkanoates. J. Mol. Struct. (Theochem) 530 (2000): 155-163.

30. Lipkowitz, K. B., Coner, B., Penterson, M. A., and Morreale, A.  
Enantioselective binding in gas chromatography: A computational study of chiral selection by permethyl- $\beta$ -cyclodextrin. J. Phys. Org. Chem. 10 (1997): 311-322.
31. Beier, T., and Höltje, H.-D. Modified cyclodextrins as chiral selector: molecular modelling investigations on the enantioselective binding properties of heptakis(2,3-di-*O*-methyl-6-*O*-*tert*-butyldimethylsilyl)- $\beta$ -cyclodextrin. J. Chromatogr. B 708 (1998): 1-20.
32. Jesus, M. B. de, Pinto, L. de M. A., Fraceto, L. F., Takanata, Y., Lino, A. C. S., Jaime, C., and Paula, E. de. Theoretical and experimental study of a praziquantel and  $\beta$ -cyclodextrin inclusion complex using molecular mechanic calculations and  $^1\text{H}$ -nuclear magnetic resonance. J. Pharmaceut. Biomed. Anal. 41 (2006): 1428-1432.
33. Morris, G. M., Goodsell, D. S., Huey, R., Hart, W. E., Halliday, S., Belew, R., and Olson, A. J. [Online], 2000. Available from:  
<http://www.scripps.edu/pub/olson-web/doc/autoflex/parameters.html>  
[2001, November 20]
34. Ratanasak, K. Quantitative structure activity relationship and molecular docking of antimalarial tricyclic 1,2,4-trioxane derivatives. Master's Thesis, Department of Chemistry, Faculty of Science, Chulalongkorn University, 2003.
35. Tonmunphean, S. Quantum chemistry and QSAR of antimalarial artemisinin and its derivatives. Doctoral dissertation, Department of Chemistry, Faculty of Science, Chulalongkorn University, 2000.
36. Goodsell, D. S., Morris, G. M., and Olson, A. J. Automated docking of flexible ligands: Applications of AutoDock. J. Mol. Rec. 9 (1996): 1-5.

37. Leach, A. R. Molecular modelling: principles and applications. 2<sup>nd</sup> ed. England: Prentice Hall, 2001.
38. Levine, I. N. Quantum chemistry. 5<sup>th</sup> ed. USA: Prentice Hall, 2000.
39. Hill J.-R., Subramanian L., and Maiti, A. Molecular modeling techniques in material sciences. USA: Taylor & Francis Group, 2005.
40. Gokel, G. W. Dean's Handbook of Organic Chemistry. 2<sup>nd</sup> ed. New York: McGraw-Hill, 2004.
41. Kaye, G. W. C., and Laby, T. H. Tables of Physical and Chemical Constants. UK: Bookcraft, 1995.



สถาบันวิทยบริการ  
จุฬาลงกรณ์มหาวิทยาลัย





**APPENDICES**

สถาบันวิทยบริการ  
จุฬาลงกรณ์มหาวิทยาลัย

## Appendix A

### Glossary

**Adjusted retention time ( $t'_R$ )** is the absolute retention of a compound on a stationary phase. This value is calculated by subtracting the time of unretained compound ( $t_M$ ) from the compound's retention time ( $t_R$ ), according to:

$$t'_R = t_R - t_M$$

**Correlation coefficient ( $R^2$ )** is a number between 0 and 1, which indicates the degree of linear relationship between two variables.

**Distribution constant ( $K$ )** is defined as the concentration ratio of a compound in a stationary phase and in a mobile phase.  $K$  is related to retention factor according to the equation shown below.

$$K = \frac{C_s}{C_M} \\ = k' \cdot \frac{V_M}{V_s} = k' \cdot \beta$$

$C_s, C_M$  = concentration of a solute in stationary phase and mobile phase, respectively

$V_s, V_M$  = volume of stationary phase and mobile phase, respectively

**Number of theoretical plate ( $N$ )** is used as a measure of column efficiency. It is defined as the square of the ratio of the retention of analyte divided by peak broadening.

$$N = 16 \left[ \frac{t_R}{w_b} \right]^2 = 5.545 \left[ \frac{t_R}{w_h} \right]^2$$

$t_R$	=	retention time of a peak
$w_b$	=	peak width at base (in the same unit as $t_R$ )
$w_h$	=	peak width at half height (in the same unit as $t_R$ )

**Phase ratio ( $\beta$ )** is defined as the ratio of the volume of mobile phase ( $V_M$ ) to the volume of stationary phase ( $V_S$ ) in the column. It is a unitless value and can be calculated from column dimension by the following equation.

$$\beta = \frac{r_c}{2d_f}$$

$r_c$	=	capillary column radius
$d_f$	=	stationary phase film thickness (in the same unit as $r_c$ )

**Retention factor or capacity factor ( $k'$ )** is defined as the ratio of analyte mole in the stationary phase and mobile phase. It is equivalent to the ratio of time of analyte molecules spend in stationary phase ( $t'_R$ ) to the time that they spend in that mobile phase ( $t_M$ ). The retention factor is calculated from:

$$k' = \frac{t_R - t_M}{t_M} = \frac{t'_R}{t_M}$$

**Separation factor or selectivity ( $\alpha$ )** is a measure of the quality of peak separation expressed as a relative adjusted retention. It is calculated from the ratio of the retention factors of the two adjacent peaks, when  $k'_2 \geq k'_1$ .

$$\alpha = \frac{k'_2}{k'_1} = \frac{t_{R,2} - t_M}{t_{R,1} - t_M}$$

## Appendix B

### NMR Spectra

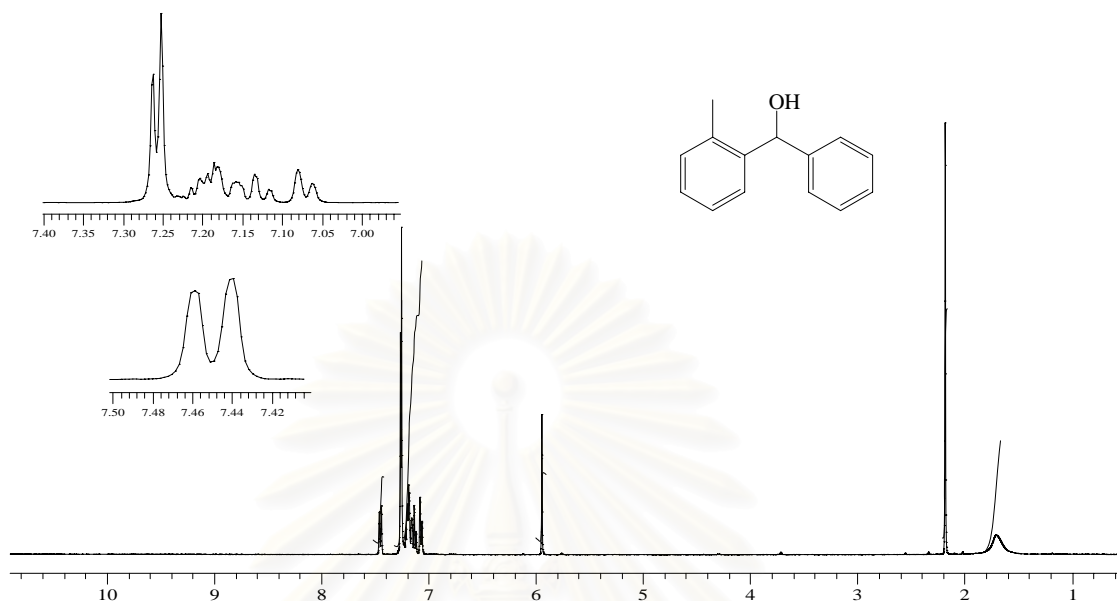


Figure B1 NMR spectrum of **2MeBen**; <sup>1</sup>H NMR (CDCl<sub>3</sub>, 400 MHz): δ 1.70 (1H, s, CHOH), 2.19 (3H, s, ArCH3), 5.93 (1H, s, CHOH), 7.05-7.24 (4H, m, ArMeH), 7.26 (4H, d, ArH), 7.45 (1H, d, ArH)

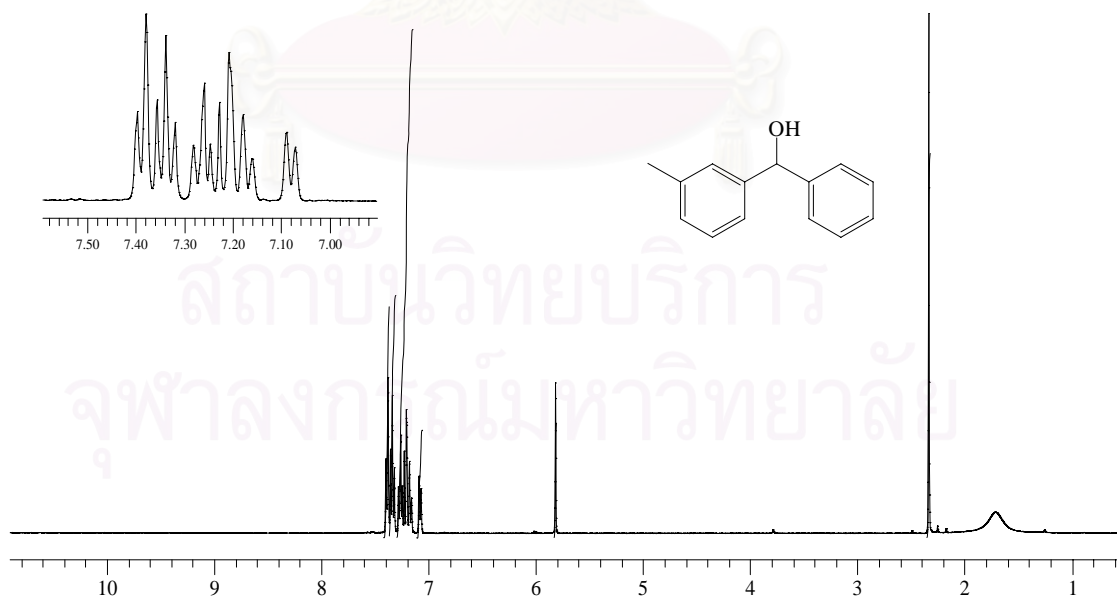


Figure B2 NMR spectrum of **3MeBen**; <sup>1</sup>H NMR (CDCl<sub>3</sub>, 400 MHz): δ 1.70 (1H, s, CHOH), 2.35 (3H, s, ArCH3), 5.84 (1H, s, CHOH), 7.08 (1H, d, ArMeH), 7.14-7.43 (8H, m, ArH)

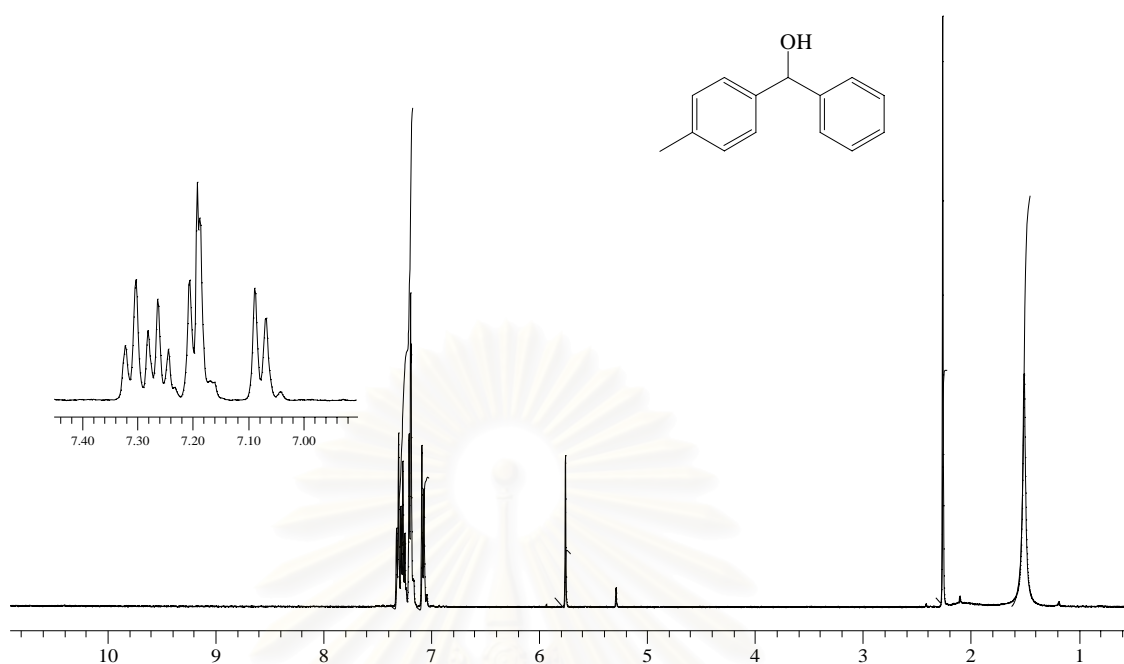


Figure B3 NMR spectrum of **4MeBen**;  $^1\text{H}$  NMR ( $\text{CDCl}_3$ , 400 MHz):  $\delta$  1.51 (1H, s, CHOH), 2.28 (3H, s, ArCH<sub>3</sub>), 5.76 (1H, s, CHOH), 7.08 (2H, d, ArMeH), 7.17-7.34 (7H, m, ArH)

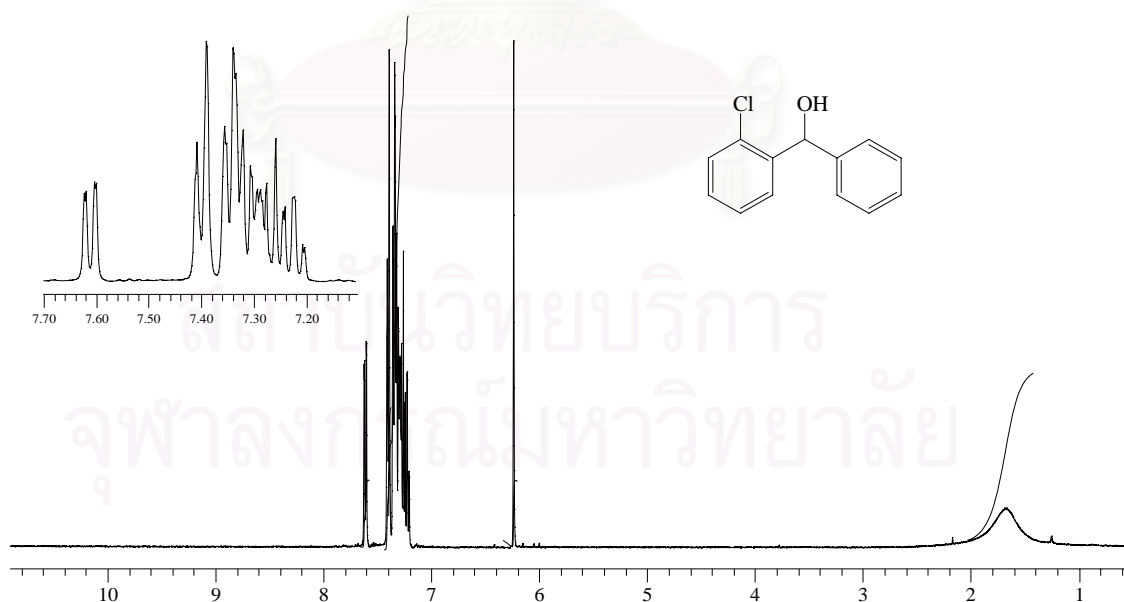


Figure B4 NMR spectrum of **2ClBen**;  $^1\text{H}$  NMR ( $\text{CDCl}_3$ , 400 MHz):  $\delta$  1.67 (1H, s, CHOH), 6.24 (1H, s, CHOH), 7.18-7.37 (6H, m, ArH), 7.40 (2H, d, ArClH), 7.61 (1H, d, ArClH)

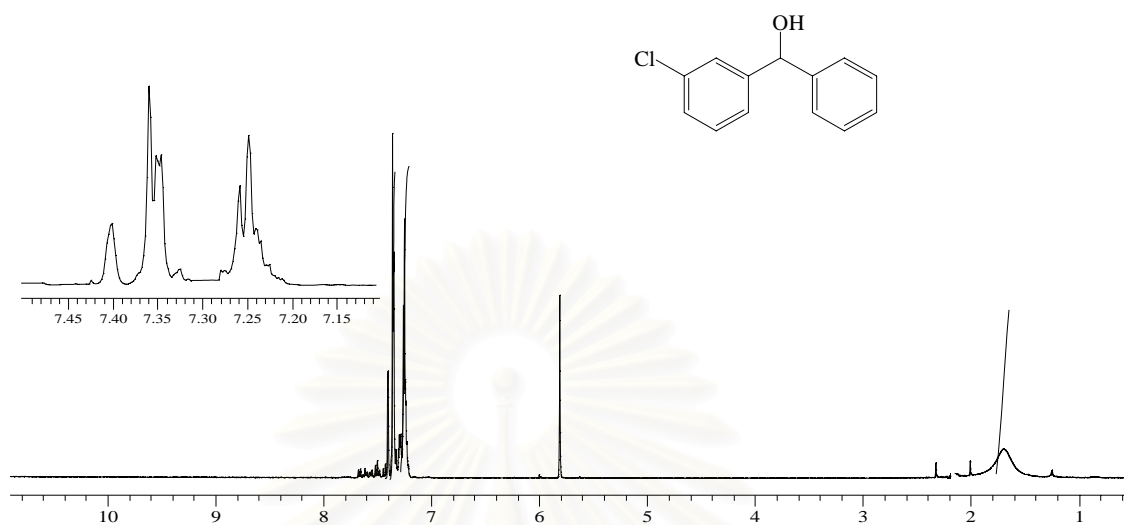


Figure B5 NMR spectrum of **3ClBen**;  $^1\text{H}$  NMR ( $\text{CDCl}_3$ , 400 MHz):  $\delta$  1.69 (1H, s,  $\text{CHOH}$ ), 5.82 (1H, s,  $\text{CHOH}$ ), 7.25 (4H, d,  $\text{ArH}$ ), 7.36 (4H, d,  $\text{ArH}$ ), 7.40 (1H, s,  $\text{ArClH}$ )

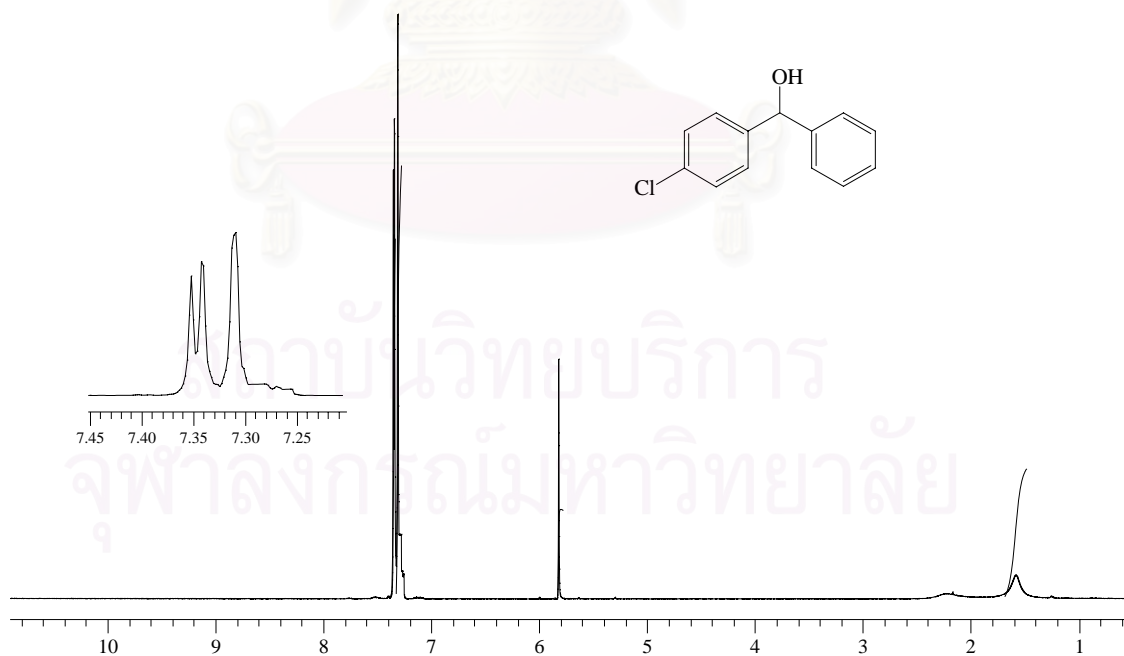


Figure B6 NMR spectrum of **4ClBen**;  $^1\text{H}$  NMR ( $\text{CDCl}_3$ , 400 MHz):  $\delta$  1.58 (1H, s,  $\text{CHOH}$ ), 5.82 (1H, s,  $\text{CHOH}$ ), 7.31 (5H, s,  $\text{ArH}$ ), 7.35 (4H, d,  $\text{ArClH}$ )

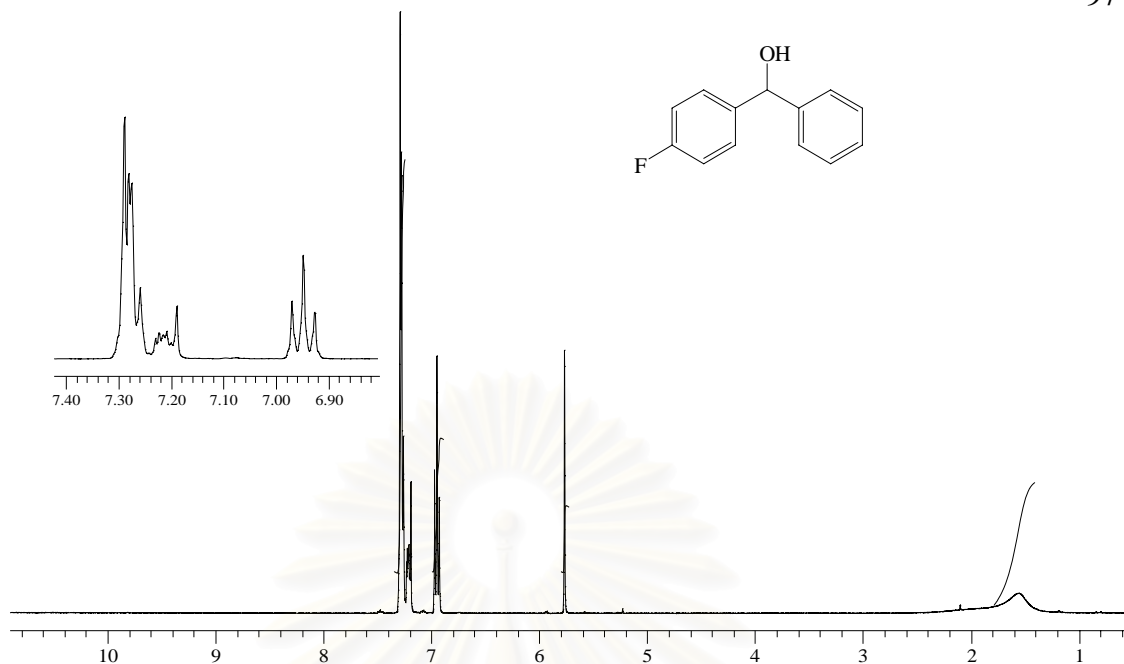


Figure B7 NMR spectrum of **4FBen**;  $^1\text{H}$  NMR ( $\text{CDCl}_3$ , 400 MHz):  $\delta$  1.57 (1H, s,  $\text{CHOH}$ ), 5.77 (1H, s,  $\text{CHOH}$ ) 6.95 (2H, t,  $\text{ArH}$ ), 7.18-7.32 (7H, m,  $\text{ArH}$ )

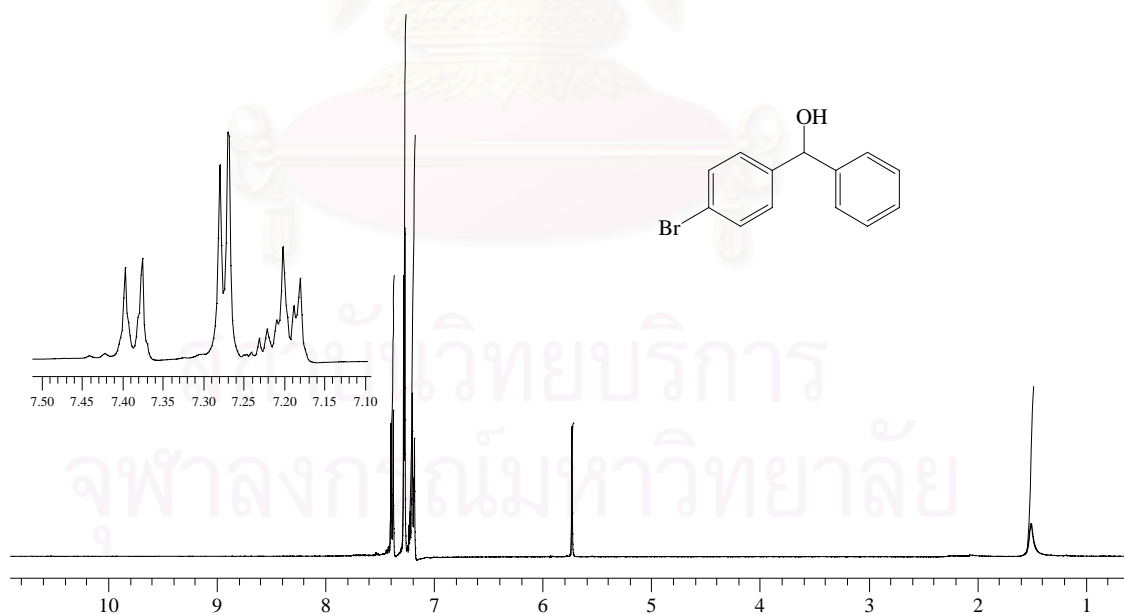


Figure B8 NMR spectrum of **4BrBen**;  $^1\text{H}$  NMR ( $\text{CDCl}_3$ , 400 MHz):  $\delta$  1.51 (1H, s,  $\text{CHOH}$ ), 5.75 (1H, s,  $\text{CHOH}$ ), 7.17-7.24 (3H, m,  $\text{ArH}$ ), 7.28 (4H, d,  $\text{ArH}$ ), 7.39 (2H, d,  $\text{ArBrH}$ )

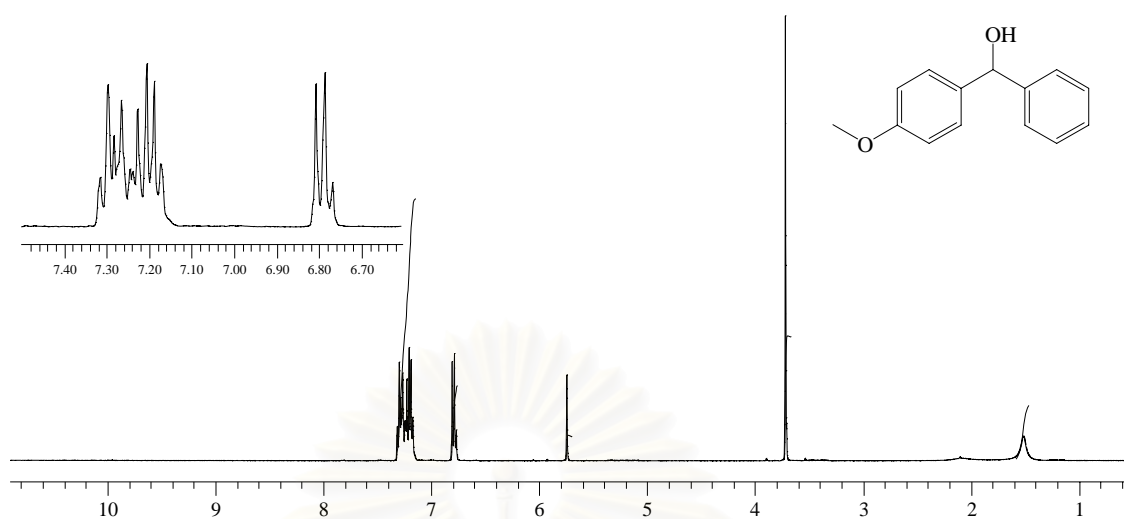


Figure B9 NMR spectrum of **4OMeBen**; <sup>1</sup>H NMR (CDCl<sub>3</sub>, 400 MHz): δ 1.51 (1H, s, CHOH), 3.72 (3H, s, CH<sub>3</sub>O), 5.75 (1H, s, CHOH), 6.79 (2H, t, ArH), 7.14-7.35 (7H, m, ArH)

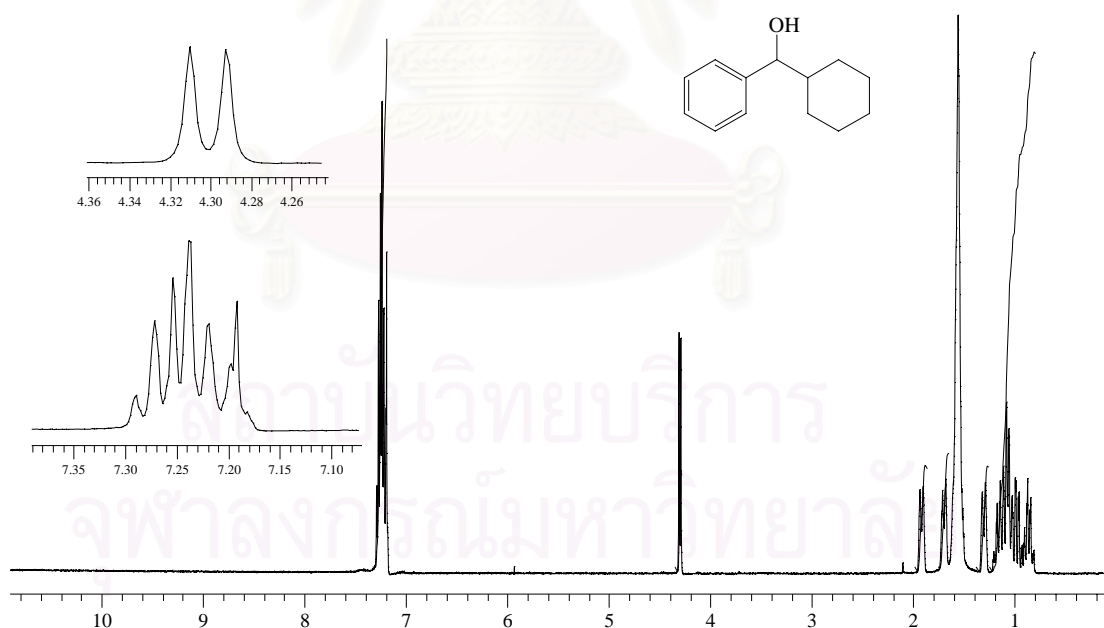


Figure B10 NMR spectrum of **24**; <sup>1</sup>H NMR (CDCl<sub>3</sub>, 400 MHz): δ 0.80-1.23 (8H, m, c-HxH), 1.30 (1H, d, c-HxH), 1.56 (1H, s, CHOH), 1.69 (1H, d, c-HxH), 1.92 (1H, d, c-HxH), 4.30 (1H, d, CHOH), 7.17-7.31 (5H, m, ArH)



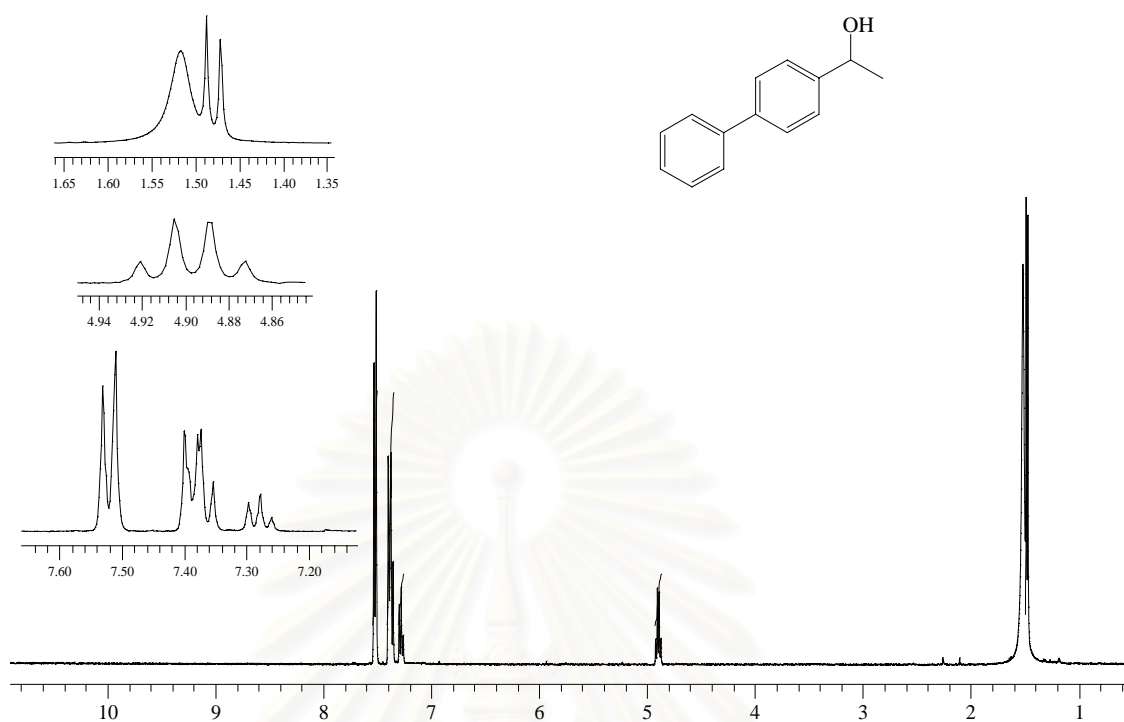


Figure B11 NMR spectrum of **4Phe**; <sup>1</sup>H NMR (CDCl<sub>3</sub>, 400 MHz): δ 1.48 (3H, d, CHCH<sub>3</sub>), 1.52 (1H, s, CHOH), 4.90 (1H, q, CHOH), 7.28 (1H, t, ArH), 7.34-7.42 (4H, m, ArH), 7.52 (4H, d, ArH)

สถาบันวิทยบริการ  
จุฬาลงกรณ์มหาวิทยาลัย

## Appendix C

### Thermodynamic Studies

**Table 1** Equations and correlation coefficient of some alcohols obtained from  $\ln k'$  vs.  $1/T$  plots on OV-1701 column

analyte	Equation: $\ln k' = m(1/T)+c$		$R^2$
	m	c	
2MeBen	7350.9	-14.451	0.9996
3MeBen	7408.3	-14.596	0.9996
4MeBen	7379.8	-14.482	0.9997
2ClBen	7529.6	-14.550	0.9997
3ClBen	7839.7	-14.998	0.9997
4ClBen	7777.1	-14.850	0.9997
4FBen	7186.7	-14.382	0.9996
4BrBen	8034.6	-15.016	0.9998
4OMeBen	8025.6	-15.192	0.9998
24	6739.0	-13.720	0.9995
4Phe	7598.9	-14.676	0.9997
2but	3994.8	-13.03	0.9997
2pen	4212.9	-12.772	0.9997
2hex	4595.1	-13.044	0.9998
3hex	4544.7	-12.958	0.9997
2hep	4988.4	-13.401	0.9997
3hep	4925.8	-13.281	0.9997
2non	5823.7	-14.320	0.9997
3non	5757.8	-14.195	0.9997
2unde	6615.6	-15.184	0.9998

**Table 2** Equations and correlation coefficient of all alcohols obtained from  $\ln k'$  vs.  $1/T$  plots on ASiMe column

analyte	less retained enantiomer			more retained enantiomer		
	Equation: $\ln k' = m(1/T)+c$		$R^2$	Equation: $\ln k' = m(1/T)+c$		$R^2$
	m	c		m	c	
1	6504.9	-15.356	0.9998	6647.4	-15.676	0.9998
2	7657.2	-15.355	0.9994	7679.0	-15.400	0.9994
3	7632.7	-15.320	0.9997	7877.2	-15.814	0.9997
4	6754.1	-14.535	0.9993	7096.1	-15.236	0.9992
5	7167.4	-15.266	0.9992	7198.8	-15.334	0.9991
6	5940.4	-14.455	0.9998	6035.2	-14.680	0.9999
7	6642.0	-15.308	0.9990	6795.1	-15.652	0.9991
8	6667.3	-15.201	0.9997	6765.2	-15.421	0.9997
9	6631.3	-14.905	0.9997	6788.2	-15.251	0.9998
10	7046.1	-15.773	0.9992	7203.0	-16.118	0.9991
11	7477.1	-15.848	0.9994	7598.4	-16.099	0.9992
12	7263.7	-16.277	0.9998	-		
13	6357.9	-14.745	0.9999	6498.3	-15.060	0.9999
14	6463.1	-14.864	0.9997	6550.4	-15.067	0.9998
15	6649.9	-14.979	0.9997	-		
16	6315.8	-14.687	0.9998	6320.1	-14.697	0.9998
17	6691.7	-15.117	0.9997	-		
18	6905.5	-15.412	0.9996	6982.6	-15.586	0.9995
19	6793.5	-15.097	0.9998	6891.4	-15.319	0.9997
20	7520.3	-17.258	0.9995	7721.5	-17.712	0.9993
21	7116.8	-16.580	0.9997	7226.0	-16.825	0.9997
22	8019.3	-15.851	0.9997	8095.6	-16.009	0.9997
23	6861.2	-15.283	0.9994	7182.2	-15.961	0.9994

analyte	less retained enantiomer			more retained enantiomer		
	Equation: $\ln k' = m(1/T)+c$		$R^2$	Equation: $\ln k' = m(1/T)+c$		$R^2$
	m	c		m	c	
24	7306.4	-14.865	0.9987	7434.1	-15.125	0.9984
2Br	7037.8	-15.256	0.9992	7388.2	-15.982	0.9992
3Br	8191.1	-17.450	0.9989	8278.1	-17.640	0.9988
4Br	7721.4	-16.420	0.9995	7785.8	-16.560	0.9995
F4Br	8417.2	-17.826	0.9992	8452.1	-17.899	0.9992
2Cl	6646.2	-14.811	0.9991	7064.0	-15.688	0.9992
3Cl	7829.4	-17.093	0.9990	7917.6	-17.285	0.9989
4Cl	7304.7	-15.955	0.9995	7375.2	-16.109	0.9995
F4Cl	8043.9	-17.453	0.9995	8097.6	-17.566	0.9995
2F	5943.2	-14.119	0.9992	6376.6	-15.047	0.9992
3F	6701.4	-15.566	0.9991	6913.4	-16.028	0.9989
4F	6389.2	-14.927	0.9993	6484.3	-15.137	0.9991
F4F	7138.1	-16.447	0.9995	7214.3	-16.610	0.9994
4Et	7020.4	-15.614	0.9992	7070.7	-15.722	0.9991
4Bu	7681.1	-16.282	0.9991	7761.8	-16.453	0.9989
4tBu	7290.2	-15.792	0.9995	7401.3	-16.033	0.9995
2NO <sub>2</sub>	7785.0	-16.166	0.9991	7956.3	-16.524	0.9986
3NO <sub>2</sub>	8019.8	-16.143	0.9994	8104.8	-16.318	0.9994
4NO <sub>2</sub>	8086.4	-16.171	0.9994	8115.6	-16.232	0.9994
3CN	8774.2	-17.944	0.9993	8974.7	-18.352	0.9991
4CN	8344.4	-17.052	0.9993	8378.7	-17.124	0.9993
2OMe	6671.1	-14.771	0.9991	7056.4	-15.581	0.9991
3OMe	7175.4	-15.644	0.9995	7286.4	-15.883	0.9994
4OMe	6588.8	-14.814	0.9994	-		
2Me	6420.3	-14.630	0.9994	6685.1	-15.201	0.9993
3Me	6678.5	-15.259	0.9994	6810.4	-15.545	0.9993

analyte	less retained enantiomer			more retained enantiomer		
	Equation: $\ln k' = m(1/T)+c$		$R^2$	Equation: $\ln k' = m(1/T)+c$		$R^2$
	m	c		m	c	
4Me	6588.8	-15.077	0.9993	6641.8	-15.195	0.9993
2CF3	6332.7	-15.093	0.9991	6665.4	-15.791	0.9992
3CF3	6781.9	-15.829	0.9997	6972.3	-16.257	0.9996
4CF3	6751.3	-15.645	0.9994	6854.4	-15.873	0.9993
4OCF3	6732.8	-15.671	0.9991	6820.6	-15.859	0.9989
4Phe	8540.3	-16.564	0.9987	8579.3	-16.644	0.9985
24Cl	7918.5	-16.676	0.9993	7967.2	-16.779	0.9992
25Cl	7635.0	-16.038	0.9995	8609.9	18.008	0.9992
34Cl	7536.2	-15.617	0.9996	7598.4	-15.749	0.9996
24F	6771.5	-16.013	0.9996	6926.5	-16.360	0.9996
25F	6970.4	-16.324	0.9995	8141.8	-18.833	0.9988
26F	5900.9	-14.335	0.9999	6014.9	-14.600	0.9999
34F	6855.6	-15.888	0.9999	6968.0	16.146	0.9999
35F	7831.0	-18.065	0.9991	8187.4	-18.839	0.9993
24Me	7026.0	-15.547	0.9993	7083.6	-15.671	0.9991
25Me	6853.3	-15.208	0.9990	7183.0	-15.899	0.9984
34Me	6965.4	-15.389	0.9994	7011.3	-15.488	0.9992
triF	6827.4	-16.087	0.9997	6885.1	-16.222	0.9996
tetraF	6762.9	-15.829	0.9997	7053.2	-16.476	0.9996
pentaF	6311.9	-15.267	0.9998	6347.0	-15.351	0.9998
2but	4647.9	-14.187	0.9997	-		
2pen	5090.5	-14.585	0.9998	5152.1	-14.745	0.9999
2hex	5408.1	-14.725	1.0000	5506.3	-14.966	0.9999
3hex	5360.7	-14.649	0.9999	5414.9	-14.786	0.9999
2hep	5911.1	-15.348	0.9999	5991.3	-15.546	0.9999
3hep	5789.4	-15.103	0.9999	5910.3	-15.392	0.9999

analyte	less retained enantiomer			more retained enantiomer		
	Equation: $\ln k' = m(1/T)+c$		$R^2$	Equation: $\ln k' = m(1/T)+c$		$R^2$
	m	c		m	c	
2oc	6546.7	-16.232	0.9997	6633.7	-16.441	0.9997
3oc	6451.6	-16.077	0.9997	6555.8	-16.320	0.9998
4oc	6422.0	-16.027	0.9997	6489.8	-16.194	0.9997
2non	7226.5	-17.355	0.9992	7315.2	-17.563	0.9993
3non	6996.6	-16.860	0.9993	7115.5	-17.136	0.9994
2unde	7776.1	-17.642	0.9996	7851.0	-17.816	0.9997
2MeBen	8101.9	-15.944	0.9989	8128.2	-15.999	0.9987
3MeBen	8426.0	-16.611	0.9983	8474.1	-16.710	0.9980
4MeBen	8409.7	-16.525	0.9985	8446.6	-16.601	0.9982
2ClBen	8169.4	-15.788	0.9994	8275.9	-16.001	0.9992
3ClBen	8938.7	-17.158	0.9987	9025.5	-17.333	0.9984
4ClBen	9034.5	-17.292	0.9986	9093.9	-17.412	0.9982
4BrBen	9173.7	-17.184	0.9986	9214.2	-17.266	0.9984
4FBen	8246.8	-16.464	0.9985	8294.9	-16.563	0.9982
4OMeBen	8549.8	-16.203	0.9991	-		

สถาบันวิทยบริการ  
จุฬาลงกรณ์มหาวิทยาลัย

**Table 3** Thermodynamic parameters of some alcohols calculated from van't Hoff plots of  $\ln k'$  vs.  $1/T$  on OV-1701 column

analyte	$-\Delta H$ (kcal/mol)	$-\Delta S$ (cal/mol.K)
2MeBen	14.61	17.74
3MeBen	14.72	18.03
4MeBen	14.66	17.80
2ClBen	14.96	17.94
3ClBen	15.58	18.83
4ClBen	15.45	18.54
4FBen	14.28	17.61
4BrBen	15.96	18.87
4OMeBen	15.95	19.22
24	13.39	16.29
4Phe	15.10	18.19
2but	7.94	14.92
2pen	8.37	14.41
2hex	9.13	14.95
3hex	9.03	14.78
2hep	9.91	15.66
3hep	9.79	15.42
2non	11.57	17.48
3non	11.44	17.23
2unde	13.15	19.20

**Table 4** Thermodynamic parameters of all alcohols calculated from van't Hoff plots of  $\ln k'$  vs.  $1/T$  on ASiMe column

analyte	enthalpy term (kcal/mol)			entropy (cal/mol.K)		
	$-\Delta H_1$	$-\Delta H_2$	$-\Delta(\Delta H)$	$-\Delta S_1$	$-\Delta S_2$	$-\Delta(\Delta S)$
1	12.93	13.21	0.28	19.54	20.18	0.64
2	15.21	15.26	0.05	19.54	19.63	0.09
3	15.17	15.65	0.48	19.47	20.45	0.98
4	13.42	14.10	0.68	17.91	19.30	1.39
5	14.24	14.30	0.06	19.36	19.50	0.14
6	11.80	11.99	0.19	17.75	18.20	0.45
7	13.20	13.50	0.30	19.45	20.13	0.68
8	13.25	13.44	0.19	19.23	19.67	0.44
9	13.18	13.49	0.31	18.65	19.33	0.68
10	14.00	14.31	0.31	20.37	21.06	0.69
11	14.86	15.10	0.24	20.52	21.02	0.50
12	14.43	14.43	0.00	21.37	21.37	0.00
13	12.63	12.91	0.28	18.33	18.95	0.62
14	12.84	13.02	0.18	18.56	18.97	0.41
15	13.21	13.21	0.00	18.79	18.79	0.00
16	12.55	12.56	0.01	18.21	18.23	0.02
17	13.30	13.30	0.00	19.07	19.07	0.00
18	13.72	13.87	0.15	19.65	19.99	0.34
19	13.50	13.69	0.19	19.03	19.47	0.44
20	14.94	15.34	0.40	23.32	24.22	0.90
21	14.14	14.36	0.22	21.97	22.46	0.49
22	15.93	16.09	0.16	20.52	20.84	0.32
23	13.63	14.27	0.64	19.40	20.74	1.34
24	14.52	14.77	0.25	18.57	19.08	0.51
2Br	13.98	14.68	0.70	19.34	20.79	1.45



analyte	enthalpy term (kcal/mol)			entropy (cal/mol.K)		
	$-\Delta H_1$	$-\Delta H_2$	$-\Delta(\Delta H)$	$-\Delta S_1$	$-\Delta S_2$	$-\Delta(\Delta S)$
3Br	16.28	16.45	0.17	23.70	24.08	0.38
4Br	15.34	15.47	0.13	21.66	21.93	0.27
F4Br	16.72	16.79	0.07	24.45	24.59	0.14
2Cl	13.21	14.04	0.83	18.46	20.2	1.74
3Cl	15.56	15.73	0.17	22.99	23.37	0.38
4Cl	14.51	14.65	0.14	20.73	21.04	0.31
F4Cl	15.98	16.09	0.11	23.71	23.93	0.22
2F	11.81	12.66	0.85	17.08	18.93	1.85
3F	13.32	13.74	0.42	19.96	20.88	0.92
4F	12.69	12.88	0.19	18.69	19.11	0.42
F4F	14.18	14.33	0.15	21.71	22.03	0.32
4Et	13.95	14.05	0.10	20.05	20.27	0.22
4Bu	15.26	15.42	0.16	21.38	21.72	0.34
4tBu	14.49	14.71	0.22	20.41	20.89	0.48
2NO <sub>2</sub>	15.47	15.81	0.34	21.15	21.86	0.71
3NO <sub>2</sub>	15.94	16.10	0.16	21.1	21.45	0.35
4NO <sub>2</sub>	16.07	16.13	0.06	21.16	21.28	0.12
3CN	17.43	17.83	0.40	24.68	25.49	0.81
4CN	16.58	16.65	0.07	22.91	23.05	0.14
2OMe	13.26	14.02	0.76	18.38	19.99	1.61
3OMe	14.26	14.48	0.22	20.11	20.59	0.48
4OMe	13.09	13.09	0.00	18.46	18.46	0.00
2Me	12.76	13.28	0.52	18.10	19.23	1.13
3Me	13.27	13.53	0.26	19.35	19.92	0.57
4Me	13.09	13.20	0.11	18.99	19.22	0.23
2CF <sub>3</sub>	12.58	13.24	0.66	19.02	20.41	1.39
3CF <sub>3</sub>	13.48	13.85	0.37	20.48	21.33	0.85

analyte	enthalpy term (kcal/mol)			entropy (cal/mol.K)		
	$-\Delta H_1$	$-\Delta H_2$	$-\Delta(\Delta H)$	$-\Delta S_1$	$-\Delta S_2$	$-\Delta(\Delta S)$
4CF3	13.41	13.62	0.21	20.12	20.57	0.45
4OCF3	13.38	13.55	0.17	20.17	20.54	0.37
4Phe	16.97	17.05	0.08	21.94	22.10	0.16
24Cl	15.73	15.83	0.10	22.16	22.37	0.21
25Cl	15.17	17.11	1.94	20.89	24.81	3.92
34Cl	14.97	15.1	0.13	20.06	20.32	0.26
24F	13.45	13.76	0.31	20.85	21.54	0.69
25F	13.85	16.18	2.33	21.46	26.45	4.99
26F	11.73	11.95	0.22	17.51	18.04	0.53
34F	13.62	13.85	0.23	20.60	21.11	0.51
35F	15.56	16.27	0.71	24.92	26.46	1.54
24Me	13.96	14.08	0.12	19.92	20.17	0.25
25Me	13.62	14.27	0.65	19.25	20.62	1.37
34Me	13.84	13.93	0.09	19.61	19.80	0.19
triF	13.57	13.68	0.11	20.99	21.26	0.27
tetraF	13.44	14.01	0.57	20.48	21.77	1.29
pentaF	12.54	12.61	0.07	19.36	19.53	0.17
2but	9.24	9.24	0.00	17.22	17.22	0.00
2pen	10.11	10.24	0.13	18.01	18.33	0.32
2hex	10.75	10.94	0.19	18.29	18.77	0.48
3hex	10.65	10.76	0.11	18.14	18.41	0.27
2hep	11.75	11.90	0.15	19.53	19.92	0.39
3hep	11.50	11.74	0.24	19.04	19.61	0.57
2oc	13.01	13.18	0.17	21.28	21.70	0.42
3oc	12.82	13.03	0.21	20.97	21.46	0.49
4oc	12.76	12.89	0.13	20.87	21.21	0.34
2non	14.36	14.54	0.18	23.51	23.93	0.42

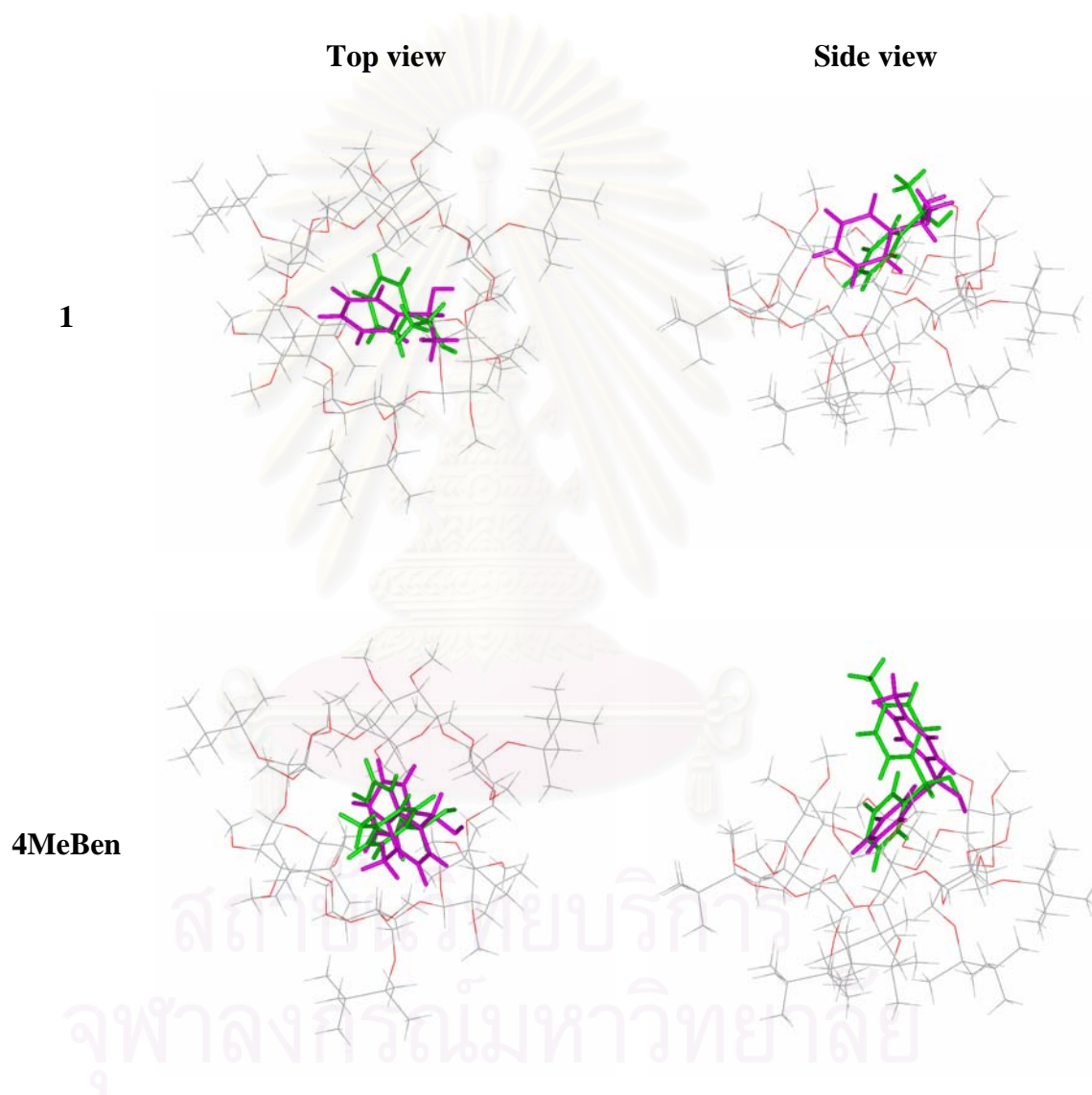
analyte	enthalpy term (kcal/mol)			entropy (cal/mol.K)		
	$-\Delta H_1$	$-\Delta H_2$	$-\Delta(\Delta H)$	$-\Delta S_1$	$-\Delta S_2$	$-\Delta(\Delta S)$
3non	13.90	14.14	0.24	22.53	23.08	0.55
2unde	15.45	15.60	0.15	24.08	24.43	0.35
2MeBen	16.10	16.15	0.05	20.71	20.82	0.11
3MeBen	16.74	16.84	0.10	22.03	22.23	0.20
4MeBen	16.71	16.78	0.07	21.86	22.02	0.16
2ClBen	16.23	16.44	0.21	20.40	20.82	0.42
3ClBen	17.76	17.93	0.17	23.12	23.47	0.35
4ClBen	17.95	18.07	0.12	23.39	23.63	0.24
4BrBen	18.23	18.31	0.08	23.17	23.34	0.17
4FBen	16.39	16.48	0.09	21.74	21.94	0.20
4OMeBen	16.99	16.99	0.00	21.22	21.22	0.00

สถาบันวิทยบริการ  
จุฬาลงกรณ์มหาวิทยาลัย

## Appendix D

### Docking configuration

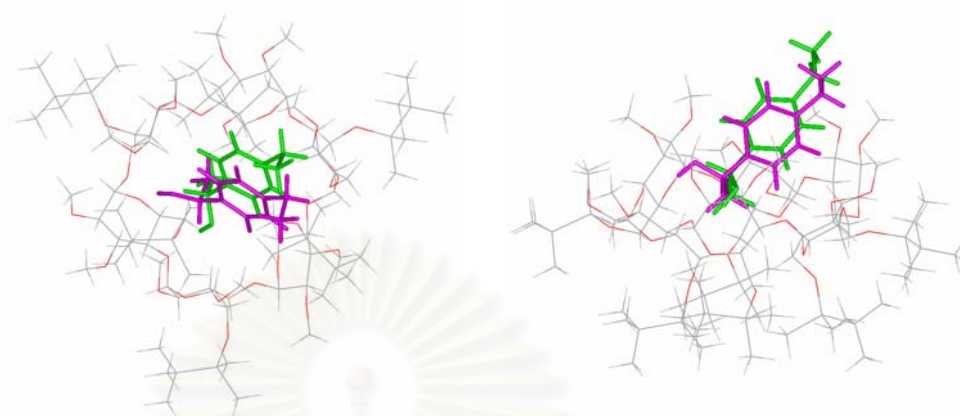
Figure D1 Docking configuration between ASiMe and *R*-enantiomer (green) and *S*-enantiomer (pink) of analytes



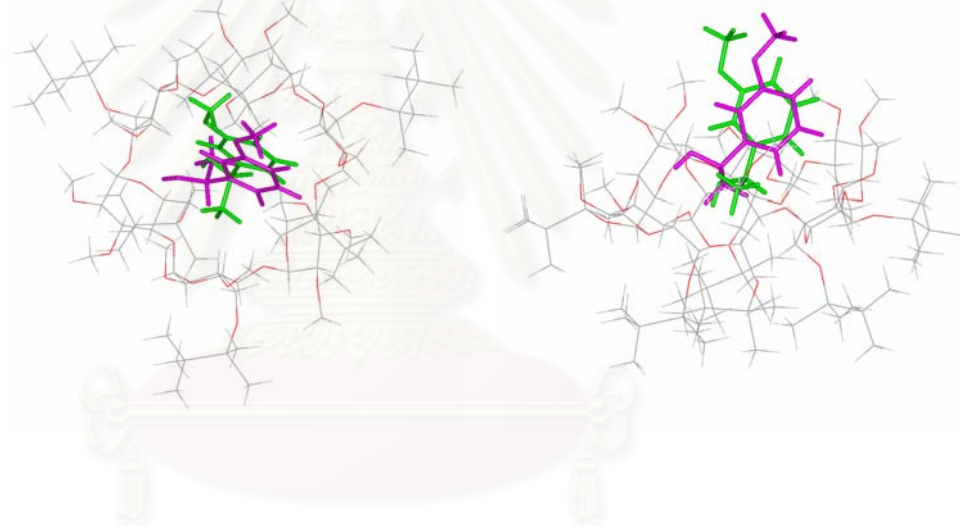
Top view

Side view

4Et



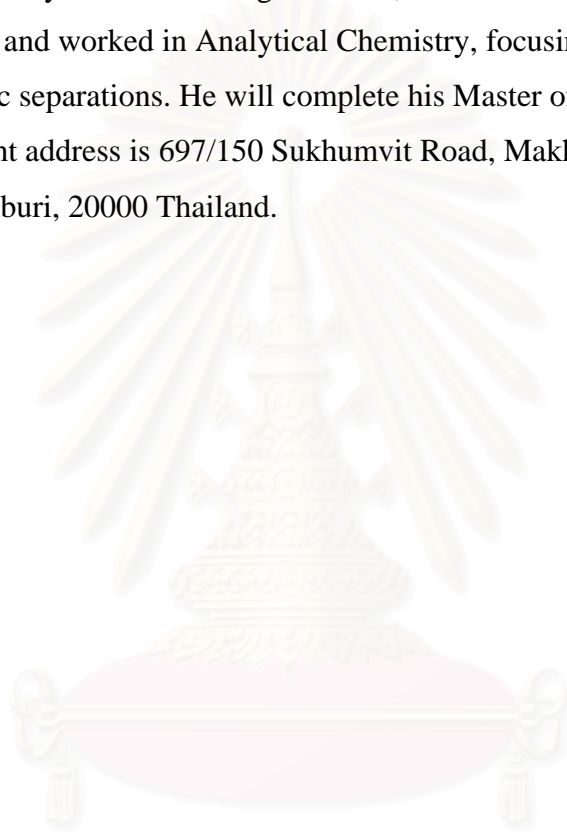
3OMe



สถาบันวิทยบริการ  
จุฬาลงกรณ์มหาวิทยาลัย

## VITA

Mr. Todsapon Pothisamutyothin was born on Monday 27<sup>th</sup> September, 1982 in Chonburi, Thailand. He finished Burapha University Demonstration School, concentration of Math and Science in 2000. He entered the Department of Chemistry, Faculty of Science, Chulalongkorn University and received a Bachelor of Science Degree in Chemistry in 2004. After graduation, he continued his graduate study at the same university and worked in Analytical Chemistry, focusing on the chromatographic separations. He will complete his Master of Science Degree in April 2007. His current address is 697/150 Sukhumvit Road, Makhamyong, Mueang Chonburi, Chonburi, 20000 Thailand.



สถาบันวิทยบริการ  
จุฬาลงกรณ์มหาวิทยาลัย